Halcyon

33rd Annual
American Helicopter Society International
Student Design Competition

Final Proposal
UMD Graduate Student Team

UNIVERSITY OF MARYLAND

Alfred Gessow Rotorcraft Center
Department of Aerospace Engineering
University of Maryland
College Park, MD 20740 U.S.A.

Lauren Trollinger
Graduate Student (Team Leader)
trollinger.lauren@gmail.com

Timothy Kreutzfeldt
Graduate Student
tkreutz@umd.edu

Br. Marius Strom
Graduate Student
brmariustor@gmail.com

Yong Su Jung
Graduate Student
jung9053@gmail.com

Luke Smith
Graduate Student
lsmith1@terpmail.umd.edu

Olivia Gonzalez
Graduate Student (Sikorsky)
omgierman@gmail.com

Eliza Perez-Sanchez
Graduate Student (Sikorsky)
eliza.perez25@gmail.com

Richard Quiñones
Graduate Student (Sikorsky)
richardquinones@gmail.com

Dr. Bharath Govindarajan
Faculty Advisor
bharath@umd.edu

Dr. Vengalatore Nagaraj
Faculty Advisor
vnagaraj@umd.edu

Dr. Inderjit Chopra
Faculty Advisor
chopra@umd.edu

Alfred Gessow Rotorcraft Center
Department of Aerospace Engineering
University of Maryland
College Park, MD 20740 U.S.A.

To the American Helicopter Society:

The members of the University of Maryland Graduate Student Design Team hereby grant AHS full permission to distribute the enclosed Executive Summary and Final Proposal for the 33rd Annual Design Competition as they see fit.

Thank you,

The UMD Design Team

ACKNOWLEDGEMENTS

The *Halcyon* design team wishes to acknowledge the following people for their invaluable discussion, guidance, and support throughout the course of this project.

University of Maryland Faculty

Dr. Inderjit Chopra – Alfred Gessow Professor and University Distinguished Professor, Director of Alfred Gessow Rotorcraft Center (AGRC), Dept. of Aerospace Engineering, University of Maryland, College Park

Dr. Vengalattore T. Nagaraj – Senior Research Scientist, Dept. of Aerospace Engineering, University of Maryland, College Park

Dr. Bharath Govindarajan – Asst. Research Scientist, Dept. of Aerospace Engineering, University of Maryland, College Park

Industry Professionals

Dr. Ashish Bagai – Program Manager, Tactical Technology Office, DARPA

Charley Kilmain – Rotor and Drive System Design, Bell Helicopter, Textron, Inc.

Capt. Samantha Lang – 41st Airlift Squadron Pilot, 19OG/Operations Group and 19 AW/Airlift Wing, Little Rock AFB

Mark Alber – Manager, Advanced Concepts at Sikorsky Aircraft

Special thanks to:

Dr. Ananth Sridharan
Dr. Anubhav Datta
Dr. Vikram Hrishikeshavan
Joseph Schmaus
William Staruk
Elizabeth Ward
Daigo Shishika
Stacy Sidle
Justin Winslow

Contents

List of Figures

List of Tables

Nomenclature

Symbol	Units	Description
AR	–	Aspect ratio
BL	–	Blade loading coefficient
DL	lb/ft^2	Disk loading
c	ft	Rotor chord
C_d	–	Drag coefficient
C_{d_0}	–	Zero-lift drag coefficient
C_f	–	Skin friction coefficient
C_l	–	Lift coefficient
C_T	–	Thrust coefficient
$C_{l_{\text{stall}}}$	–	Maximum lift coefficient
f	–	Fineness ratio
FF	–	Form factor
$GTOW$	lbs	Gross takeoff weight
M	–	Mach number
N_b	–	Number of blades
R	ft	Rotor radius
ρ	slugs/ft^3	Air density
Q	–	Interference factor
R	–	Reynolds number
S	ft^2	Wing planform area
S_{ref}	ft^2	Reference area
S_{wet}	ft^2	Wetted area
σ	–	Solidity
V_{stall}	ft/s	Stall speed
V_{tip}	ft/s	Tip speed
W	lbs	Weight

RFP Requirements and Compliance

Mission Profile Requirements	Design Solution	Section
Vehicle shall be fully contained within the internal dimensions of the C-130J cargo bay	Compact quadrotor biplane tailsitter design complies with C-130J loading regulations	3.4
Vehicle shall carry a minimum of 500 lbs of payload	Each *Halcyon* aircraft carries 508 lb of payload	3.1
Vehicle shall not jeopardize the safety of the C-130J or its crew	Halcyon powers up only when the aircraft is outside the C-130J cargo bay, and locks onto its rail system to prevent movement	11.4
Vehicle shall not jeopardize the safety of the people on the ground	Low rotor downwash from 50 ft (15 m) hover prevents injury to ground personnel from flying debris	14.5
Vehicle shall be deployed at 15,000 ft ISA and 140 knots equivalent airspeed	*Halcyon* is launched at the given conditions and is designed to stabilize and spin up the rotors after launch	12.4.1
Vehicle shall arrest its descent and transition to autonomous flight by 11,000 ft ISA (1,000 ft AGL)	*Halcyon* stabilizes and gains full control by 13,900 ft ISA (3,900 ft AGL)	12.4.1
Payload shall be delivered from a precision no-wind hover at 10,050 ft ISA (50 ft AGL) by tether	Payload is delivered according to the RFP specifications using an FAA-certified helicopter rescue hoist	12.4.4
Payload shall impact the ground at less than 5 fps and at precise GPS coordinates	The underslung payload impacts the ground at less than 5 ft/s even in gusts of 20 ft/s	12.4.4
Payload delivery in hover shall not take longer than 60 seconds	The control system enables the underslung payload to impact the ground at less than within 30 seconds even in gusts of 20 ft/s	12.4.4
After releasing the tether, the vehicle shall travel a minimum distance of 50 nm to a base for recovery	With full fuel tanks, *Halcyon's* low-power cruise enables a range of up to 124 nm	9.3
The vehicle shall land at precise GPS coordinates at 4,000 ft ISA	Three-tier navigation system ensures *Halcyon* is capable of precise geolocation	11.6

1 Introduction

The western coast of South America experiences more than 25% of the world's strongest earthquakes, characterized as a magnitude of 8.0 or higher on the Richter Scale [1]. These earthquakes leave communities without access to the most basic necessities: food, water, medicine, and shelter. Local airports often cannot accommodate the sudden influx of emergency aircraft, and may be incapacitated in the aftermath of a natural disaster. Fixed wing aircraft rely on functioning runways and are usually far from the epicenter where aid is most needed. Even cargo air-dropped using the U.S. military's most precise parachute system can drift up to 250 ft (75 m) off-target [2] and may never reach the intended recipients without additional ground support to locate and retrieve the cargo.

Vertical Take-Off and Landing (VTOL) aircraft are often used for disaster relief because they need no runways and can perform precision hover and hoist operations; however, full-scale helicopters still require large debris-free areas to hover close to the ground or to land. Commercially available unmanned aerial vehicles (UAVs), used for surveying the area and searching for survivors, are too small to deliver supplies to those in need. To address these issues, the 2015 AHS Student Design Competition Request for Proposal (RFP) called for a hover-capable autonomous unmanned aerial vehicle capable of delivering 500 lb (230 kg) of emergency aid to South American earthquake victims after deployment from the cargo bay of a C-130J Super Hercules, as illustrated in Fig. 1.1.

FIGURE 1.1: Disaster relief mission over the mountains of South America.

Through the application of innovative design concepts and proven technology based on recent advances in serial hybrid electric propulsion, the University of Maryland Design Team presents *Halcyon*, a quadrotor biplane tailsitter that offers unprecedented payload capacity for providing aid to disaster victims in an operationally safe, mission flexible package.

The design philosophy during this process concentrated on a few key performance parameters: maximizing payload, emphasizing safe operation, and using simple, currently available technology to minimize development and operation costs. Furthermore, *Halcyon* is designed to aid the disaster relief effort beyond completing the specified mission by providing kitted aircraft for on-site assembly, a modular structure for easy access to Line-Replaceable Units (LRUs), and multi-mission capability. This design philosophy resulted in *Halcyon*, a 1,520 lb (690 kg) autonomous UAV designed for disaster response at every level.

- *Halcyon* combines the exceptional control authority and hover efficiency of a quadrotor with airplane-like cruise efficiency to enable precision hover, extended range and endurance, and a 70 knot (130 km/hr) cruise speed at 10,000 ft (3,050 m)

- Biplane wings naturally stabilize the vehicle in deployment after launch without the use of cumbersome, single-use parachutes or additional mechanically complex devices
- Each *Halcyon* unit carries 508 lb (230 kg) of payload, and six units pack into the C-130J cargo hold to deliver a total of 3,045 lb (1,381 kg) in a single mission
- Simple, low maintenance design minimizes production and operational costs
- Stored in a self-contained kit complete with tooling, *Halcyon* is easily assembled in minutes for immediate disaster response
- Serial hybrid-electric propulsion supports a simple, lightweight transmission
- Four variable-speed rotors provide rapid response to input control to withstand gusty environments
- Advanced sensor suite enables day and night operation, flight in adverse conditions and degraded visual environments, optical and thermal image processing for mapping and search-and-rescue efforts, and sense-and-avoid procedures to ensure the safety of other aircraft and personnel
- Precise navigation capability and intelligent imaging keep *Halcyon* on target, even after a disaster when natural landmarks or structures may shift or be destroyed
- Additional flight sensors enable precision maneuvering between *Halcyon's* vertical hover and horizontal cruise flight modes

2 Mission Requirements

As Fig. 2.1 illustrates, the mission is to deploy from the cargo bay of a C-130J at 15,000 ft (4,600 m) at International Standard Atmosphere (ISA) conditions and 140 knots (260 km/hr), descend into a precision hover, deliver the payload from 50 ft above the ground at 10,050 ft (3,060 m) ISA using a sling cable, then fly for 50 nautical miles (92 km) to a predetermined base. The mission may be conducted in remote, high-altitude locations over disaster areas that may be strewn with debris, fallen trees, and downed communication lines. Additionally, the aircraft may encounter mountainous terrain, adverse weather conditions and degraded visual environments, and polluted or contaminated air. System redundancy and safety is of particular importance for these reasons as well as ensuring the protection of ground personnel and disaster victims awaiting emergency supplies.

1. **Deployment and descent:** Each of the six *Halcyon* aircraft will be sequentially launched from the cargo hold of the C-130J at an altitude of 15,000 ft ISA (5,000 ft above ground level, or AGL) and at a forward velocity of 140 knots (260 km/hr) equivalent airspeed, 176 knots (324 km/hr) true air speed (KTAS). A lithium-ion battery powers *Halcyon* when the aircraft is in free-fall. A second battery powers the autopilot and sensor suite through the duration of the aircraft's operation, ensuring an uninterrupted supply of power to the avionics system regardless of altitude, orientation, or gravitational forces.

   Regardless of initial orientation during launch, *Halcyon's* center of gravity is located to naturally pitch down into a vertical dive. This nose-down orientation ensures air flows

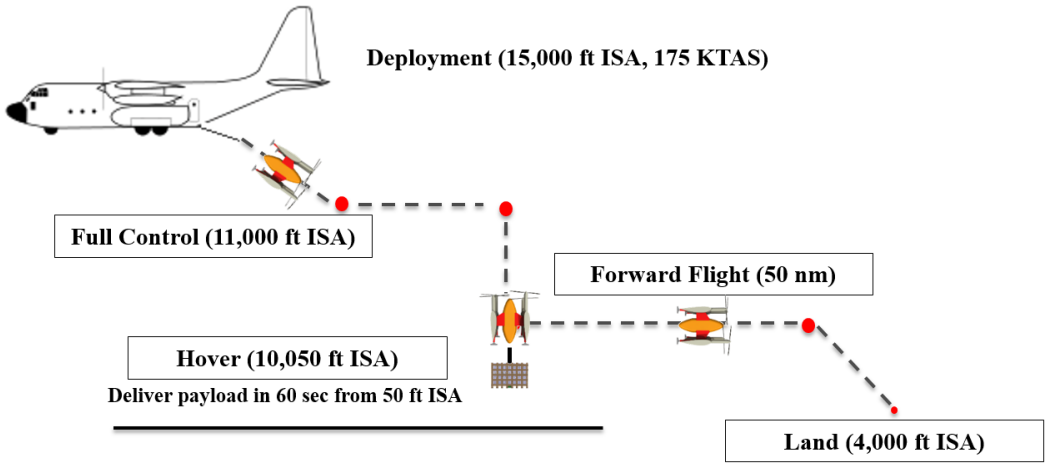

FIGURE 2.1: Mission profile.

over the rotors in a favorable direction, avoiding vortex ring state when the rotors spin up. Actuated flaps on each wing deflect to pull out of the vertical dive into a horizontal flight mode while gyroscopic sensors signal the proprotors to spin up when *Halcyon* attains level cruise. Thirty seconds after launch, the turbo-generator can provide full power to the electric transmission and the battery is disengaged. The aircraft thus enters level, autonomous flight at about 13,900 ft (4,240 m), well above the 11,000 ft requirement mandated by the RFP.

2. **Precision hover and package delivery:** The drop zone is located at 10,000 ft ISA. *Halcyon* identifies the payload delivery point by the provided GPS coordinates, transitions into edgewise flight, and settles into a precision hover 50 ft (15.2 m) above the ground. Though the RFP stipulates a no-wind hover condition during payload delivery, *Halcyon* is designed to deliver the payload in accordance with the requirements even in gusts up to 12 knots (6 m/s), as discussed in Section 12.4.4. The hoist releases the payload and lowers it by a tether such that it impacts the ground within 30 seconds at less than 5 ft/s (1.5 m/s). After delivery, the aircraft detaches the tether from the package, retracts the cable, and transitions into wing-borne cruise to travel back to the recovery location.

3. **Cruise, descent, and landing:** *Halcyon* will transition out of hover and into forward flight mode using its four variable-speed rotors to travel at least 50 nm (92 km) to a recovery location for retrieval. The base is located at 4,000 ft ISA at known GPS coordinates, as specified in the RFP. *Halcyon* is equipped with enough fuel for a 5 minute hover before landing to account for air traffic control, in addition to 10% reserve fuel for loiter. During cruising flight and after delivering the supplies, *Halcyon* requires 20% less power. The excess power output from the turbo-generator is used to recharge the batteries that power the aircraft through deployment and to the sensors and avionics.

4. **Reload and Re-deploy:** *Halcyon's* specially designed landing gear easily attaches to castering wheels for ground handling, as described in Section 3.3.1. These features allow *Halcyon* to be ready for a new mission in a short time, requiring only the time required to fill the fuel tanks (90 seconds) and load up the next payload for delivery (2 minutes).

2.1 Multi-Mission Capabilities

Though the basic mission described in the RFP requires the delivery of 500 lb of payload and a minimum range of 50 nm, *Halcyon* is designed with mission flexibility in mind. Owing to *Halcyon's* unique overlapping proprotors, six aircraft loaded with more than 500 lb of payload each can be simultaneously carried within the C-130J cargo hold. Each *Halcyon* unit satisfies every specification listed in the RFP, and the deployment of multiple *Halcyon* aircraft capable of completing the prescribed mission enables a higher level of mission capability. In the immediate aftermath of a disaster, a wide array of supplies and emergency equipment must reach critical areas as soon as possible. Water, shelter, and medicinal supplies must be delivered to disaster victims within 72 hours to maximize the chance of survival. With the ability to deploy six *Halcyon* aircraft and a total of 3,046 lb of supplies with every C-130J flyover, more emergency aid can reach disaster victims scattered over a large area within the critical 72 hour window and many more lives can be saved. All six *Halcyon* could focus deliveries on one designated area, or the aircraft could deliver supplies to six widespread locations. This system of systems approach enables unparalleled mission flexibility and ensures that relief teams respond to a specific event with mission-tailored methods.

In addition to delivering six times the payload requirement stated in the RFP in a single mission, *Halcyon* was designed for extended range missions. The basic mission requires a minimum range of 50 nautical miles from the payload delivery zone. Due to likelihood of encountering terrain, rough weather conditions, and the need to reach remote towns or villages, increased range capability is a key feature of this disaster relief vehicle. To account for such considerations, *Halcyon* is designed to carry enough fuel to comfortably travel 300% farther than the requirement when flying the mission specified in the RFP. The aircraft's serial hybrid-electric propulsion system is driven by a single turboshaft engine, which powers an electric generator. The biplane tailsitter is uniquely suited to long-range missions, as the ability to fly like an airplane minimizes the power required to cruise. Additionally, range can be increased simply by swapping potential payload for fuel, which is particularly useful for delivery missions with smaller or lighter payloads such as first aid kits or MREs.

Disasters occur in many forms, and *Halcyon* is exceptionally suited for responding to situations in the wake of a disaster that may be inaccessible by human response teams and may involve hazardous tasks. As an autonomous UAV, *Halcyon* can be employed in disaster response efforts in a number of ways:

- **Delivery of emergency supplies:** After a disaster has occurred, *Halcyon* can deliver large quantities of much-needed food, water, medical supplies, tools, tents and temporary shelters, and basic amenities to victims. *Halcyon* can sustain a precision hover even in windy conditions, and is equipped with a FAA-certified variable-speed helicopter rescue hoist to ensure safe, controlled delivery of the package. The ability to deploy multiple *Halcyon* aircraft per mission allows six times the emergency supplies to reach victims with one flight of the C-130J.
- **Reconnaissance and mapping:** *Halcyon* is outfitted with a wide array of sensors and navigational equipment utilized to survey the area after a disaster. Blocked roads, destroyed bridges, and other damaged infrastructure can be mapped, evacuation routes planned, and information relayed to other branches of the relief effort, thus saving time when it is most crucial.

- **Search and rescue:** Search and rescue (SAR) efforts are most critical in the first 72 hours following a disaster to locate survivors. While manned SAR missions can lead to crew fatigue and an increased likelihood of missing survivors among the rubble, autonomous UAVs like *Halcyon* can continue the search as far as necessary, only briefly stopping to replace fuel and batteries.

- **Logistics support:** *Halcyon* can serve as temporary telecommunication platforms or be used to set up wireless or radio communication networks. Multiple *Halcyon* aircraft can aid with route planning around fallen trees and buildings, blocked roads, and downed power lines, identifying and communicating the best path to and from a rescue area to ground vehicles or personnel.

- **High altitude response:** *Halcyon* is capable of operation at high altitudes (10,000 ft ISA). Augmented by backup lithium-ion batteries, *Halcyon* can sustain flight in polluted-air environments or at altitudes beyond the capability of air-breathing engines for 2 minutes at maximum power.

- **Fire suppression:** Wildfires pose a severe threat to would-be rescuers, and a typical light helicopter can only deliver 120 gallons/bucket of retardant. Deploying all six *Halcyon* aircraft from a single C-130J would deliver over 360 gal of fire suppression agents to various locations simultaneously to smother the flames.

- **CBRNE countermeasures:** Chemical, Biological, Radiological, Nuclear, and Explosive (CBRNE) hazards pose a grave threat to humans, and therefore are best investigated by autonomous UAVs like *Halcyon*. With the addition of certain sensors, multiple aircraft could canvass a large area and take instrument data and visual recordings to survey the site of a CBRNE disaster.

3 Concept of Operations

Designing a VTOL disaster relief vehicle to fit within the constraints of a C-130J cargo hold is challenging, and therefore a broad variety of configurations were considered before the quadrotor biplane tailsitter was selected as the most appropriate design for this mission. This configuration was chosen because it demonstrated the ability to meet all the requirements dictated by the RFP, including transportation and launch via a C-130J fixed-wing aircraft, precision hover capability, and high payload capacity.

The quadrotor biplane tailsitter provides maximized payload-carrying capacity in a compact, easily transported package. Completely contained within a 9 ft x 9.7 ft x 8 ft (2.7 m x 3.0 m x 2.4 m) space, *Halcyon* easily fits within the 40 ft x 119 in x 9 ft (12.2 m x 3.02 m x 2.7 m) C-130J cargo bay while still complying with Defense Transportation Regulations (DTR) clearances detailed in Section 3.4.2. Four variable-speed electric motors housed within the rotor hubs provide the necessary power and precision control in flight by independently operating four 6.64 ft (2.02 m) diameter rotors. Rotors are positioned such that diagonally-opposed rotor pairs are at the same height, and adjacent rotors overlap by 15% of the radius. Allowing the rotors to overlap not only allows for a larger radius, decreased disk loading, and greater stall margin, but the overlapping design also enables the close packing of up to six assembled and fully-loaded *Halcyon* vehicles within the C-130J cargo hold. Two wings, each of which possesses a flap capable of a 25° deflection, provide deployment stabilization during launch as well as

TABLE 3.1: Pallet options considered.

Pallet Type	Thickness (in / mm)	Cost	Weight (lb / kg)
463L Pallet	2.25 / 57.2	Not Available	168 / 76.4
Plywood Sheet	1.13 / 28.6	$55.00	189 / 85.7
Plywood Sheet with Frame	4.50 /114	$23.00	119 / 54.0
Aluminum Sheet	0.12 / 3.00	$67.00	12.2 / 5.54
Wooden Pallet	5.00 / 127	$25.00	50.0 / 22.7
Plastic Pallet	5.00 / 127	$90.00	7.00 / 3.18

the transition into a low power, fuel efficient airplane-like cruise. A serial hybrid propulsion system provides a simple, lightweight transmission and mission flexibility through extendable range capabilities. A variable-speed helicopter rescue hoist provides precision payload delivery, and an autonomous flight control and navigation system supports intelligence, surveillance, and reconnaissance (ISR) missions as well as resupply and delivery operations.

3.1 *Halcyon* Kit Assembly

Designed for simplicity and rapid response, *Halcyon* can be delivered to strategic locations near a disaster zone as a self-contained kit complete with requisite tooling. Made primarily from lightweight carbon composite, *Halcyon* is assembled in minutes with just five tools included with the kit: an impact driver, screw driver, allen key, right-angle torque wrench, and push puller. This system enables large-scale delivery and on-site assembly to maximize response time during relief efforts.

FIGURE 3.1: *Halcyon* kit option.

3.2 Preparing the Payload

The deliverable payload consists of three components: (1) 18 cases of water bottles weighing just over 500 lb (230 kg), (2) a plastic pallet to support the bottles, and (3) the cargo net to ensure integrity of the payload. Each item is commercially available and ready to use, enabling the *Halcyon* to be mission-ready with minimal lead time. The water bottles alone weigh 508 lb, so great care was taken in choosing payload delivery accessories that minimize total payload weight.

A support system for the water bottles is necessary to prevent rupture in transit. Several options were considered, including metal-reinforced military pallets such as the 463L, standard wooden pallets, and thin aluminum metal pallets: the corresponding thickness, cost, and weight of each are shown in Table 3.1. Though each option is physically capable of fitting within the cargo bay of the *Halcyon* vehicle, minimizing the weight of external packaging enables more emergency payload to be carried. A plastic pallet was the ultimate selection because it offered 43% less weight for comparable cost. The plastic pallet used in *Halcyon* is strong enough to carry four times the payload weight, is commercially available, and can be re-purposed as furniture, shelter material, support for other supplies, and a number of other needs after the payload is delivered.

To protect the payload during delivery, an industrial-grade cargo net fully surrounds the cases

of water stacked on the plastic pallet; this net is included in the 463L pallet universal payload system. Made from a polyester webbing manufactured to military standards, these commercially available nets are extremely durable and lightweight. The net selected for the *Halcyon* cargo system weighs just 17 lb (7.71 kg) and is capable of lifting 4,500 lb (2,041 kg). Delivered to the target location along with the pallet and payload, the net can also be repurposed and reused by the relief teams on the ground.

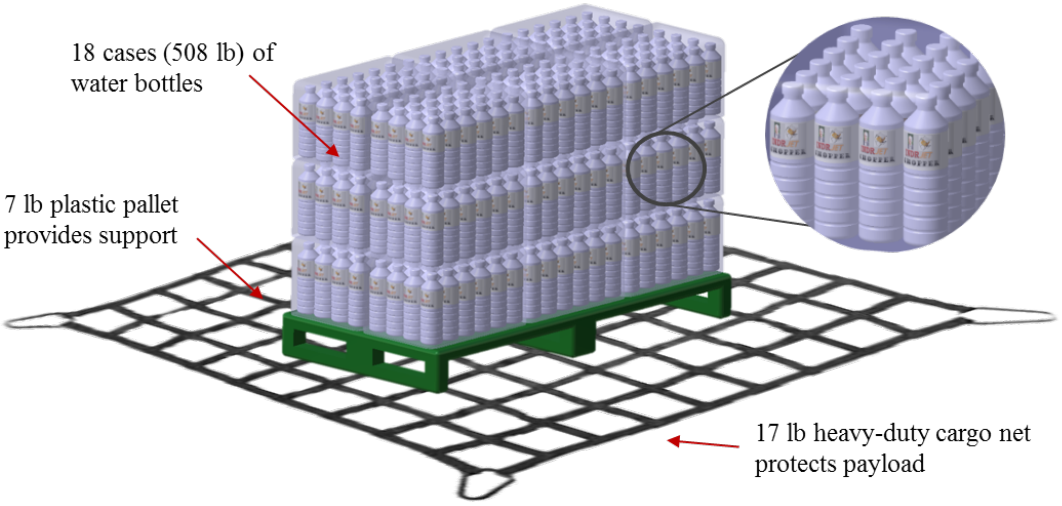

FIGURE 3.2: Mission payload consists of water, plastic pallet, and industrial strength cargo net.

3.3 Loading and Unloading *Halcyon*

Halcyon employs simple payload integration to allow supplies to be loaded or unloaded from the cargo bay with no more than two ground handlers.

Halcyon rests upright on its landing gear, with the rotor plane parallel to the ground, during all ground handling operations. The fuselage has a streamlined shape with clamshell doors that open to reveal the cargo bay. When *Halcyon* rests on the ground, these doors can be fully opened to allow unrestricted access to the cargo bay. The doors are manually operated by a single person using handles on each door for loading or unloading. When the doors are removed, the payload can be rolled directly under the vehicle. The mission payload, which consists of the required 500 lb of water, the plastic pallet, and the cargo net has a maximum clearance of 8 in (20 cm) between the top of the package and the bottom edge of the airframe. Any available ground handling equipment, such as commercially available forklifts, dollies, and baggage carts found at almost any tool supplier, may be used to place the payload. *Halcyon* is also designed with an optional set of detachable castering wheels that enable ground personnel to roll the vehicle directly over the payload. These heavy-duty handling wheels are discussed in Section 3.3.1.

Once the payload is in position, the hoist hook is lowered from inside the vehicle and attached to the cargo net. Ground personnel then engage the hoist to lift the payload into its position inside the cargo bay. *Halcyon's* system prioritizes safety and simplicity by automating the loading procedures as much as possible and providing all necessary handling equipment. *Halcyon* is equipped with the TALON Auto-Loc Cargo Hook, shown in Fig. 3.3, which can pick up or drop

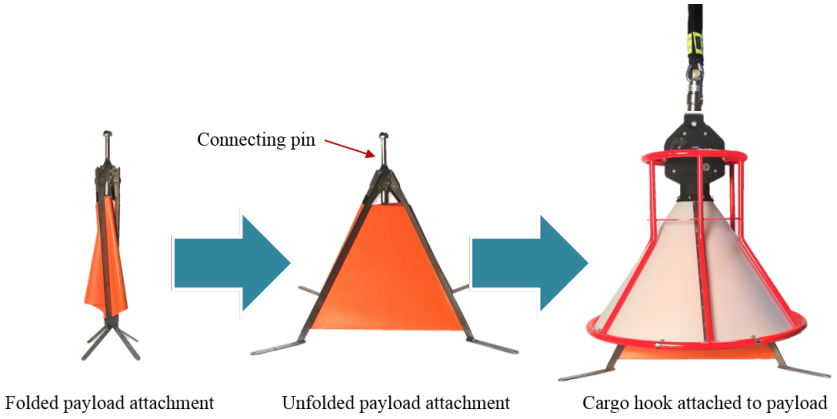

FIGURE 3.3: Pressure-sensitive auto-locking cargo hook enables autonomous payload delivery.

off payloads autonomously. The hook itself can be fitted to use with any hoist. A target cone is placed on the payload and left at the pick up or drop off location. The hook is lowered on top of the target, and pressure sensors detect its presence in the capture area. The hook then grabs the target, and the payload can be raised into the cargo bay. Therefore, if no personnel are available at the supply delivery zone, *Halcyon* is still able to deliver the payload with complete autonomy and complete the specified mission.

3.3.1 Ground Handling

Ground handling involves two modes: skids for C-130J operation and wheeled landing gear for ground operations. The skids interface directly with the standard 436L cargo rails installed in the C-130J, allowing for ease of loading. Once on the ground, a set of ground handling wheels, developed for the Bell 206 Jet Ranger, can be installed via attachment points on the vehicle's skids. The wheels integrate with the skids in a similar manner as shown in Fig. 3.4.

The wheels also allow for *Halcyon* to be loaded into the C-130J cargo hold when a K-loader (or similar device) is not available. Instead, with the C-130J cargo door lowered and appropriate ramps in place, a fully loaded *Halcyon* can be wheeled directly into the cargo hold. The wheels can then be detached, allowing *Halcyon's* skids to rest on the Universal Cargo Handling Rail. This use of the cargo rail system allows for ease of deployment of the *Halcyon* from the C-130J, since directionality is automatically enforced by the rails.

FIGURE 3.4: Dual-mode landing gear.

The skids are designed such that the lower skid will never impede *Halcyon's* movement inside the C-130J. A polyethylene guide plate ensures that directionality is maintained as the vehicle is moved on the cargo rails and that the skids cannot slip off of the rails in case the C-130J experiences turbulence. The skids are extended such that *Halcyon* will always have four points of contact as it moves towards the exit ramp of the C-130J. The skid tips are shaped to ensure that as *Halcyon* tips over the edge of the deployment ramp, no part of the vehicle impacts the C-130J.

3.4 C-130J Packing

Halcyon's staggered rotor design enables multiple vehicles to be stored in close proximity, as shown in a representation of the C-130J's cabin space in Fig. 3.5. This allows a total 6 vehicles to be deployed by a single C-130J, allowing for a total of 3,045 lb (1380 kg) of food, water, shelter, medical, or other supplies to be delivered per mission.

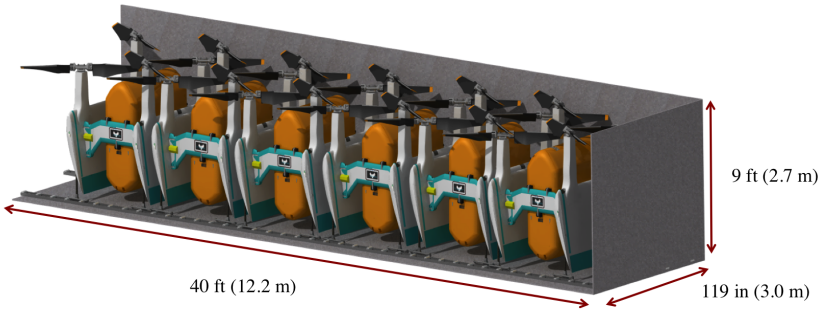

FIGURE 3.5: C-130J packing scheme.

3.4.1 C-130J Allowable CG Travel

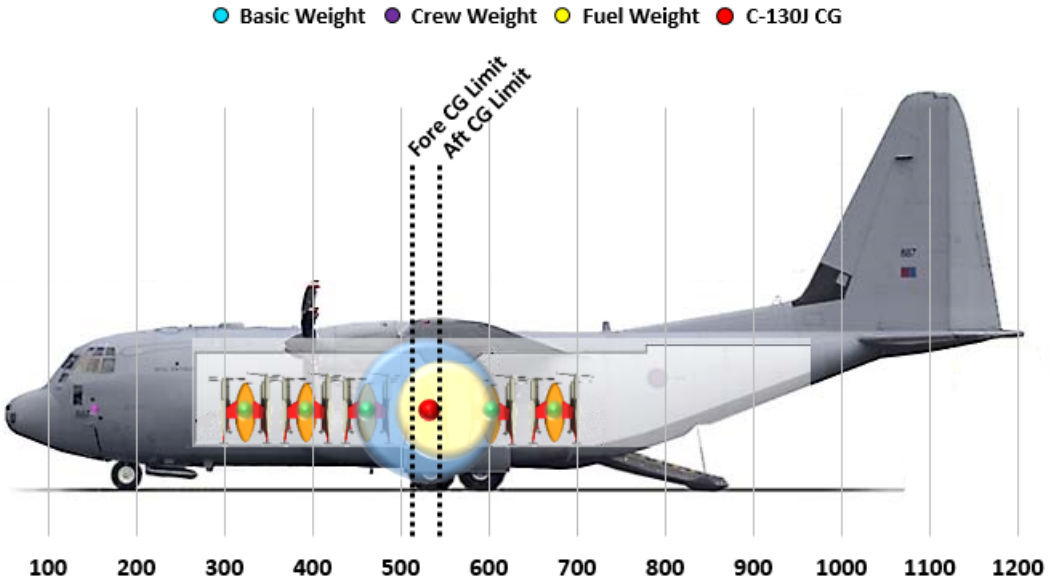

FIGURE 3.6: C-130J operates within its allowable CG travel of 21%-30% MAC.

In a given aid delivery mission, the C-130J will have minimal personnel on board, including flight crew and a loadmaster. Based on a typical fuel consumption of 4,000 lb/hr (1,818 kg/hr), the C-130J's fuel state is assumed to be 38,000 lb (17,273 kg) at the time of deployment. As the 6 vehicles are deployed from the C-130J, CG travel is within the maximum allowable range for this aircraft, which is 21% to 30% of its wing mean aerodynamic chord (MAC). To stay within this range, however, requires that one *Halcyon* vehicle be launched at a time and that each is pushed to the ramp from its storage location.

Given this procedure of launching one vehicle at a time, it is not possible for *Halcyon* to force the C-130J to exceed its flight envelope. While such a breach is possible if multiple vehicles are placed at the cabin door, so long as at least one additional vehicle is located forward of station 481 the aircraft is within its operating limits as shown in Fig. 3.6.

3.4.2 DTR Compliance

As *Halcyon* may see action in coordination with military aircraft, it is important that it complies with the Defense Transport Regulations (DTR) to ensure safety of personnel onboard the parent aircraft. The following criteria, taken from the C-130J load planning datasheet in DTR-III-V-16, are required for all payloads onboard a C-130J [3].

1. Maximum cargo weights: "Pallet positions 1-4: 10,355 lb; Pallet positions 5: 8,500 lb" (DTR III-V-15, V-4)
2. "Maximum heights are as follows. 102 inches for large, single items of cargo placed on pallets...[the] maximum height for cargo located forward of fuselage station 381 or positioned on the airplane ramp is restricted to 76 inches." (DTR III-V-16, V-4)
3. "In terms of width, cargo must be 14 inches from the sides of the airplane, without passengers. Without dual rails installed, the cargo compartment floor is limited to 105 5/8 inches wide." (DTR III-V-16, V-4)

Beginning with the first point, even the maximum weight of six fully-loaded *Halcyons* comes to 9,172 lb (4,169 kg), hence there are no combined loadings that could possibly exceed the maximum weight for any given pallet position nor the payload capacity of the parent aircraft of 35,000 lb (15,909 kg).

As seen in Fig. 3.7(a), the red region represents the 14 in. corridor (required in (1)) such that the rear of the aircraft can be reached in the event of an emergency. Similarly, this corridor is required such that the loadmaster can facilitate *Halcyon's* deployment. The yellow region represents buffer zone imposed by the maximum height limitation. It is worth noting that the height restriction forward of station 381 is due to an inward tapering of the cabin ceiling.

By superimposing *Halcyon* on the DTR limitations in Fig. 3.7(b), it is evident that *Halcyon* complies with each buffer zone with the exception of its rotor blades. These blades, the lowest of which is 7.6 ft (2.3 m) above the floor of the cabin, exceed the width restrictions imposed by the DTR by 8 in. (20 cm), leaving a 6 in. (15 cm) buffer between the blade tips and the cabin walls.

According to Air Force Instruction 11-2C-130 (*C-130 Operations Procedures*) Part 4.2.4, "If the aisleway requirement in paragraph 4.2.3. cannot be achieved on missions carrying crew only or mission-essential personnel (MEP) authorized by operations order/plan...MAJCOM A3/DO is authorized to waive this requirement based on MAJCOM Stan/Eval evaluation and recommendation." Based on this instruction, the height of the rotor blades, and current waivers regularly given by Air Force loadmasters, this intrusion should not pose an issue to certification and deployment of the vehicle. Furthermore, based on a dynamic simulation of the vehicle as it departs the C-130J ramp, the rotor blades have been shown to maintain a minimum 6 in. (15 cm) clearance from the parent aircraft during all phases of loading and deployment [4].

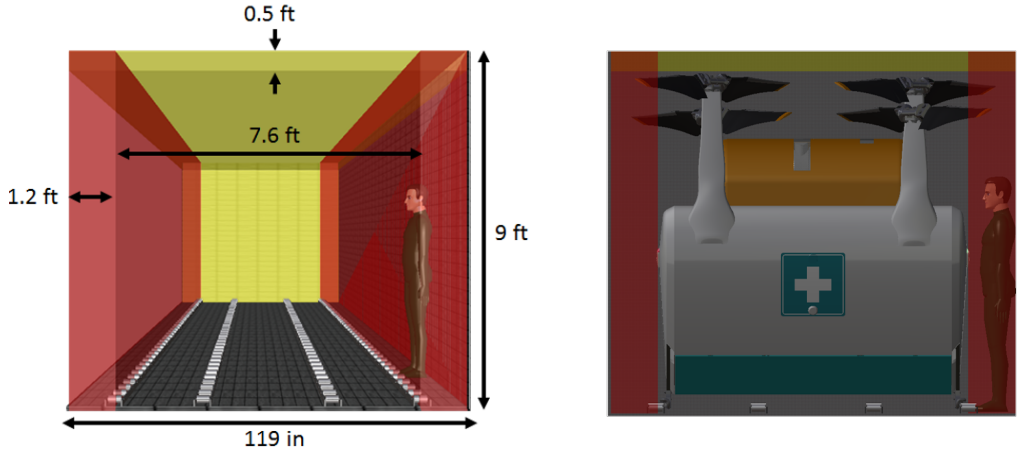

(a) Required buffer zones

(b) Halcyon in the C-130J cabin

FIGURE 3.7: Interior packing constraints within C-130J cargo bay.

3.5 Multi-Vehicle Operation

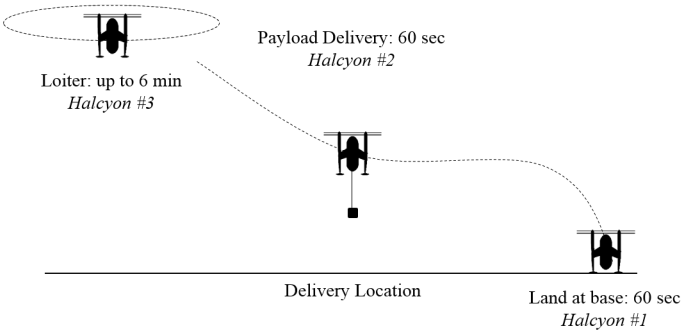

FIGURE 3.8: *Halcyon* holding pattern for multi-vehicle delivery.

The *Halcyon* system is unique because multiple aircraft are utilized to complete the mission, and therefore special considerations must be made to address the interaction and operation of multiple *Halcyon* vehicles. A holding pattern is necessary to ensure safe operation and prevent any accidents when all six *Halcyon* vehicles are called upon to deliver 3,045 lb (1,380 kg) of payload to a single drop zone.

The first *Halcyon* vehicle transitions into hover over the drop zone and delivers the payload while the other five vehicles arrive and maintain a steady loiter nearby. When the first vehicle completes delivery, it transitions into cruising forward flight and begins its journey to the recovery location while the second *Halcyon* vehicle begins payload delivery procedures. This process is repeated until all six vehicles have delivered their payload.

To account for this procedure and ensure that the last vehicle to deliver the payload has sufficient fuel to loiter, each vehicle's fuel tanks are sized for an additional 39 lb (17.7 kg) of fuel to accommodate an 18 minute holding pattern. This time period includes, for each vehicle, 60 seconds for transitioning into and out of precision hover, 60 seconds for payload delivery, and 60 seconds for landing at the recovery location.

By sizing the fuel tanks for additional loiter time, *Halcyon* is fully capable of the mission illustrated in Fig. 3.8. It should be noted that *Halcyon's* internal avionics and flight planning systems govern all in-flight operation, and therefore impose no additional responsibilities on the C-130J flight crew or ground control operators.

4 Vehicle Configuration Selection

A vast range of configurations were considered for this mission, including a conventional single main rotor helicopter, autorotative aerodynamic decelerator (AAD), stopped rotor, variable rotor radius/disc rotor, thrust-augmented compound, lift-augmented compound, fan-in-wing/fan-in-body, tiltrotor, and tailsitter. Each aircraft configuration was ranked in a Pugh decision matrix according to the design drivers listed in Section 4.1, and the top five vehicle configurations then underwent a subsequent Pugh decision matrix to determine the optimal rotor number and layout for the given mission. The down-selection process began by identifying the most important selection criteria for the mission detailed in the RFP using an Analytical Hierarchy Process (AHP). A Pugh decision matrix was utilized to select the optimal vehicle and rotor configuration for this mission's unique deployment requirements.

4.1 Selection Criteria: Voice of the Customer

The RFP requires the design of an aircraft capable of carrying a minimum payload of 500 lb of water bottles to a high-altitude disaster zone. The size of the vehicle is constrained by the size of the C-130J cargo hold from which it will be deployed. Other requirements include delivering the payload from a 50 ft precision hover in less than 60 seconds and a subsequent minimum cruise distance of 50 nm to a base location for recovery.

To perform a comprehensive comparison for such a broad range of configurations, a set of selection criteria was developed to highlight the most important aspects of an air launched, unmanned disaster relief vehicle. These are listed, in no particular order, below:

- **Deployability:** The chosen configuration must be capable of withstanding the deployment velocity of 176 KTAS, achieving stable flight immediately after release, and entering controlled, autonomous flight by the time it falls to an altitude of 11,000 ft ISA.
- **Flight Safety:** This aircraft will operate over a disaster zone in a remote location, where the delivery of basic necessities may be the key to survival for victims of the disaster. For this reason, flight safety is a major design driver. In case of emergency, the aircraft must be able to survive a loss of power and safely land away from disaster victims or ground personnel so its payload can be recovered.
- **Personnel Safety:** To protect crew members within the close quarters of the C-130J cargo bay, the rotors must not be allowed to spin up while the aircraft is inside the C-130J cargo bay. There should be a sufficient gap between the rotor plane and the head height of crew members. The aircraft must have low rotor downwash to prevent injury to people on the ground and to prevent blowing around debris or wreckage left behind in the aftermath of the disaster.
- **Payload Capacity:** A major criterion for selecting a configuration is to maximize payload carrying capacity. Multiple aircraft, each carrying as much payload as possible, should be sized to fit within the C-130J cargo bay.

TABLE 4.1: Prioritized selection criteria provided by the AHP matrix.

	Flight Safety	Technological Risk	Payload Capacity	Forward Flight	Deployability	Personnel Safety	Cost	Normalized Priority	Rank
Flight Safety	1.00	3.00	0.50	3.00	0.25	0.80	5.00	**0.153**	**3**
Technological Risk	0.33	1.00	0.20	2.00	0.20	0.50	2.00	**0.083**	**5**
Payload Capacity	2.00	5.00	1.00	4.00	0.80	2.00	6.00	**0.253**	**2**
Forward Flight	0.33	0.50	0.25	1.00	0.20	0.30	3.00	**0.060**	**6**
Deployability	4.00	5.00	1.25	5.00	1.00	5.00	8.00	**0.260**	**1**
Personnel Safety	1.25	2.00	0.50	3.33	0.20	1.00	4.00	**0.150**	**4**
Cost	0.20	0.50	0.17	0.33	0.13	0.25	1.00	**0.041**	**7**

- **Technological Risk:** The chosen configuration must be robust and demonstrate reliable performance even over long periods of disuse. The aircraft should depend on technology with a high Technology Readiness Level (TRL). Proven technology should be preferred during the configuration selection.
- **Cost:** The design should aim to decrease production, operation, and maintenance costs as much as possible by taking advantage of recyclable materials and reducing the use of overly complex mechanisms and unduly specialized components.
- **Forward Flight Performance:** Forward flight performance is related to the vehicle's speed and range. The disaster area is assumed to be a remote location over mountainous terrain, and therefore a larger range is desirable. More aid can be delivered if the overall cycle time of the mission is decreased.

4.2 Selection Criteria: Analytical Hierarchy Process

Each of the selection criteria was ranked according to its relative importance to the mission specified in the RFP using an Analytical Hierarchy Process (AHP). This ranking process allowed the team to prioritize the selection criteria, and thereby choose a configuration to reflect the most critical aspects of the disaster relief mission. This prioritization is shown in Table 4.1.

The selection criteria, listed across the top-most row and left-most column, are ranked relative to one another according to their importance to a successful mission. For example, the first column is Flight Safety. Starting from the top row and working down to the bottom, each design driver is ranked more (> 1.0) or less (< 1.0) important than Flight Safety. Once each column in the AHP matrix is filled out, the AHP values within each column are normalized by the column sum, then averaged by row. This gives a Normalized Priority for each row, which can be ordered from largest to smallest value to provide the ranking.

The resultant AHP matrix shows that high payload capacity and stable, controlled deployment are mission critical. These will be the drivers behind the entire configuration selection process. The primary objectives vital to the success of the mission are flight safety, personnel safety, and technological risk. The secondary mission objectives are forward flight performance and cost.

4.3 Considered Configurations

A wide range of vehicle configurations were considered for the disaster relief mission specified in the RFP; each of these is shown in Fig. 4.2. The advantages and disadvantages of each

configuration are discussed in this section. Because of the mission requirements, desirable configurations could be sized such that multiple vehicles, each capable of completing the entire mission independently, could be deployed simultaneously. Suitable designs should also achieve passive stabilization after ejection from the C-130J, withstand the high aerodynamic forces and moments experienced in the initial seconds of deployment, and have a low disk loading and a high power loading. A radar plot showing the top-scoring configurations for the mission is shown in Fig. 4.1.

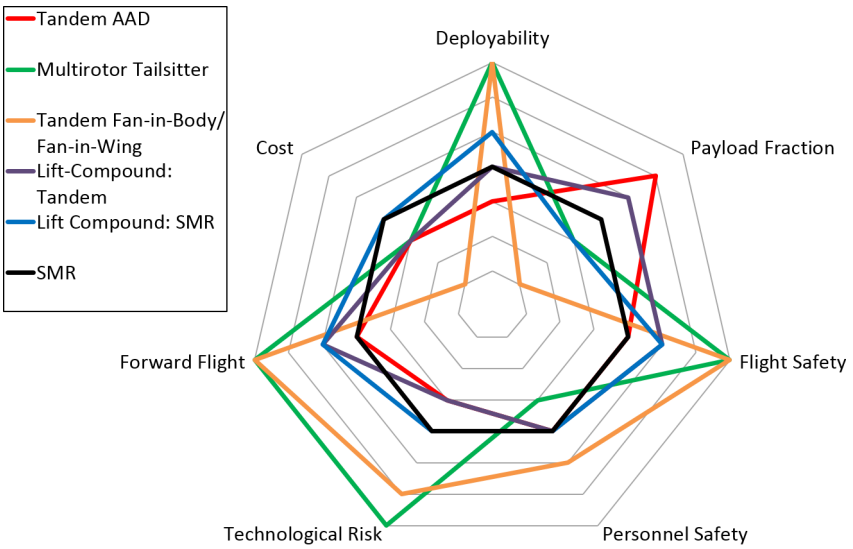

FIGURE 4.1: Radar plot showing the results of the initial Pugh decision matrix.

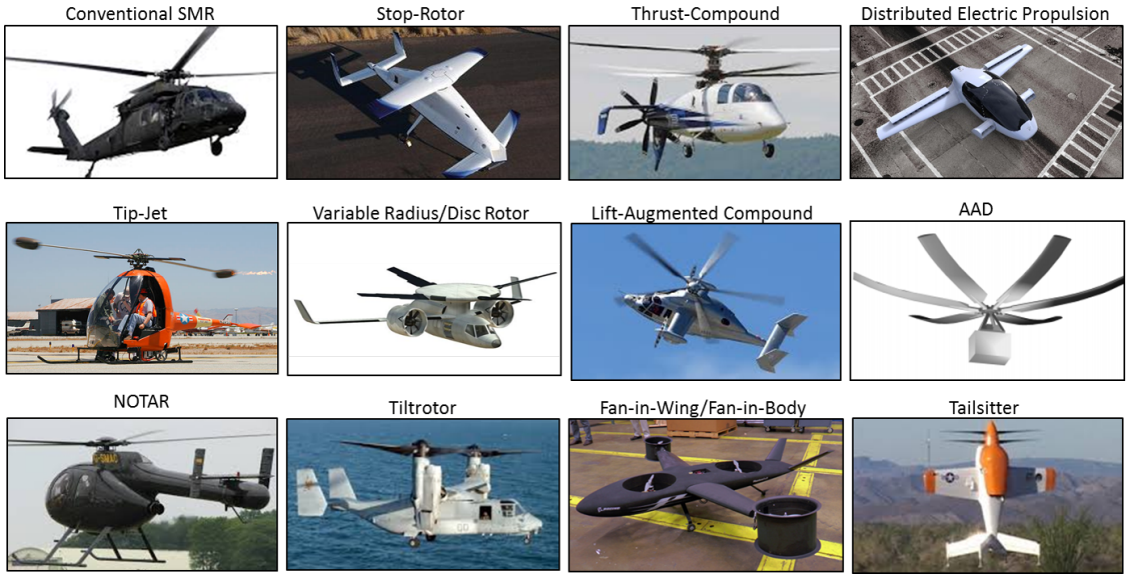

FIGURE 4.2: Configurations considered in the selection process.

4.3.1 Single Main Rotor (SMR)

Conventional SMR helicopters were the baseline against which all other configurations were compared in the Pugh decision matrix in Table 4.2. Multiple single main rotor (SMR) helicopters were examined for this mission.

- Conventional SMR/TR: These helicopters have good endurance, paylan oad capacity, and hover efficiency, but also have a large footprint because of the tailboom and a potentially exposed tail rotor that could pose a safety risk to C-130J flight crew.
- Fenestron SMR: The shrouded tail rotor is safer for ground personnel, but has the same disadvantages of a conventional SMR.
- Tip-Jet SMR: Though excellent in autorotation, a tip-jet SMR would have to be very large to carry the minimum payload, and would face the same problem as a SMR in exiting the cargo hold at an angle.
- NOTAR: Despite an advantage of not having a long tail boom take up valuable space in the cargo hold, the high speeds at which the helicopter is deployed would overpower the coanda effect used to achieve stable flight.
- Autonomous Aerodynamic Decelerator (AAD): Similar to a conventional SMR, the AAD's rotor blades tend to be more flexible and are designed specifically for autorotative descent, where the blades unfold as they spin faster due to centrifugal loading. AADs have been investigated for reentry vehicles, package delivery, and aircraft deployment applications [5]. Though these rotors are very tolerant of high aerodynamic loads, the technology readiness level of large-scale AADs with high payload-carrying capacity is extremely low.

4.3.2 Stopped Rotor

The stopped rotor configuration was initially attractive because the strong, rigid rotors could withstand high aerodynamic loads and double as lifting wings in high speed flows similar to those encountered during deployment. These designs suffer from decreased rotor efficiency and low technology readiness level.

4.3.3 Variable Diameter Rotors

Variable diameter rotors have an advantage in deployment at high speeds. Retracted rotors can resist higher aerodynamic forces and have a smaller footprint. However, variable diameter rotors are mechanically complex and have a low TRL, so this configuration was not a practical option.

4.3.4 Fan-in-Wing/Fan-in-Body

The fan-in-wing/fan-in-body configuration can be very efficient in hover, and tilt-fan designs are good for high speed and long range missions. In addition, the shrouded rotors are extremely safe for C-130J personnel. These rotors are enclosed by a fuselage or wing area, limiting their size as compared to an unshrouded design. This leaves little internal space for carrying a payload.

4.3.5 Tiltrotor/Tiltwing

A major advantage of tiltrotors is that these aircraft take off vertically and then transition into a faster and more efficient forward flight cruise. Tiltrotors are designed with a high disk loading because of their smaller-diameter proprotors, which have a high downwash that is unfavorable for delivering a slung load. Tilting the rotors (and the wing that supports them) requires bulky mechanisms and complex shafting, which detracts from the overall payload fraction. Though the proprotors offer better cruise efficiency than a rotor in edgewise flight, they are susceptible to whirl flutter and require thick wings for support.

4.3.6 Compound Helicopters

Lift- and thrust-compound and helicopters are well-suited for high speed cruise. However, this configuration would have a worse efficiency in hover because of the rotor wash over the wing. Additionally, a large wing is challenging to fit within the C-130J. Thrust-compound designs are ideal for high speed cruise, but this is not primarily a high-speed mission and there is little benefit to payload capacity by adding vertical propellers or ducted fans.

4.3.7 Distributed Electric Propulsion

Distributed Electric Propulsion (DEP) has seen a noticeable increase in popularity in recent years. DEP is appealing because it is much less complex than a traditional mechanical propulsion system; it is also an environmentally responsible form of aviation that relies on battery power, and therefore has no carbon-based emissions. A major challenge of DEP aircraft, however, is the availability of a battery with sufficient specific energy to provide the aircraft with both meaningful range and payload capacity. Recent designs such as the European Space Agency's Lilium Jet have batteries with low specific energies resulting in very low power loading [6].Since high payload capacity is a mission critical selection criterion, a DEP design was not selected for the given mission.

4.3.8 Tailsitter

The multirotor tailsitter is an attractive configuration because of superior control authority, small footprint, and unique flight capabilities. Multiple smaller-diameter rotors can facilitate the use of an electric transmission, which enables immediate response and a simple control scheme. Multiple rotors also provide multiple thrust vectors for precise control, steady hover, and gust tolerance. Like the tiltrotor, it is capable of hover but can transition into forward flight without auxiliary control surfaces, enabling a smoother flight profile, airplane-like range and speed, and extended mission capability. One disadvantage of the tailsitter configuration is that its smaller-diameter proprotors may not have the capability to autorotate in case of power loss in hovering flight. This problem is addressed by wings which enable gliding flight and provide control while maintaining a small footprint.

The tailsitter configuration ranked the highest in the final Pugh decision matrix because of its small footprint, heavy payload capacity, potential gliding ability, and rotor/motor redundancy in case of power failure in flight.

Wt.	Design Goal	SMR and AAD	Stopped Rotor	Variable Diameter	Thrust-Compound	Lift-Compound	Fan-in-Wing / Fan-in-Body	Tailsitter	Tiltrotor / Tiltwing
9	Deployability	0	2	-3	0	1	3	3	2
8	Payload Fraction	0	-2	-2	-1	-1	-3	-2	-2
6	Flight Safety	0	-1	-2	0	1	-3	-1	-1
5	Personnel Safety	0	0	-1	0	0	1	-2	-2
4	Technological Risk	-1	-1	-3	-1	-1	-1	-1	-1
2	Forward Flight	0	1	0	1	1	3	3	3
1	Cost	0	-2	-3	-1	-1	-3	-1	-2
	Total Weight	**-4**	**-8**	**-75**	**-11**	**4**	**-11**	**-4**	**-14**

TABLE 4.2: Preliminary Pugh decision matrix shows various vehicle configurations ranked against the weighted selection criteria.

4.4 Pugh Decision Matrix

The Pugh decision method was used to quantitatively rank potential vehicle configurations against the sorted set of selection criteria. Each vehicle configuration listed in Section 4.3 was compared against each of the selection criteria ranked by Table 4.1 and given a relative score. These results are presented in Table 4.2. Multiplying this score by the weights of the selection criteria and summing the scores provides a comparison of all rotorcraft configurations. Therefore, a higher total weight reflects a more optimal rotary-wing configuration.

Because the mission requires a precision hover, no pure fixed wing design was considered. Additionally, configurations that were dependent on the use of parachutes during deployment were not chosen. Parachutes are not overly compatible with non-shrouded rotors, and therefore present a threat to the flight safety of the aircraft. Furthermore, parachutes detached after deployment litter an already chaotic scene; though the used parachute could be retracted back into the aircraft if there were no threat of tangling with the rotors, the development of such a system would add an unnecessarily complicated mechanism and another potential failure mode. Parachutes also require trained personnel, or "riggers", to properly prepare the packs for the next deployment. To protect the payload, only configurations able to carry the full payload internally were considered. Slung loads expose the payload to a potentially dangerous weather environment and present some stabilization problems during ejection from the C-130J cargo hold.

4.5 Rotor Configuration

The top five vehicle configurations from the preliminary Pugh decision matrix were the AAD, lift-compound AAD, tailsitter, fan-in-body/fan-in-wing, and stopped rotor variations. These were put through a secondary configuration Pugh decision matrix to compare each vehicle configuration with various rotor layouts. Single rotor, coaxial rotors, tandem rotors (including fore-and-aft, side-by-side, and overlapping rotor configurations), and intermeshing (synchronous) rotors were considered for each vehicle configuration. The final Pugh decision matrix laid the following out for comparison, where each configuration is compared relative to one another using the SMR AAD as a baseline:

- Autorotative Aerodynamic Decelerator (AAD): SMR, coaxial, tandem, and synchronous rotors.
- Lift-compound AAD: SMR, coaxial, tandem, and intermeshing rotors.

- Stopped rotor: SMR, coaxial, and tandem rotors. Synchronous rotors considered too dangerous for high aerodynamic loads and sudden starts and stops.
- Fan-in-body/fan-in-wing: tandem. Tandem rotors considered necessary to provide balance and ample cargo space.
- Tailsitter: multirotor. Multiple rotors considered necessary to achieve adequate payload capacity.

FIGURE 4.3: (a) AAD (b) Lift-compound AAD (c) Stopped Rotor (d) Fan-in-body/Fan-in-wing, and (e) Tailsitter were chosen as the top five vehicle configurations.

In order to make these comparisons, all configurations are considered to be sized to fit within the C-130J cargo bay, and therefore each rotor is assumed to be as large as the width of the cargo bay allows. For example, a side-by-side tandem rotor layout would have smaller-diameter rotors than a fore-and-aft tandem rotor configuration, thereby limiting payload capacity for the same number of rotors. Coaxial systems would allow for two rotors equal in size to a SMR configuration, thereby increasing payload capacity by doubling rotor area within the same small footprint.

Coaxial, intermeshing, and overlapping rotors could present issues in deployment if the high impulsive aerodynamic loads cause the rotor blades to hit one another, and this risk must be taken into account when determining the best configuration for this mission. Increasing rotor rigidity by adding stronger, heavier materials is undesirable, as it results in a heavier aircraft.

Smaller, more rigid rotor blades are less likely to result in blade strike, whereas larger rotor configurations are more likely to flex into one another. Adding rigidity or additional support structure to prevent blade strike negatively affects the rotor weight and decreases the payload fraction.

Intermeshing rotors also do not allow for RPM control of the vehicle, and instead require a more complicated, control scheme involving collective and cyclic controls. Intermeshing rotors demonstrate decreased control authority because the swashplate controls are slow to respond.

Table 4.3 shows that compared with the baseline SMR AAD, the multirotor AAD systems are less desirable during the mission's deployment segment because the high flap angles that make an AAD excel in autorotation are likely to cause blade or fuselage strike. Alternatively, multiple rotors help to increase the vehicle's payload capacity and are preferable for fitting within the constraints of the C-130J interior. Flexible rotors, desirable in autorotation for decreased hub and blade loads, may not be as desirable in powered flight — synchropters, in particular, exhibit difficulty at high speeds if high loads case the blades lag. Multirotor AADs are untested technology, and therefore Table 4.3 reflects a lower TRL level and higher costs for development and testing. Single main rotor AAD prototypes have been built and tested, but there have been no full scale flights.

Lift-compound AADs are similiar to AADs with wings or wing-like structures that provide additional lift. The increased downwash over the wings in all rotor variants decreases the payload

TABLE 4.3: Secondary Pugh decision matrix shows various rotor layouts for each of the top vehicle configurations.

Wt.	Design Goal	AAD				Lift-Compound AAD				Stopped Rotor			Fan-in-Body / Fan-in-Wing	Tail Sitter
		SMR	Coax	Tandem	Sync	SMR	Coax	Tandem	Sync	SMR	Coax	Tandem	Tandem	Multirotor
9	Deployability	0	-2	-1	-3	1	-1	0	-2	2	-1	1	3	3
8	Payload Fraction	1	3	3	2	0	2	2	1	-2	-1	-1	-3	-1
6	Flight Safety	0	0	0	0	1	1	1	1	-2	-2	-2	3	3
5	Personnel Safety	0	0	0	0	0	0	0	0	0	0	0	1	-1
4	Technological Risk	0	-2	-1	-2	0	-2	-1	-2	1	-2	-2	2	3
2	Forward Flight	0	0	0	-1	1	1	1	0	2	1	2	3	3
1	Cost	0	-1	-1	-1	0	-1	-1	-1	-1	-2	-2	-3	-1
	Total Weight	**8**	**-3**	**10**	**-22**	**17**	**6**	**19**	**-13**	**-3**	**-37**	**-17**	**37**	**49**

capability in hover, and this is reflected in the table. Flight safety increases with the assumption that the wings are large enough to enable gliding flight, and likewise the lift-compound AAD variants have slightly increased forward flight performance and deployability. The cost and technological risk of implementing a simple wing structure is considered minimal, and therefore there is no difference in cost or TRL between AADs and lift-compound AADs.

Deployed with a stopped rotor that starts up after it leaves the C-130J, a stopped rotor vehicle is desirable for its ability to glide initially after launch and for its strong, rigid blades that can withstand high impulsive loads. Multiple rotor variants can be less efficient, since a coaxial rotor system can have 20% more hub drag than a single rotor. The inefficiency of elliptical airfoils, characteristic of stopped rotor designs, results in decreased payload fraction and poor autorotation capability. The low technology readiness level of these rotorcraft and high cost to develop and test make the stopped rotor, particularly the multirotor variants, a less feasible option despite its aptitude for deployment from the C-130J.

Only a tandem fan-in-wing and fan-in-body configuration is considered in this secondary decision matrix in order to account for internal payload carriage and balanced lift. The fan-in-wing design has enhanced deployability and performance in forward flight because its tiltable rotors shrouded within wings produce propulsive and lifting force simultaneously, and the ducted design fully protects the flight crew and ground personnel. The fan-in-wing/fan-in-body designs have a severely decreased payload capacity because of the lack of internal cargo space and downwash from the rotors on low-slung cargo. Current work on fan-in-wing/fan-in-body suggests a high cost to develop, but since similar prototypes have been successfully flown this configuration received a high TRL level score.

The multirotor tailsitter has the advantage of deploying in "airplane mode", which is also extremely advantageous for higher-speed and longer-range forward flight performance as well as gliding flight in the event of power failure. Exposed rotors near human height negatively impact the safety of flight and ground crews, and the necessary addition of a wing or lifting body negatively affects payload fraction in hover due to rotor downwash. The cost of such a vehicle is slightly less than a simple AAD because the tailsitter would have to be modified for air-launch and payload delivery; however, similar tailsitter designs have been designed and flown very successfully, and thus the tailsitter scores the highest in this decision matrix.

The results of this second Pugh matrix clearly showed the merits of the multirotor tailsitter, but a more detailed analysis was needed to choose the optimal multirotor configuration for this

FIGURE 4.4: Considered tailsitter configurations include a (a) standard quadrotor, (b) coaxial quadrotor, (c) angled quadrotor, and (d) overlapping quadrotor.

mission. A standard quadrotor was compared to a coaxial rotor system, an angled quadrotor design, and overlapping quadrotors (see Fig. 4.4) and run through a detailed sizing analysis for an aircraft that could carry 550 lb (250 kg) of payload, 10% more than the RFP requirement.

The sizing methodology described in Section 5 predicted the rotor radius, disk loading, and blade loading coefficient (i.e., stall margin) for each of the multirotor tailsitter variations. Though all aircraft were sized to carry 550 lb of payload, the overlapping quadrotor could fit 6 vehicles within the C-130J, one more than the angled quadrotor and two more than the coaxial and standard quadrotor configurations. The overlapping quadrotor was compared to an overlapping quadrotor biplane variant to assess the power requirements in the cruise part of the mission, which accounts for most of the vehicle's time in the air, and the result clearly shows the benefits of a biplane configuration for low-power cruise. Sized correctly, the wings are also useful for stabilizing the vehicle during its deployment phase. For these reasons, the overlapping quadrotor biplane tailsitter was selected as the optimal payload delivery vehicle for this mission.

5 Preliminary Vehicle Sizing

An alternative to conventional air-drop delivery, *Halcyon* was designed to be easily packed within a confined space, maintain a high stall margin during deployment, and perform an efficient hover during payload delivery. The vehicle's weight class, coupled with its control through differential RPM, imparts *Halcyon* with several unique systems not found on conventional rotorcraft. An in-house sizing algorithm based on the methodology of Tishchenko and the Army's Aero Flight Dynamics Directorate (AFDD) empty weight model was developed specifically to estimate the weight, geometry, and power requirements of a vehicle in the tailsitter configuration. Constraints were placed on the vehicle's radius and stall margin to comply with the vehicle's mission requirements. This section will describe the specifics of the sizing algorithm and present a set of trade studies that led to the selection of the vehicle's geometry.

5.1 Sizing Mission

The AFDD weight model determines the empty weight of a vehicle based on historical trends in the size and weight of small and large scale helicopters. Although this model, along with the Tishchenko sizing method, is well-validated over a wide range of weight classes, the majority of its data is based on the single main rotor configuration. Several modifications were made to better estimate *Halcyon's* weight and power requirements. The first step of vehicle sizing was to divide the mission profile, as specified in the RFP, into discrete mission segments. Figure 5.1 provides an overview of the four mission segments stated in the RFP: (1) deployment from a C-130J, (2) precision hover after achieving stable flight, (3) cruise 50 nautical miles to a known base, and (4) hover until landing.

Aside from the deployment stage, the power required for each mission segment can be reasonably estimated from modified momentum theory equations for a rotor in hover and axial flight, with

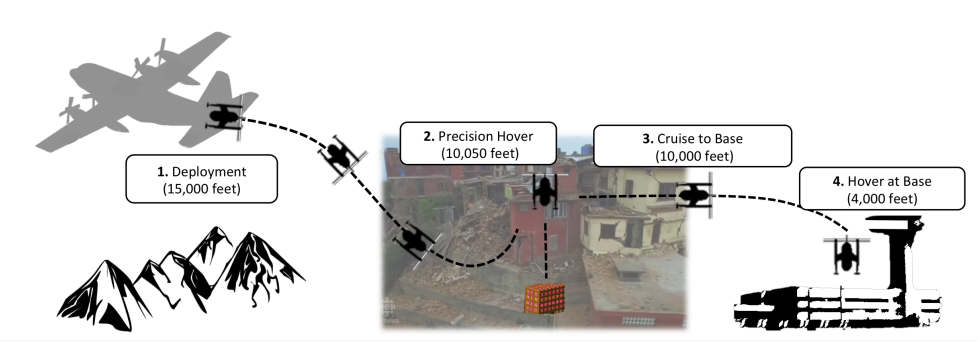

FIGURE 5.1: Mission profile detailing deployment from a C-130J, payload delivery, and return to base.

corrections for non-ideal flow effects and rotor interference. In deployment, the vehicle is constantly changing its orientation and the thrust condition of each of the four rotors. Due to the time-dependency of thrust, the power output during deployment is difficult to model without a detailed flight dynamics analysis. For this early stage of vehicle sizing, the rotor was assumed to never exceed more than 10% of the hover power, an assumption that is confirmed in Section 12.4. In place of a deployment model, initial sizing placed an emphasis on hover stall margin to ensure the rotors do not stall during deployment. The final sizing mission consists of only a hover at high altitude, a cruise at high altitude, and a second hover at low altitude.

5.2 Sizing Methodology

The *Halcyon* sizing algorithm is an iterative procedure based on the Tishchenko methodology for rotorcraft sizing [7]. Along with the RFP mission profile, the sizing method is initialized by a set of user-defined performance inputs, each of which form the basis for an estimation of the vehicle's gross takeoff weight (GTOW). Relevant vehicle component weights, including the airframe, rotor blades, and wings, are estimated from the AFDD component weight models, modified to reflect the tailsitter configuration. Component weights that do not apply to the tail-sitter configuration, such as a tail rotor or an articulated rotor hub, were eliminated from the sizing algorithm. The algorithm was outfitted to size a turbine-driven propulsion system, a battery-driven propulsion system, or a combination turbine-battery propulsion system.

An overview of the sizing procedure is summarized in Fig. 5.2 and more thoroughly described below:

1. The mission profile and initial vehicle data are treated as inputs. Initial vehicle data consists of geometric parameters and performance parameters. Geometric parameters include inputs related to the geometry of the rotor and wings, such as disk loading, blade aspect ratio, and wing aspect ratio. Performance parameters are related to the efficiency of the vehicle in hover and cruise, including figure of merit (FM), propulsive efficiency (η_P), the hover download factor, and the flat plate area. When sizing *Halcyon*, a low figure of merit, a low propulsive efficiency, and high flat plate area were assumed to over-estimate the vehicle's power installed and fuel weight. The flat plate area was estimated from the square cube law for helicopter flat plate area [8] .

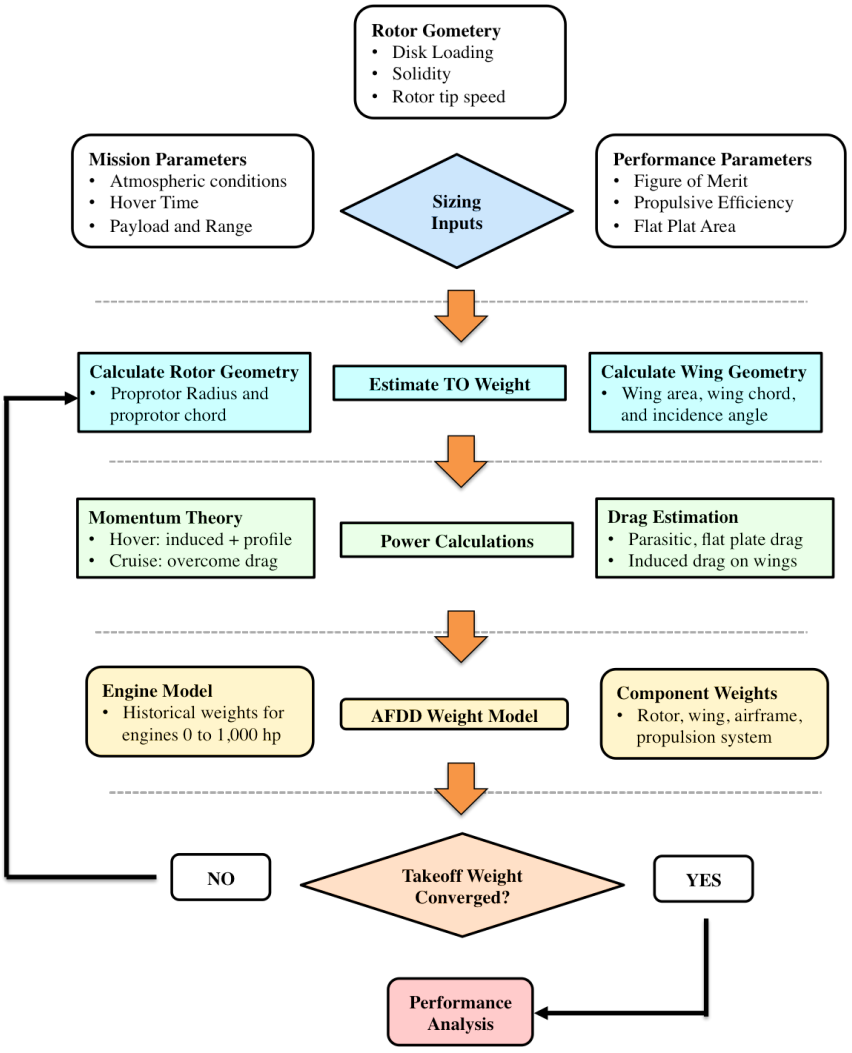

FIGURE 5.2: Summary of the methodology for initial vehicle sizing.

2. The takeoff weight is initialized to an initial condition based on a guess of the vehicle's size. The sizing algorithm is robust and converges to the same takeoff weight regardless of the initial condition.

3. The rotor disk size is calculated from the user-defined disk loading, takeoff weight, and hover downwash factor. The wing area is calculated from the user-defined wing aspect ratio, span constraints from the C-130J cargo bay, and an assumed wing maximum lift coefficient.

4. The power required in hover is calculated from basic momentum theory equations using the rotor geometry, assumed figure of merit, and assumed hover downwash factor.

5. The power required in cruise is calculated based on an estimation of the total vehicle drag. The vehicle drag is assumed to have three main components: parasitic drag from the fuselage, induced and profile drag from the wings, and drag arising from interference between the fuselage and wings.

6. The mission segment that requires the most power is used to calculate the total power installed. If a the vehicle is assumed to have a gas-powered propulsion system, the total

power installed is calculated from the engine lapse rate equations at altitude. If the vehicle is assumed to have an electric propulsion system, the power required simply becomes the power installed, and battery weight is calculated from an assumed specific energy.

7. Empty weight is calculated using the AFDD component weight models and a list of necessary on-board equipment.

8. Takeoff weight is calculated by summing the estimated empty weight, the assumed payload weight, and the fuel weight from each segment. If the takeoff weight is not within 0.1% of the initialized takeoff weight, the entire process is repeated until the GTOW reaches convergence.

The final output of the *Halcyon* sizing algorithm is the rotor disk geometry, the wing geometry, and an estimate for the vehicle GTOW. These initial values were used as a starting point for completing detailed component analysis of the wing design, the rotor blade design, and the propulsion system design. As component design became more detailed, the sizing algorithm was continuously updated to more accurately represent the vehicle's component weights.

5.3 Design Drivers

When designing *Halcyon*, constraints were placed on rotor, wing, and overall geometry to ensure compliance with the vehicle's mission requirements. The primary constraints are related to the vehicle's packing within the C-130J and the vehicle's stall margin during hover. The RFP specifies that the vehicle must fit within a 40 ft (length) x 119 in (width) x 9 ft (height) cargo bay, accounting for appropriate clearance in each direction. As a quad-rotor tail-sitter, *Halcyon* was designed with two sets of tandem, overlapping blades aligned along the width of the cargo bay. Therefore, two rotor diameters (with overlap) must fit comfortably within a width of 119 in (3.02 m). Section 3.4 found that within the C-130J cargo bay, the maximum allowable radius for a tandem, overlapping quadrotor is 3.40 ft (1.04 m). During sizing, any design that resulted in a radius greater than 3.4 ft was eliminated from consideration.

The second primary constraint is related to the vehicle's thrust in deployment. When developing the sizing mission, the deployment stage was neglected due to the difficulty of developing a flight dynamics model simultaneously with vehicle sizing. A constraint was placed on hover blade loading to ensure that if deployment was to require a higher thrust than hover, the rotor blades would not stall. A blade loading of 0.16 is typically associated with the onset of stall at outboard blade sections. For *Halcyon*, any design that produced a blade loading greater than 0.15, i.e. any stall margin less than 10%, was eliminated from consideration.

A final constraint was placed on the rotor disk loading. A high disk loading corresponds to a high downwash velocity in rotor wake, an especially difficult problem for tethered payload deliveries. A low disk loading, however, is associated with a small rotor radius, a feature that conflicts with *Halcyon's* tight packing constraint. Therefore, the vehicle's storage requires the upper limit on disk loading to be relatively high, with the understanding that disk loading should be kept as low as possible to minimize downwash. As a compromise, an upper limit of 16 lb/ft^2 (78 kg/m^2) was placed on the rotor disk loading.

Table 5.1 summarizes the primary design drivers for the present mission. Typical design drivers for a rotorcraft, including gross takeoff weight and power installed, were not constrained by the RFP and were considered secondary design drivers.

TABLE 5.1: Design constraints as taken from the mission profile.

Design Driver	Constraint	Mission Segment
Disk Loading	16 lb/ft^2	Hover
Rotor Radius	3.40 ft	Packing and Deployment
Blade Loading Coefficient	0.15	Hover

5.4 Trade Studies

The final geometric configuration for *Halcyon* was the result of an extended parametric study based on the sizing mission. The sizing algorithm determined the effect of disk loading, solidity, and tip speed on the rotor radius and blade loading coefficient. Final values for these parameters were chosen based on how well a given design fit within the constraints set by the RFP. The outcome of this section will be a set of vehicle geometries, including blade radius, solidity, and propulsion system type, to be used as guidelines for individual component design in later sections.

5.4.1 Selection of Disk Loading and Aspect Ratio

Rotor disk loading and aspect ratio each have a specific effects on blade radius and blade loading coefficient. A high disk loading is associated with a small rotor radius but a high downwash velocities. A low aspect ratio (i.e., a high solidity) is associated with a low blade loading coefficient but high profile power on the rotor blades. The final disk loading and aspect ratio were selected as a compromise between fitting within the storage constraints and performing efficiently in hover and cruise.

Figure 5.3 shows the effect of disk loading and blade aspect ratio on radius and blade loading coefficient. In this plot, horizontal lines represent a constant disk loading, and vertical lines represent a constant blade aspect ratio. Each black dot represents a single unique design point. The final disk loading and aspect ratio were chosen by applying the mission's design constraints to Fig. 5.3. Disk loadings lower than 12 lb/ft^2 (59 kg/m^2) are shown to produce a rotor radius that exceeds the packing constraint. Disk loadings greater than 12 lb/ft^2 reduce the effective radius but also require a lower blade aspect ratio to meet the blade loading constraint. Low blade aspect ratios increases the total power required to hover. To meet the design constraints and still operate efficiently in hover, a disk loading of 12 lb/ft^2 and a blade aspect ratio of 5 were selected for the *Halcyon*.

Note that the disk loading and blade aspect ratio were chosen assuming two blades on each of *Halcyon's* four rotors. Increasing the number of blades would lower the blade loading coefficient, a desirable property for *Halcyon*, but a high number of blades also complicates the vehicle's storage. With 3 or 4 blades per rotor, less than 6 vehicles are likely to be stored within the C-130J cargo bay. To maximize the number of total vehicles stored during one flight, *Halcyon* was limited to a maximum of two blades per rotor.

5.4.2 Selection of Hover Tip Speed

Hover tip speed strongly influences a rotor's blade loading coefficient. Figure 5.4(a) shows the variation in blade loading with tip speed under a fixed solidity and disk loading. As tip speed increases, the blade loading decreases, providing a better stall margin by decreasing the hover

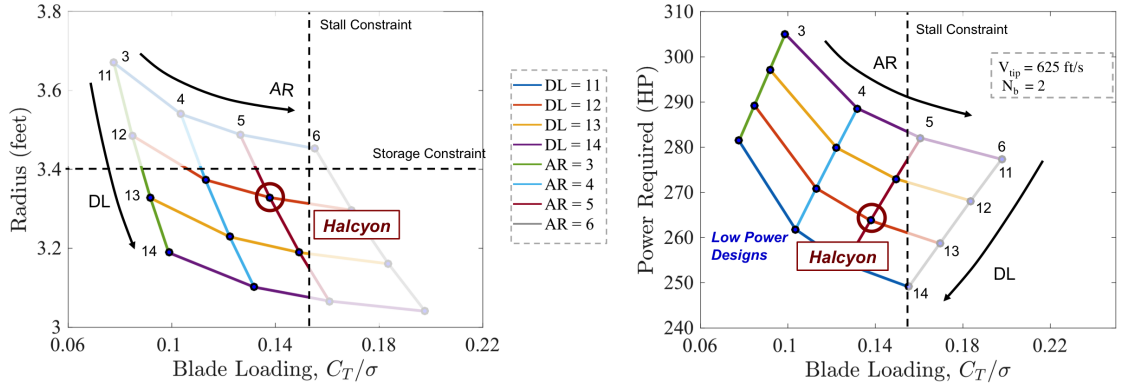

FIGURE 5.3: The impact of disk loading and aspect ratio on rotor radius, stall margin, and power required.

thrust coefficient. Higher tip speeds, however, are associated with higher power requirements and a high takeoff weight, as shown by Fig. 5.4(b). A hover tip speed of 625 ft/s (190 m/s) was selected to minimize the takeoff weight while still remaining well within the constraint on stall margin. This hover tip speed produces a blade loading coefficient of $C_T/\sigma = 0.138$ and a takeoff weight of 1,520 lb (690 kg). This design point was chosen as a compromise between sufficient blade loading and efficiency in hover and cruise.

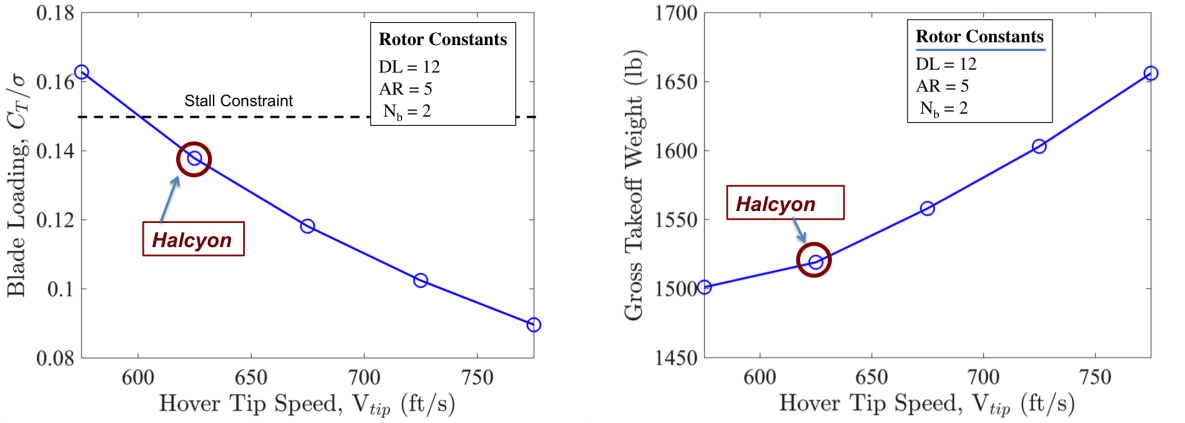

(a) Effect of hover tip speed on blade loading coefficient.

(b) Effect of hover tip speed on vehicle takeoff weight.

FIGURE 5.4: Selection of hover tip speed.

5.4.3 Selection of Wing Aspect Ratio

Halcyon's wings serve two primary functions: to stabilize the vehicle during deployment and to lift the vehicle's full weight during cruise. Both functions drive the wing toward a large surface area. In deployment, a larger wing area improves the vehicle's pitch stability, a concept discussed in detail in Section 12.4. In cruise, a larger wing area reduces the wing incidence angle required to lift the vehicle and, in turn, reduces the total wing drag. During initial sizing, emphasis was placed on maximizing the total wing area, with the understanding that increased wing area increases the overall vehicle weight. Section 3.4 found that a single wing is limited a maximum

wing span to 7.6 ft (2.3 m). As a way of maximizing wing area, all potential wing designs were assumed to have a wing span of 7.6 ft.

Figure 5.5(a) shows the variation in takeoff weight with wing aspect ratio. As the aspect ratio of the wing increases, the takeoff weight decreases, a result of the fixed wing span. When wing span is assumed to be constant, increasing the aspect ratio leads to a reduction in the total wing area, which reduces the weight of the wing and the total weight of the vehicle. Figure 5.5(b) shows the variation in expected wing incidence angle with wing aspect ratio. Again, an increase in aspect ratio corresponds to a decrease in wing area, which in this figure, amounts a loss in total lifting surface. With less lifting surface, the wings are required to cruise at a higher incidence angle to support the total vehicle weight, increasing the total wing drag. As a compromise between added weight and wing incidence angle, a wing aspect ratio of 1.6 was chosen for *Halcyon*. This low aspect ratio allows a large lifting surface to fit within the C-130J but is also associated with performance losses due to 3-D effects. A more detailed aerodynamic analysis of the wings is presented in Section 7.

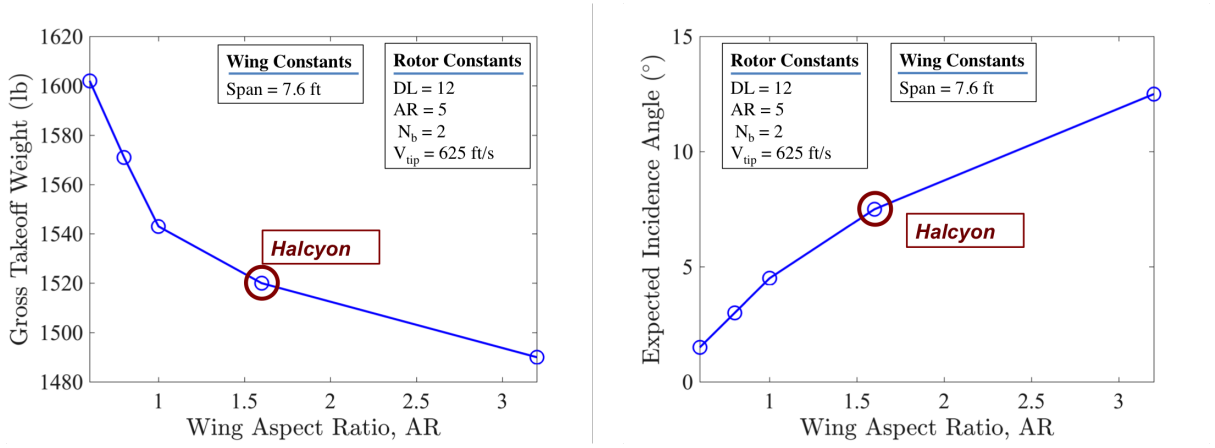

(a) Effect of wing aspect ratio on vehicle takeoff weight.

(b) Effect of wing aspect ratio on estimated incidence angle.

FIGURE 5.5: Selection of wing aspect ratio.

5.5 Propulsion System Sizing

A variety of propulsion systems, each with a different combination of power source and transmission, were considered to optimize *Halcyon's* energy output. One goal of the design was to promote overall system simplicity and maximize redundancy. Therefore, special attention was to finding an alternative to the complex mechanical transmission found on conventional rotorcraft. Although demonstrated on helicopters of all sizes, mechanical transmissions have a large number of moving parts and require frequent maintenance. *Halcyon's* final propulsion system design features a turboshaft engine, an electric generator, and an electric transmission. This section will detail the methodology for choosing the propulsion system configuration.

Four types of propulsion system were considered for *Halcyon*, each representing a different method of power generation and vehicle control. The four options are illustrated in Fig. 5.6 and summarized in the table below:

- A "full mechanical" propulsion system consists of a gas-powered turboshaft engine and a series of connecting gears. Vehicle control is achieved by implementing variable collective

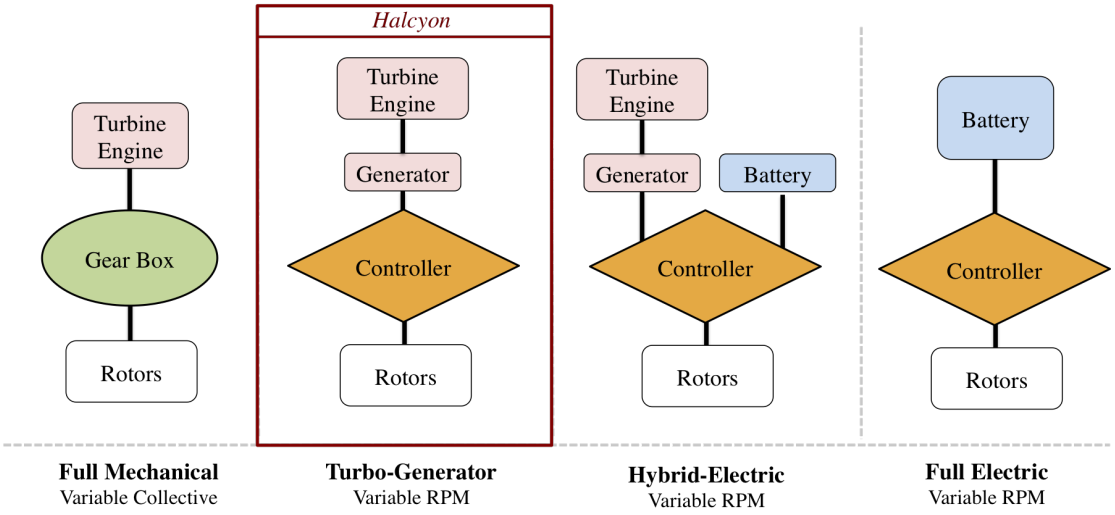

FIGURE 5.6: Conceptual sketches of a full mechanical, turbo-generator, hybrid-electric, and full electric propulsion system.

pitch on each rotor. Although a proven system, the full mechanical option suffers from high maintenance and a large number of moving parts.

- A "turbo-generator" consists of a turboshaft engine that powers an electric generator. The generator is connected to an electrical transmission, and four variable torque motors control the vehicle through differential thrust. By eliminating a gearbox, the turbo-generator is a mechanically simpler system but suffers from the additional weight of its generator and motors.

- A "hybrid-electric" propulsion system consists of both a turboshaft engine and a battery. Like the turbo-generator option, the two power sources connect to an electric generator and an electric transmission. By offloading the power required of the turboshaft, a hybrid electric system reduces the weight of the turbine at the expense of adding battery weight. An ideal hybrid-electric system reduces more weight than it gains.

- A "full electric" propulsion system is powered by a single large battery. The battery connects directly to the controllers and stability is achieved through differential RPM. The advantages of a full electric system include the elimination of all mechanical components and a non-existent carbon footprint; however, full electric systems require a very heavy battery to meet the energy demands of a 50 nautical mile cruise.

To compare the four candidate propulsion systems to compare the effect of each propulsion system on *Halcyon's* takeoff weight. When sizing the turbine, a weight model was developed to size the engine based on five commercial turboshafts in the 250 hp – 500 hp weight class. When sizing the batteries in the hybrid-electric and full electric options, the total battery was was calculated using a value for specific energy based on a survey of commercially available high-energy batteries. The battery in the hybrid-electric option was sized to provide half the total power during hover, such that it served as a midway point between the full mechanical and the full electric options.

Table 5.2 shows the results of the propulsion system weight analysis. The full electric option was eliminated because of the excessive weight required to power the vehicle. By having a

TABLE 5.2: Weight comparison of the four candidate propulsion systems.

	Full Mechanical	**Turbo-Generator**	**Hybrid-Electric**	**Full Electric**
Takeoff Weight	1460 lbs	1520 lbs	1630 lbs	2289 lbs
Battery Weight	0	0	78.6 lbs	942 lbs
Turbine Weight	162.9 lbs	164.7 lbs	155.3 lbs	0
Battery Power	0	0	143.5 hp	402 hp
Turbine Power	452.0 hp	480.0 hp	307.0 hp	0

battery as its only source of power, the full electric option requires a battery to supply power throughout the vehicle's entire 50 nautical mile cruise, leading to an overly heavy battery. The hybrid-electric option was eliminated based on a comparison with the turbo-generator. Both of these options have the same transmission and control method, but the hybrid-electric option adds an additional 100 lb (45 kg) to the takeoff weight, despite its turbine having half the power output of the turbo-generator option. This is a result of the engine weight model used in the present analysis, reproduced in Fig. 5.7. Based on this historical data, the weight of a turbine engine varies very little between an output of 300 hp (hybrid-electric option) and 500 hp (the turbo-generator option). By including a battery and reducing the power of the turbine, the hybrid-electric option adds battery weight without subtracting significant turbine weight.

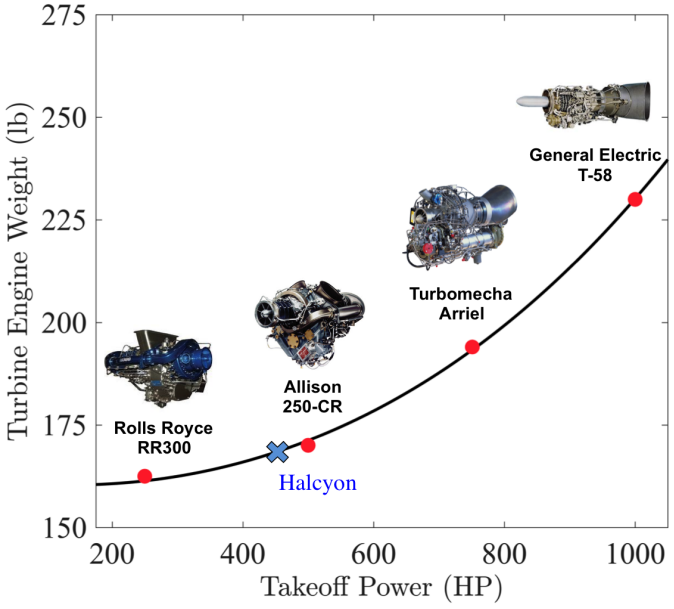

FIGURE 5.7: Turbine engine sizing model based on commercial turboshafts.

The final two options were the turbo-generator option and the full mechanical propulsion system. The final selection was based on overall system complexity. A full mechanical option minimizes the vehicle's takeoff weight at the expense of high maintenance and high number of redundancies. The turbo-generator option boasts an easily maintained electric transmission at the expense of only 60 pounds of additional vehicle weight. The turbo-generator option was chosen to emphasize system simplicity and maintainability.

5.6 Results of Preliminary Sizing

Table 5.3 shows the rotor and wing parameters produced by initial vehicle sizing. These parameters are frozen during individual component design of the vehicle's rotor blades, wings, propulsion system, and airframe structure.

TABLE 5.3: Result of preliminary sizing analysis.

Parameter	**Value (English)**	**Value (Metric)**
Takeoff Weight	1,519 lb	690 kg
Empty Weight Fraction	0.60	–
Payload Fraction	0.33	–
Fuel Weight Fraction	0.07	–
Disk Loading, DL	12 lb/ft^2	59 kg/m^2
Power Loading, PL	7.4 lb/hp	4.5 kg/kW
Blade Loading, C_T/σ	0.138	–
Blade Radius	3.32 ft	1.01 m
Blade Aspect Ratio	5	–
Thrust Weighted Solidity, σ_e	0.115	–
Hover Tip Speed	625 ft/s	190 m/s
Power Installed	480 hp	360 kW
Number of Blades	2	–
Number of Wings	2	–
Wing Aspect Ratio	1.6	–
Wing Span	7.6 ft	2.3 m
Wing Area, s_{wing}	36.1 ft^2	3.4 m^2

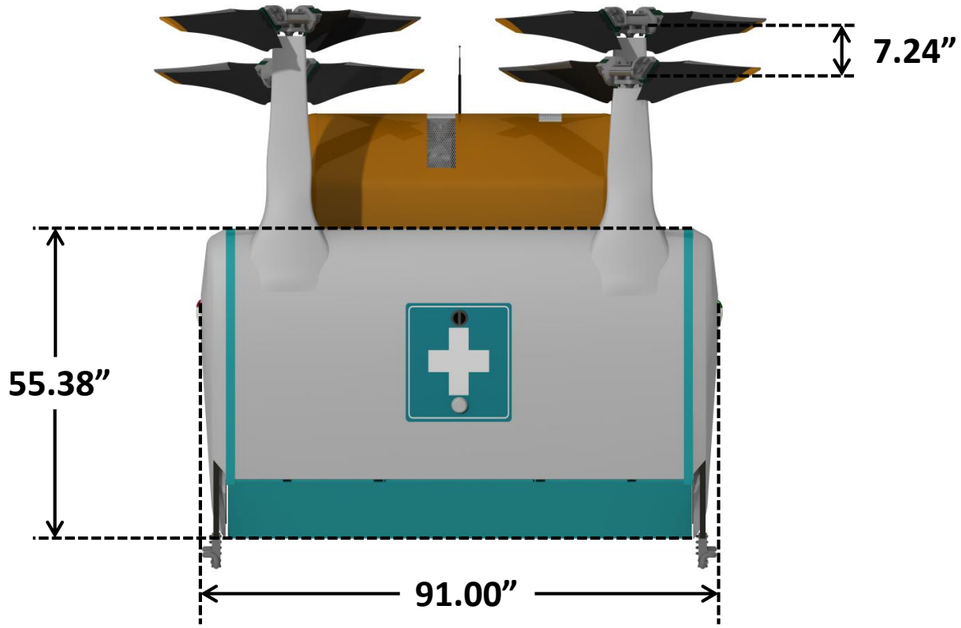

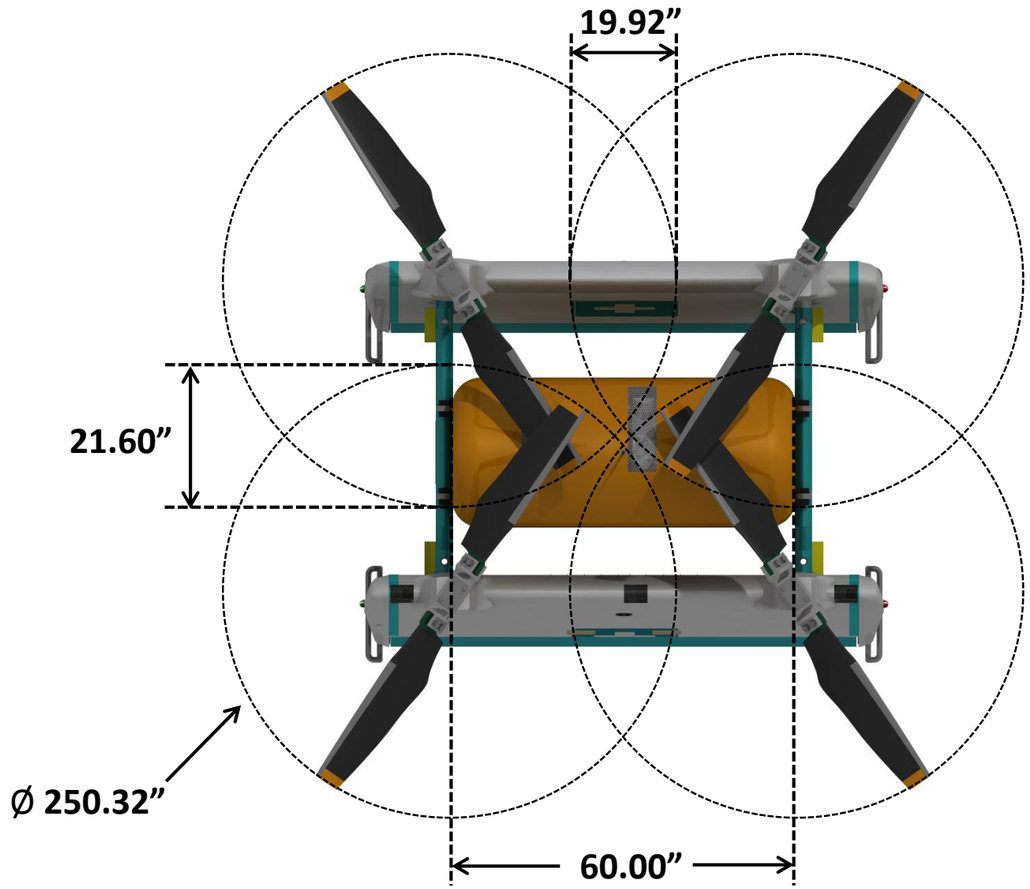

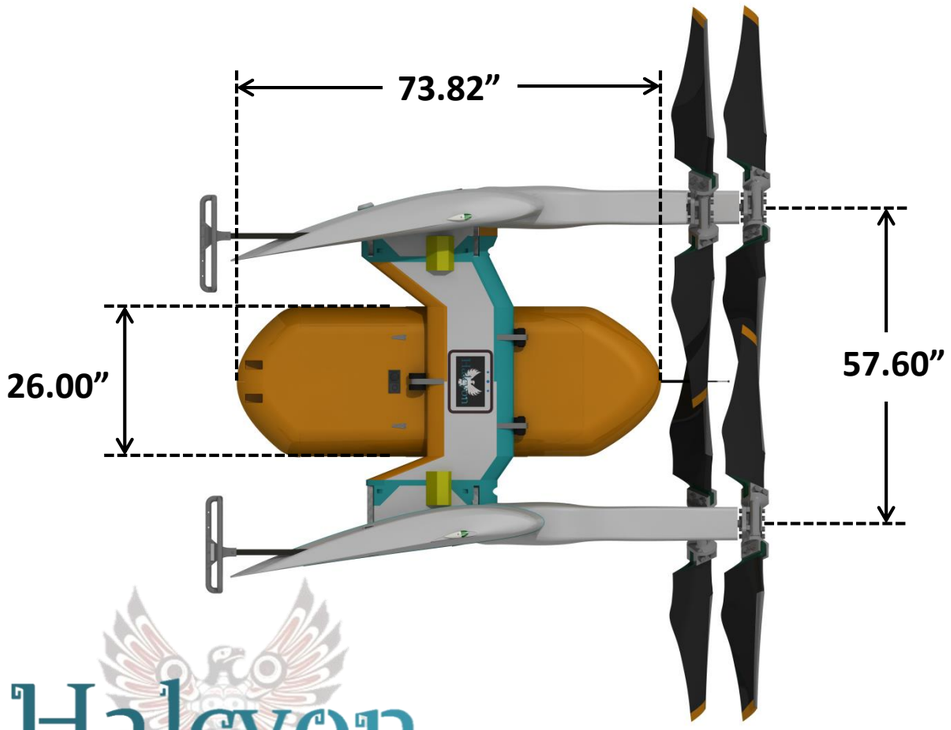

Weight	GTOW	1519 lb (690 kg)	Rotor & Power	Disk Loading	12 lb/ft^2 (59 kg/m^2)
	Payload Weight	508 lb (231 kg)		c_T/σ	0.138
	Empty Weight Fraction	0.60		Power Loading	7.4 lb/hp (4.5 kg/kW)
	Payload Fraction	0.33		Radius	3.32 ft (1.01 m)
	Fuel Weight Fraction	0.07		Hover Tip Speed	625 ft/s (190 m/s)
Wing	Wing Area	36.1 ft^2 (3.4 m^2)		Cruise Tip Speed	713 ft/s (217 m/s)
	Wing Aspect Ratio	1.6		Installed Power	480 hp (360 kW)

Halcyon

UNIVERSITY OF MARYLAND

6 Proprotor Design

The *Halcyon* disaster relief vehicle is designed for three flight modes: hover, cruise, and deployment. Each flight mode represents a drastically different set of aerodynamic and structural design challenges. Aerodynamically, since *Halcyon* hovers as a rotor but cruises as a propeller, the vehicle is required to operate efficiently in both hover and axial flight, despite the dissimilar design drivers associated with each flight mode. Proprotor geometry, including blade twist, taper, and collective angle, must be chosen to bridge the gap between an optimum hovering rotor and an optimum propeller. Structurally, the vehicle is required to withstand the unsteady aerodynamic loads imposed during deployment in addition to aerodynamic, inertial, and vibratory loads during hover and cruise. Since *Halcyon* is controlled by differential RPM, the proprotors operate over a wide range of rotational speeds and experience a wide range of vibration frequencies. This section will describe the complete methodology for selecting a blade geometry and structural design, noting how proprotor design affects vehicle performance in each flight mode.

6.1 Proprotor Aerodynamic Design

Halcyon operates either as a helicopter in hover or a propeller in axial flight. Therefore, the aerodynamic design of *Halcyon's* proprotors was driven by the geometric differences between an optimum hovering rotor and an optimum propeller. The optimum twist distribution of a hovering rotor (one that is not required to perform in forward flight) is hyperbolic, even though a typical helicopter blade features a moderate linear twist to operate in forward flight [8]. The optimal twist distribution of a propeller is also hyperbolic, but a propeller operates under very different inflow conditions compared to a hovering rotor. On one hand, a rotor in hover operates at a high thrust condition and a small total inflow compared to a propeller in axial flight. On the other hand, a propeller in axial flight operates at a very high inflow at the rotor plane, requiring a high collective angle, but with a low thrust condition compared to hover. Consequently, an ideal proprotor design represents a compromise between the twist distribution of an optimum hovering rotor and the twist distribution of a propeller.

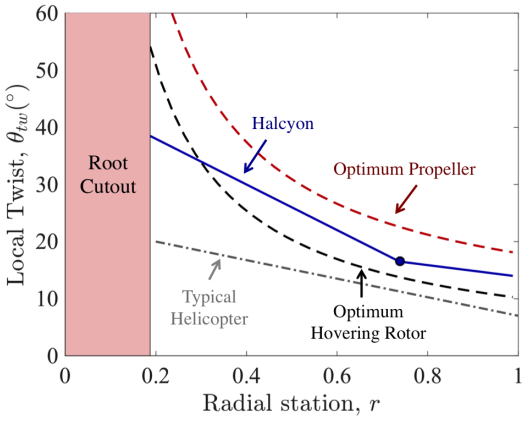

(a) *Halcyon* compared to the optimum propeller and hovering rotor

***Halcyon* Proprotor Design**		
Inboard Twist	12°/ft	39.4°/m
Outboard Twist	3°/ft	9.8°/m
Twist Junction	0.75	
Collective (Fixed)	40°	
Taper Ratio	3:1	
Hover RPM	1,800 RPM	
Cruise RPM	1,950 RPM	
Figure of Merit	0.79	
Propulsive Efficiency	0.68	

(b) *Halcyon*'s proprotor geometry

FIGURE 6.1: Overview of *Halcyon* proprotor design.

Halcyon's proprotor blades approximate hyperbolic twist with a bilinear twist distribution and a fixed collective angle. As a summary of the aerodynamic proprotor design, Fig. 6.1(a) shows *Halcyon's* blade twist distribution compared to an optimum hovering rotor and an optimum propeller. Figure 6.1(b) details the vehicle's exact proprotor geometry. The bilinear twist distribution is tuned to favor the optimum hovering rotor as a way of minimizing the vehicle's total installed power (see Section 5.1), while a fixed collective angle was chosen to minimize the system's complexity. The remainder of this section presents a detailed methodology for determining the proprotor geometry presented in Fig. 6.1(b) and quantifies the performance of this design in hover and axial flight.

6.2 Performance Metrics

For *Halcyon*, the ideal proprotor will achieve three design goals: efficiency in hover, efficiency in forward flight, and sufficient hover stall margin to ensure unstalled blades throughout all flight modes. The current analysis employs the Figure of Merit (FM), defined in Equation 6.1, to measure hover performance, and the propulsive efficiency, defined in Equation 6.2, to measure forward-flight performance. Blade loading coefficient is used to track the stall margin of a given blade design. Since blade loading depends on tip speed, the blade loading coefficient varies with RPM and is highly coupled with the aerodynamic blade design.

$$\text{FM} = \frac{P_{ideal}}{P_{actual}} = \frac{C_T^{3/2}/\sqrt{2}}{C_P} \tag{6.1}$$

$$\eta_P = \frac{C_T \mu}{C_P} \tag{6.2}$$

A benchmark for each performance parameter was determined from *Halcyon's* mission requirements. Initial sizing found that the vehicle's power installed and takeoff weight are driven by the efficiency of the hover segment. To minimize the vehicle's total power installed, a relatively high threshold of FM ≤ 0.725 was set for hover efficiency. The vehicle was designed with an understanding that a fixed collective proprotor achieves a high FM at the expense of reduced propulsive efficiency. As a way of favoring hover efficiency over cruise efficiency and in turn lowering the total installed power, a relatively low threshold of $\eta_P > 0.60$ was set for cruise performance. Finally, Section 9.1 shows that for a $C_T/\sigma < 0.138$, *Halcyon* can increase its hover thrust by 7% of the takeoff weight without encountering rotor stall. The blade loading coefficient was required to remain below a threshold of $C_T/\sigma < 0.138$ to maintain this stall margin in hover.

6.3 Methodology

The *Halcyon* proprotor design was parameterized by an a bilinear twist rate, a linear taper ratio, a fixed collective angle, and an airfoil cross-section shape. These proprotor design parameters were varied while the takeoff weight, rotor radius, and rotor solidity are held constant. The goal of blade design is to determine the optimal combination of parameters that minimize the system's complexity while meeting the hover and cruise performance benchmarks. An in-house analysis tool based on blade element momentum theory (BEMT) was developed specifically to determine the performance of each blade geometry in hover and axial flight. The BEMT solver, which has been validated on a variety of rotor and propeller designs, accounts for large angles of

attack in axial flight (no small angle approximation) and targets a given thrust through RPM variation [9].

The steps for choosing a blade design are described in Fig. 6.2, and the remainder of this section will describe the methodology used in each step.

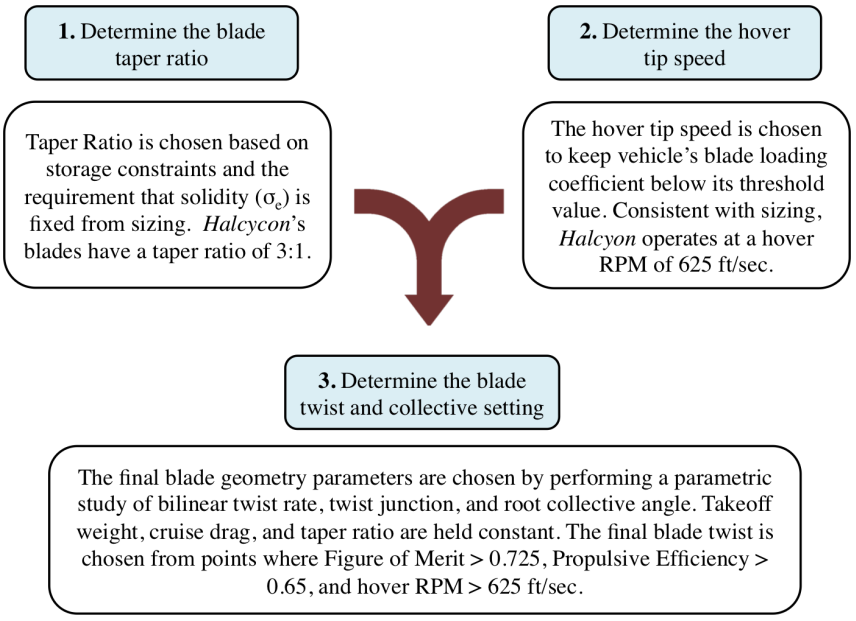

FIGURE 6.2: Step-by-step methodology for determining rotor blade geometry and operating RPM.

6.4 Blade twist and collective

Historically, blade twist has been shown to have a dominant impact on the hover and cruise performance of a proprotor, whereas taper ratio and rotor solidity have only a secondary effect. The first step of proprotor design is to define a blade twist profile, including the blade's inboard twist, outboard twist, twist junction, and collective angle. An extensive parametric study, wherein each blade twist parameter was varied independently, was performed at a constant taper ratio and rotor solidity. Inboard and outboard twist rates were varied from 15°/ft to 5°/foot, and bilinear twist junction was varied from 25% blade span to 75% blade span. The collective angle was varied from a low setting of 35° to a high setting of 55°. This sweep resulted in 1,100 blade twist profiles each tested across five different airfoil cross sections, for a total of 5,500 total independent blade designs.

Figure 6.3 shows the outcome of the blade twist parametric sweep. In this figure, hover performance, denoted by FM, is plotted on the abscissa, and the forward-flight performance, denoted by η_P, is plotted on the ordinate. The orange lines represent the benchmark values set for Figure of Merit (FM ≤ 0.725) and propeller efficiency ($\eta_P \geq 0.60$). Each marker represents a different combination of bilinear twist rate, twist junction, and collective angle. Each color corresponds to a different blade loading coefficient. Five airfoils, each of varying camber, were considered but only two, the NACA 0012 and NACA 2412, are shown here for simplicity. The NACA 2412 produced the most ideal combination of FM and η_P, while the NACA 0012 produced the least ideal. The remaining three airfoils performed somewhere within these two bounds.

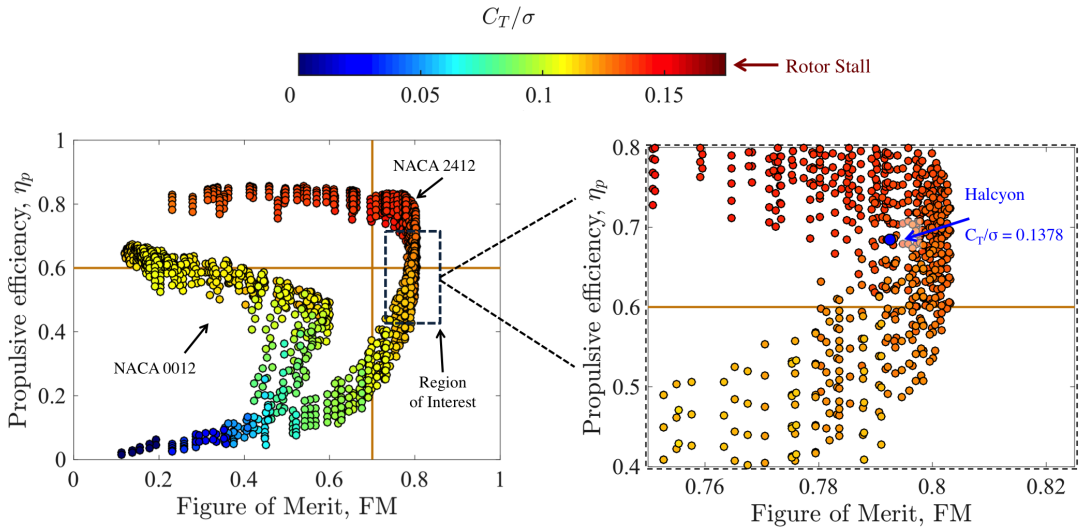

FIGURE 6.3: Hover and propulsive efficiency for two of the five proprotor airfoils considered. Dark red contours correspond to rotor stall.

The region of interest for *Halcyon* is outlined by the dotted black line in Fig. 6.3. Here, the FM is high at the expense of a relatively low η_P. If the propulsive efficiency is increased in this region, C_T/σ exceeds its threshold value and the blades approach rotor stall in hover. This parametric study reflects the challenge of designing a fixed-collective proprotor: designs that achieve high FM and η_P can only be achieved when hovering near rotor stall. The design point for *Halcyon* is marked by the dark blue dot in the enlarged region of interest. The vehicle's proprotors operate at a FM of 0.79 and a propulsive efficiency of 0.68. This point represents the maximum hover and forward flight efficiency that can be achieved in a fixed collective system without approaching rotor stall. Section 6.6 will show that the vehicle's relatively low propulsive efficiency only results in a fuel gain of 10 lb (4.5 kg) compared to a vehicle with high propulsive efficiency.

6.5 Blade Taper Ratio

Having chosen a blade twist, the next step in proprotor design is to choose a blade chord profile. Like blade twist, optimal performance in hover and axial flight is achieved with a hyperbolic distribution of blade chord, often approximated as a bilinear taper. However, historical data suggests that a chord distribution has only secondary effect on vehicle performance. Because complicated chord distributions produce minimal gains in performance, only a linear taper was considered for *Halcyon*. A short parametric study was performed on linear blade twist at constant thrust weighted solidity and blade twist. In this study, an increase in root-to-tip taper ratio from 1:1 to 4:1 resulted in only a 4% increase in Figure of Merit and a 2% increase in propulsive efficiency, a small change in performance.

Since its effects on vehicle performance are minimal, taper ratio was chosen to maximize thrust-weighted solidity and stall margin. In Section 3.4, the tight packing of *Halcyon* limits the tip chord to 0.4 ft (0.12 m). With this constraint, the blades require a root-to-tip taper ratio of 3:1 to to achieve the the thrust-weighted solidity determined in initial sizing. This taper ratio was

chosen for *Halcyon's* proprotors. The final design was modified slightly in the inboard sections to account for blade grips and dynamic tuning (see Section 6.7).

6.6 Effect on Vehicle Efficiency

Halcyon's proprotors were designed to achieve maximum performance in hover and cruise while maintaining an adequate stall margin. The final step of proprotor aerodynamic design is to confirm that each of these goals have been met. For the final blade geometry, the vehicle's performance in hover and cruise segments were considered separately. If the vehicle was found to stall during hover, or if the vehicle's cruise segment was found to require excessive fuel, the design was eliminated and a different blade twist was chosen from Fig. 6.3.

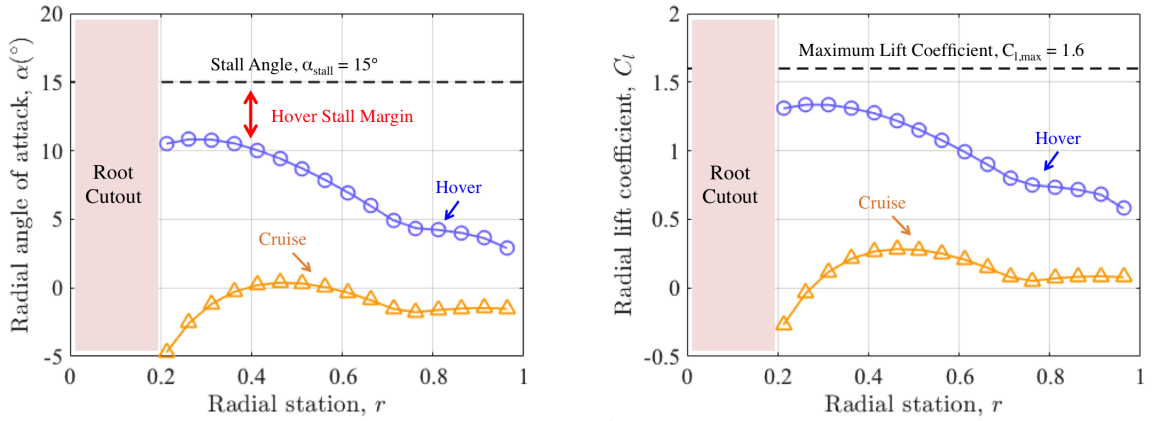

(a) Spanwise distribution of angle of attack on during hover and cruise

(b) Spanwise distribution of sectional lift coefficient during hover and cruise

FIGURE 6.4: Illustration of *Halcyon's* stall margin in hover and cruise

In hover, *Halcyon's* blade twist profile produces a very high FM of 0.79, the result of the very high operating thrust condition. Although C_T/σ provides a reasonable estimate for the hover stall margin, *Halcyon's* high hover thrust condition requires a more detailed analysis of the rotor's stall characteristics. Figure 6.4(a) shows the final spanwise distribution of angle of attack (α), and Fig. 6.4(b) shows the final spanwise distribution of lift coefficient. These figures show that the blade approaches $\alpha = 10°$ at some outboard sections of the blade, an angle near stall for many thin airfoils. A NACA -2412 airfoil was chosen for *Halcyon's* rotors because its high stall angle remains relatively unchanged across several Reynolds numbers. Based on the NACA 2412 stall angle of of attack, *Halcyon* can vary its α by up to 5° without encountering rotor stall.

In cruise, *Halcyon's* blade twist profile produces a propulsive efficiency of 0.68, a value lower than the typical propulsive efficiency of a fixed wing propeller ($0.8 < \eta_P < 0.9$). The consequence of a low propulsive efficiency is an increase in power during cruise and an increase in the vehicle's total fuel. To justify the selection of a low propeller efficiency, the fuel required by *Halcyon* was compared to a vehicle with high propulsive efficiency.

A fuel-savings analysis was completed to compare *Halcyon*, with its fixed collective angle, to a vehicle of the same takeoff weight and a variable collective angle. Variable collective proprotors have been shown to exhibit a high propulsive efficiency, a high Figure of Merit, and a high stall margin, but at the expense of increased system complexity [9]. Table 6.1 summarizes the

comparison between a fixed collective system and a variable collective system for a 50 nautical mile cruise at 70 knots. The total power required was calculated using the in-house BEMT solver, and cruise fuel required to cruise was calculated assumed a specific fuel consumption (SFC) of 0.60 lb/hp/hr, consistent with the SFC analysis in Section 10.3. Table 6.1 shows that a fixed collective system requires 47 lb (21 kg) of fuel to complete a 50 nautical mile cruise, while a variable collective system requires 36 lb (16 kg) of fuel to complete a 50 nautical mile cruise. By having only one fixed collective angle, *Halcyon* boasts a very simple proprotor system with only a 10 lb fuel weight penalty. The minimal fuel weight penalty was deemed to be worth the cost of avoiding a complex variable collective system.

TABLE 6.1: Comparison of *Halcyon* to a vehicle with variable pitch higher propulsive efficiency.

	Variable Collective Pitch	**Fixed Collective Pitch**
FM	0.79	0.79
η_P	0.86	0.68
Hover Collective	40°	40°
Cruise Collective	58°	40°
Cruise Power	71 hp (53 kW)	92 hp (69 kW)
Cruise Fuel	**36.2 lb**	**46.9 lb**

In summary, the *Halcyon* proprotor geometry consists of a bilinear twist, a 3:1 root-to-tip taper ratio, and a fixed collective angle of 40°. The vehicle efficiently hovers at a Figure of Merit of 0.79, and incorporates a 5° stall margin at its maximum thrust condition. The vehicle's propeller efficiency, although somewhat lower than typical propeller designs, completes the mission 50 nautical mile cruise at low power and with minimal fuel weight penalty. The *Halcyon* proprotor blades boasts a simple, highly efficient aerodynamic design without the need for variable collective pitch.

6.7 Structural Design

Figure 6.5 shows the top view of the rotor system. The 20% radius root cutout section consists of a titanium hub and the blade grip. The blade geometry from 20% to 40% span was designed to tailor the first flap frequency of the blade to between 1.3/rev and 1.7/rev at the operating rotor speeds. This section has little impact on the blade's aerodynamic properties due to the relatively small dynamic pressure at the inboard section of the blade. From 40% span to the tip, the blade has a 3:1 taper ratio (from root to tip). The total weight of each blade is 1.07 lb (0.49 kg).

A cross sectional view of the internal blade structure is shown in Fig. 6.6. The selection of composite materials in the spar allows the blade to resist the high flap and lag moments experienced after deployment from the C-130J. The blade was wrapped in layers of ±45 ° S-glass with epoxy to form the skin to maintain the aerodynamic shape and provide torsional stiffness. A D-spar spanning from 2% chord to 35% chord is constructed from plies of ±45 ° S-glass with epoxy to add flap and lag stiffness at the root of the blade. Rohacell 75 foam was chosen as the filler material for the mandrel and the trailing edge section to preserve the shape of the blade cross section. Care was taken to ensure that the elastic axis of the blade was located at the quarter-chord. Unidirectional fiberglass block reinforces the trailing edge and adds incremental

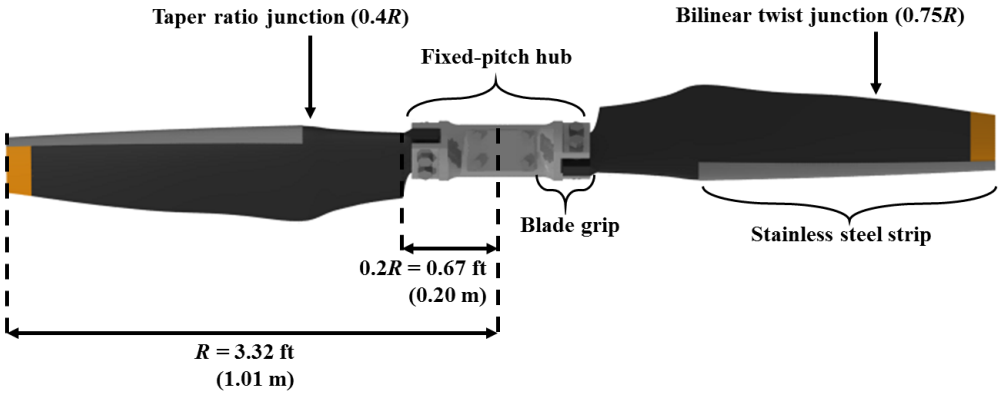

FIGURE 6.5: Top view of the rotor blades.

flap and lag stiffness. The center of gravity was aligned with the elastic axis at the quarter-chord by tungsten leading edge masses. A thin copper mesh provides electric bonding to protect the blade from lightning strike. A stainless steel strip on leading edge protects the blade from abrasion and erosion.

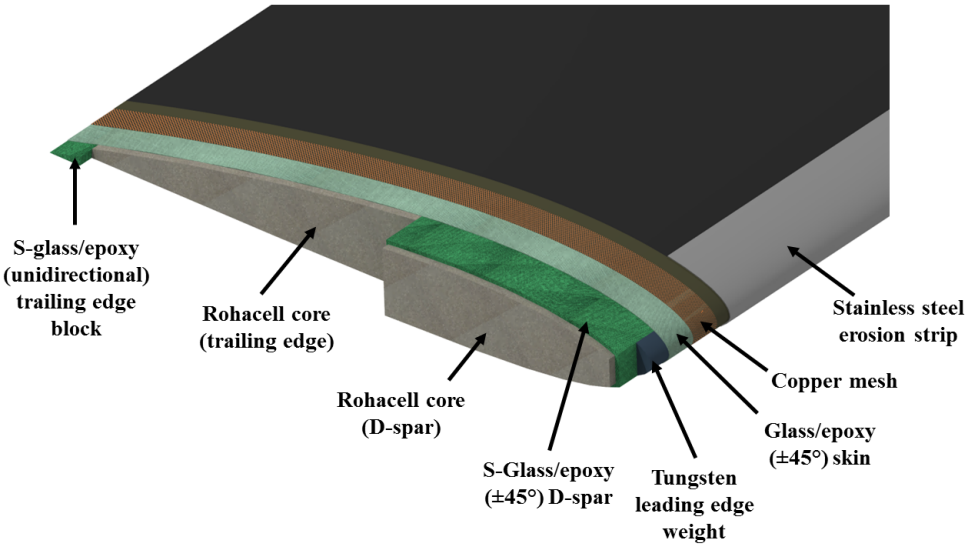

FIGURE 6.6: Cutaway view of the internal blade structure.

6.8 Rotor Blade Cross Sectional Properties

The flexural stiffness and mass per unit span were determined using cross sectional analysis. Parametric studies of the root flap and lag stresses, blade mass, and modal frequencies were conducted to determine optimal values for the spar width, spar thickness, web thickness, skin thickness, and leading edge mass. The flap and lag stiffness at the root were chosen to ensure the stresses experienced in the deployment and startup phases do not exceed the allowable limits on the spar. Properties along the blade were then manipulated to tune the modal frequencies.

The non-dimensional mass and stiffness distributions along the elastic axis of the blade are shown in Fig. 6.7. The mass and stiffness distributions of the blade grip place the effective cantilever point of the blade at the 20% radius root cutout. The stiffness and mass per unit length vary at outboard locations because of variation in chord. A tungsten tuning mass was added at the quarter-chord between 61% and 64 % span to reduce the second flap frequency of the blade. This effectively targets the location of maximum deflection in the second flap mode to reduce excitation.

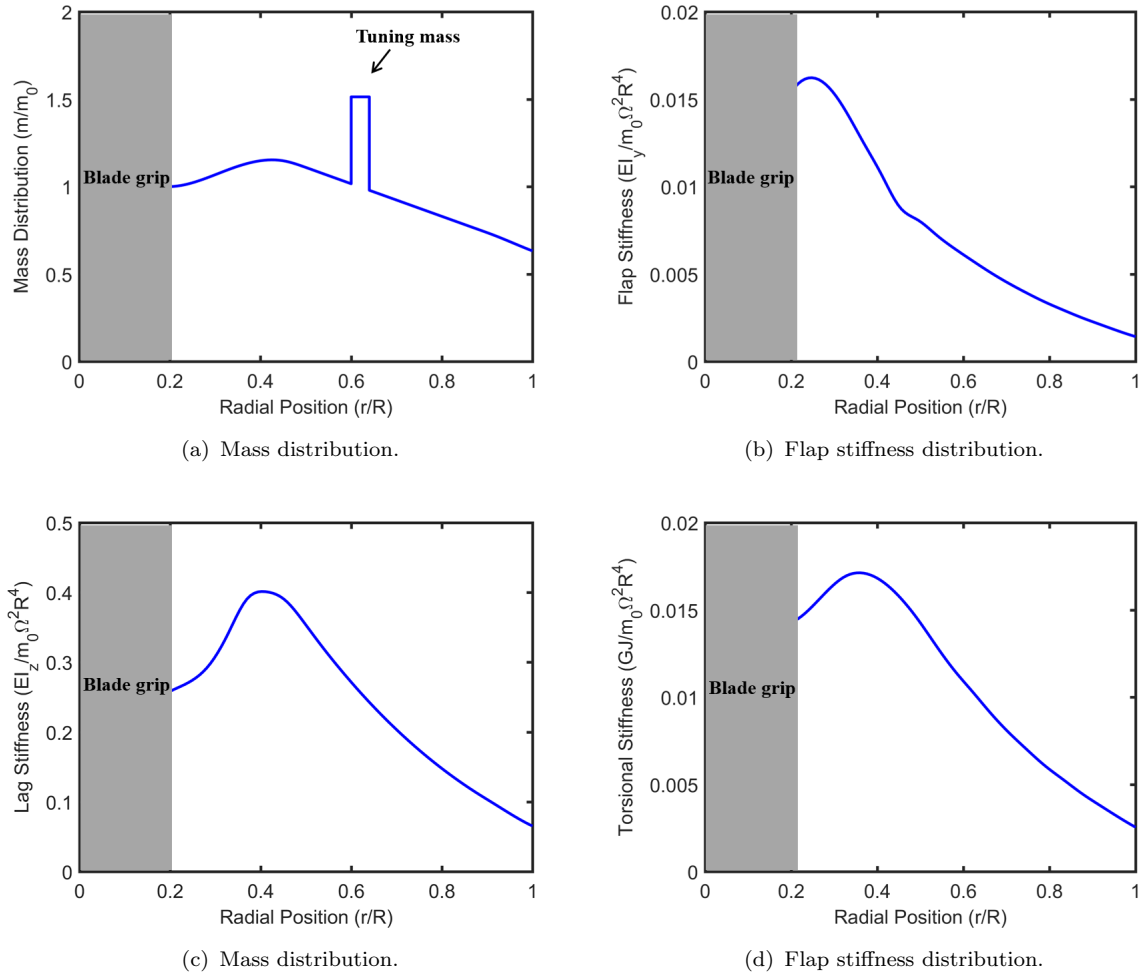

(a) Mass distribution.

(b) Flap stiffness distribution.

(c) Mass distribution.

(d) Flap stiffness distribution.

FIGURE 6.7: Spanwise mass and stiffness distributions.

Based on the given cross sectional properties of the blade, natural modes of the blades were calculated using the University of Maryland Advanced Rotor Code (UMARC). Figure 6.8 shows the fan plots for the vehicle's operational rotor speeds with and without the payload, respectively. The blade has an equivalent hinge offset of 29%. The fan plots show that the first, second, and third flap modes will not excite the 1−10/rev harmonics at any of the operating RPMs of the rotor. Blade twist between the root and tip induces coupling between the flap and lag modes. Similar to typical propeller blades, high lag stiffness contributes to high first lag frequencies at each operational rotor speed (larger than 10/rev at all RPMs considered). The first flap, lag and torsional frequencies at each rotor speed are shown in Table 6.2.

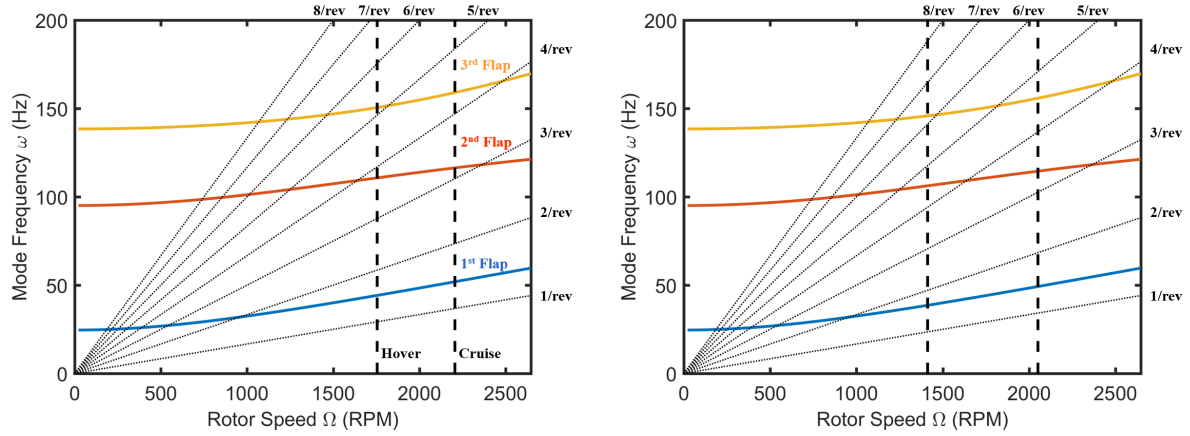

(a) Fan plot of the vehicle with the payload.

(b) Fan plot of the vehicle without the payload.

FIGURE 6.8: Fan plots of modal frequencies.

TABLE 6.2: First modal frequencies for each rotor speed.

	Condition	Rotor Speed	1st Flap	1st Lag	1st Torsion
Without Payload	Hover	1,412 RPM	1.64/rev	25.67/rev	20.29/rev
	Cruise	2,051 RPM	1.44/rev	17.87/rev	13.99/rev
With Payload	Hover	1,755 RPM	1.51/rev	20.66/rev	16.25/rev
	Cruise	2,206 RPM	1.41/rev	16.68/rev	13.01/rev

6.9 Rotor Stability

Aeroelastic instabilities from pitch-flap coupling, pitch divergence, and flap-lag coupling were considered in the design of the internal blade structure. The roots loci for pitch-flap flutter and pitch divergence are plotted in Fig. 6.9(a) with reference to the vehicle's torsional frequency. The elastic axis and the center of gravity are each aligned at the quarter-chord of the blade, which prevents the occurrence of pitch-flap flutter and pitch divergence. Figure 6.11(b) shows the eigenvalue analysis of the flap and lag modes of the rotor for each operational rotor speed at 10,000 ft (3,050 m) ISA. The flap and lag eigenvalues for hover and cruise with and without the payload are all stable. It should be noted that the inherent blade structural damping is neglected, but its inclusion will further increase the stability of the lag mode.

Other instabilities which were considered include air resonance, ground resonance, and whirl flutter. Air resonance occurs when the rigid body modes of the vehicle couple with various rotor modes, but it is not a concern due to the stiff-in-plane rotor configuration. Ground resonance involves the coupling of the rotor lag modes with the the landing gear modes, and is also not a problem for stiff-in-plane rotors. Whirl flutter involves the coupling of the modal frequencies of the wings to those of the rotor. Unlike standard tilt-rotor configurations which feature rotors attached to the ends of the wings, the attach points of *Halcyon's* rotors are mid-span, reducing their vulnerability to vibratory coupling. High bending stiffnesses of both the wings and the rotors further reduce their susceptibility to whirl flutter.

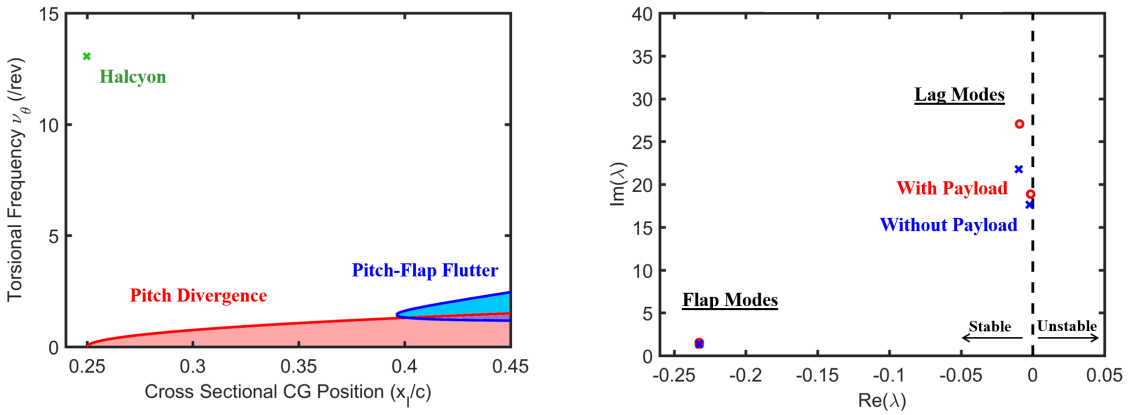

(a) Pitch-flap flutter stability plot.

(b) Flap-lag flutter eigenvalue analysis.

FIGURE 6.9: Aeroelasticity plots.

6.10 Blade Stress Analysis

The high aerodynamic forces faced by the rotor immediately after deployment from the C-130J and after the rotors begin spinning require careful consideration of the allowable stresses on the blade. In this section, the rotor blade stresses after deployment are predicted using Euler-Bernoulli beam theory. These stresses are compared to the maximum allowable stress of the spar to verify the structural integrity of the blade.

6.10.1 Deployment Procedure

After deployment, *Halcyon's* uses the passive stability of the wings to attenuate pitch oscillations and approach a steady pitch attitude. Vehicle dynamics are predicted for the first few seconds after deployment, yielding the variation of the pitch rate with time. A criterion is enforced that startup begins when the magnitude of the vehicle's pitch rate must be 10°/s for a period longer than 1 second. This condition can be easily detected using the gyroscope in the onboard avionics system. As shown in Fig. 6.10, the vehicle meets this criterion approximately 5.9 seconds after deployment. *Halcyon's* passive stability ensures that the it reaches a steady pitch attitude even it is deployed from the C-130J with an initial pitch moment.

The rotors must be locked in a non-rotating position until the vehicle has reached a steady pitch orientation to ensure the rotors will not spin in the wrong direction. To accomplish this, a torque limiter on each motor resists the aerodynamic torque of the freestream. The maximum aerodynamic torque experienced during the deployment phase is 190 ft-lb (257 Nm), which is resisted by the preset 369 ft-lb (500 Nm) limit on the torque limiter. When the steady pitch orientation criterion is met, the vehicle uses the deployment battery to provide power to the motors. The 406 ft-lb (550 Nm) maximum continuous torque of the motors is sufficient to bypass the torque limiter and begin startup. The aerodynamic torque on each rotor after deployment is shown in Fig. 6.11(a).

After using the motors to bypass the torque limiters on each rotor, the rotors begin to autorotate as a result of the aerodynamic torque from the freestream. No motor torque is used during the startup period except to initially bypass the torque limiters. The blades accelerate from 0 to 1920 RPM in a period of 1.1 seconds. A freewheel clutch disengages the each motor from the

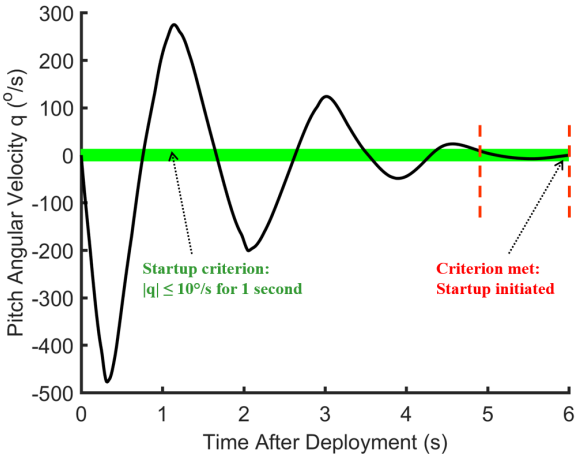

FIGURE 6.10: Pitch rate following deployment from the C-130J.

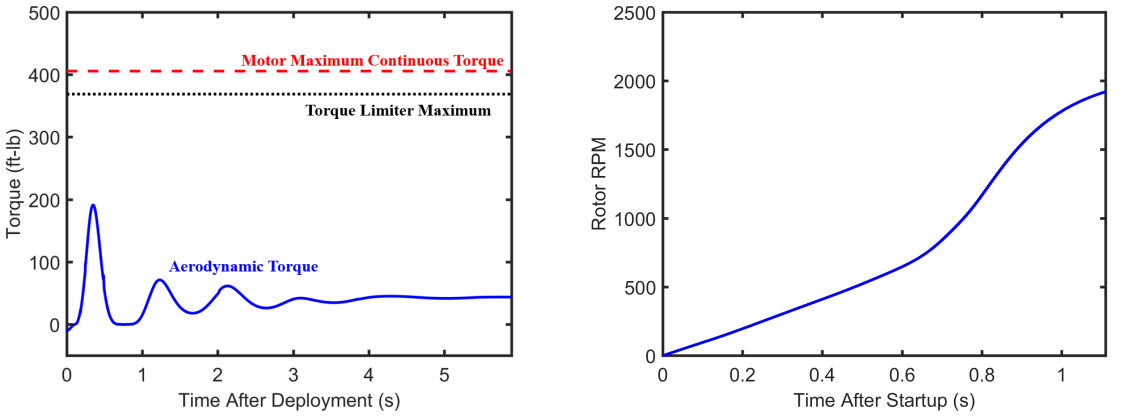

(a) Aerodynamic torque on each rotor before startup.

(b) Profile of the RPM and of each rotor after startup.

FIGURE 6.11: Freestream effects before and after startup.

rotor shaft when the rotor RPM exceeds that of the motor. This ensures that the motors are never driven by the autorotation of the rotors, which would require dissipation of a large amount of power. The clutch engages when the rotor RPM reaches 1920 RPM and the motors begin to provide torque to the rotors.

6.10.2 Root Bending Stresses

Transient vehicle dynamics are used to predict the forces on the non-rotating blades at each time step after deployment. The stresses are largest at the root, where the flap and lag moments are summed along the span of the full blade. The root stresses are compared to the maximum allowable stress of the spar to demonstrate the structural integrity of the blade.

The variation of flap and lag root bending stresses are predicted as seen in Fig. 6.12. The blade flap and lag stresses oscillate after deployment from the C-130J, and their amplitudes are attenuated as the vehicle begins to stabilize. The blade experiences a maximum flap stress of 56 ksi (383 MPa) 0.27 seconds after deployment, corresponding to the vehicle's impulsive acceleration of 60 g's after egress from the cargo bay. The spar is able to resist this flap stress with safety factor of 3.3 relative to the 186 ksi (1280 MPa) ultimate strength of S-glass with

epoxy. Due to the high lag stiffness of the spar, the maximum lag stress in the non-rotating phase of 2.3 ksi (16 MPa) is three orders of magnitude less than the ultimate stress of the material. The maximum root flap and lag bending stresses are lower during the startup stage than the deployment stage. The maximum bending stresses in the flap and lag modes are 40 ksi (274 MPa) and 0.7 ksi (5 MPa), respectively.

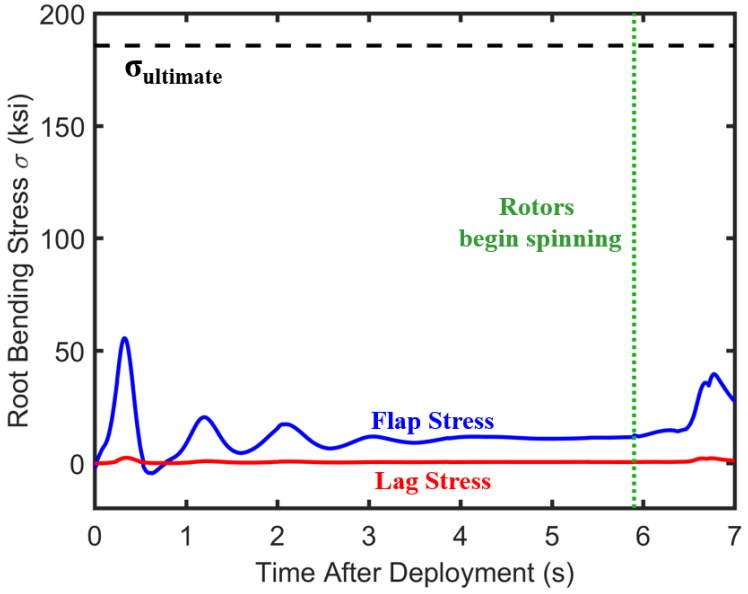

FIGURE 6.12: Flap and lag bending stresses at the root after deployment.

7 Wing Design

Halcyon's wings were designed for two purposes: flight stabilization during deployment and lift during cruise. In initial sizing, a wing span and aspect ratio were selected to maximize the vehicle's lifting surface, a property that improves performance in both performance and cruise, while still fitting within the C-130J cargo bay. The resulting wing was outfitted with an area of 36 ft^2 (3.35 m^2) and an aspect ratio of 1.6 to meet the vehicle's packing constraint. However, these parameters were chosen without accounting for non-ideal effects on the wings, including interaction effects and lift losses associated with low aspect ratio wings. This section provides a detailed description of how the wing was designed to overcome the complex, non-ideal flow environment and structural loads incurred at the *Halcyon's* wing during cruise and deployment.

7.1 Wing Aerodynamic Design

In addition to the wing area and aspect ratio, aerodynamic design of wings involves the selection of an incidence angle, an airfoil section(s), a sweep angle, and a twist rate. The wings were designed with no sweep and no taper because of the low Mach numbers (on the order of $M = 0.10$) encountered, thereby rendering effects of compressibility negligible. The wings were untwisted because of the presence of wing-mounted rotor hubs, as twisting the wings would complicate the interface between the wings and hub. Additionally, the aerodynamic benefits of twist on a low aspect ratio wings are minimal. The remaining two parameters, incidence angle and airfoil section(s), were selected based on the aerodynamics of low aspect ratio wings and the interaction between the fuselage and wings. The ideal wing design allows *Halcyon* to cruise with its fuselage

pitched at zero angle relative to the freestream, avoiding flow separation about its large elliptical shape.

7.1.1 Lift Requirement

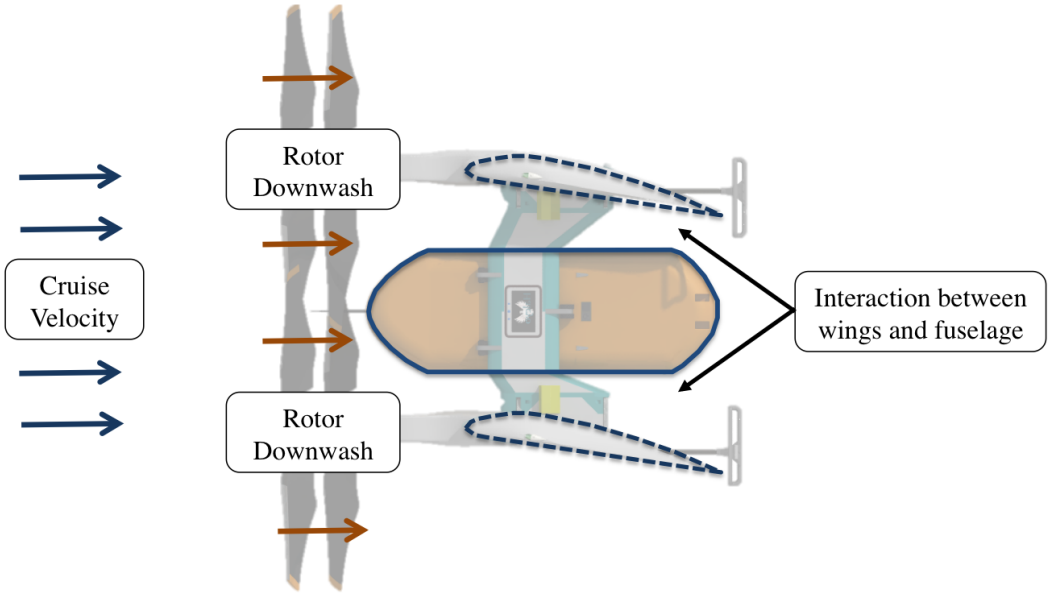

FIGURE 7.1: Overview of the dominant flow effects on *Halcyon's* wings.

Halcyon's wing geometry was selected to support the vehicle's weight in cruise after dropping the payload. Any additional lift needed in deployment was assumed to be provided by the wing's actuator flap, an assumption confirmed in Section 12.4. Based on the results of preliminary sizing, the vehicle's cruise weight is 1,012 lb (460 kg), equal to the weight of the total vehicle without its 508 lb (230 kg) onboard payload. *Halcyon's* wings were required to exceed 1,012 lb of lift in airplane mode while minimizing the body pitch of the fuselage. Although the geometry of its wings are relatively simple, *Halcyon* encounters a very complex flow at the surface of its wings, with three primary effects driving the aerodynamics: 1. Induced inflow from the rotors, 2. Interaction between the fuselage and wings, and 3. Lift losses as a consequence of low-aspect ratio. Each effect is important when choosing wing incidence angle and will be considered below.

7.1.2 Effect of Rotor Downwash

During normal operation, the wings are in the rotor downwash as two rotor hubs are mounted directly to the leading edge of each wing. The plane of one rotor disk is located 3 ft (0.9 m) from the wing leading edge, while the second rotor disk plane is located 2.3 ft (0.7 m) from the leading edge. The difference in distances arise from the tandem configuration of the rotors. The proximity of each rotor disk to the wing leading edge implies that the local dynamic pressure at the wing includes the induced inflow through the rotor. Figure 7.2(a) shows the span-wise distribution of inflow velocity as calculated from BEMT and a cruise speed of 70 knots (130 km/hr). When determining lift produced from the wings, the free stream velocity was calculated assuming an average value of induced inflow, shown in Fig. 7.2(a) to be around 5 ft/s. The total free stream velocity at the wings is, therefore, a summation of the cruise velocity and the rotor

inflow, amounting to a total free-stream velocity of 73 knots (135 km/hr). All future wing lift calculations are performed using 73 knots as the local free-stream velocity.

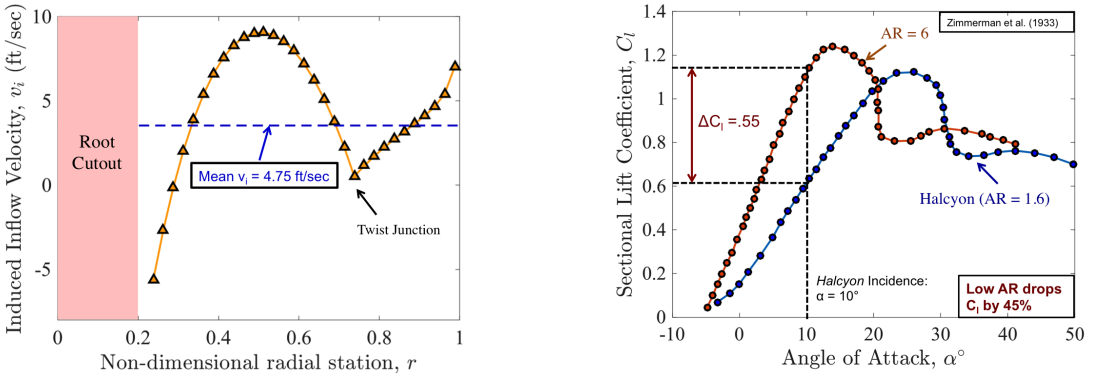

(a) Span-wise distribution of rotor inflow.

(b) Clark Y lift coefficient at several aspect ratios.

FIGURE 7.2: Effect of rotor downwash and aspect ratio.

7.1.3 Effect of Fuselage-Wing Interaction

The aerodynamic interactions between the fuselage and wings is a unique feature of *Halcyon*. To efficiently pack the vehicle within the C-130J cargo bay, the two wings are mounted in very close proximity to the fuselage, which results in the flow field of one lifting body (a wing) being highly coupled to the flow field of an adjacent lifting body (the fuselage). The resulting aerodynamics forces cannot be estimated through conventional means, as experimental values of lift coefficient do not account for proximity effects. Instead, analysis of these highly coupled aerodynamics was completed using an in-house two dimensional, inviscid computational fluid dynamics (CFD) model of the flow at the vehicle's central longitudinal plane. An unstructured grid technique was used to sufficiently generate a mesh for the three lifting bodies, and the flow condition was set at 73 knots.

Figure 7.3 shows a contour of pressure coefficient (c_p) for the two-dimensional flow between the wings and the fuselage, as generated by the in-house CFD model. The wings were designed with a NACA 4412 airfoil and pitched to an incidence angle of 10°. At the lower wing (denoted by the blue dashed box in Fig. 7.3), the high incidence angle causes a narrowing of the gap between the fuselage and wing, and a very low pressure region develops in the gap as a consequence of the Venturi effect. At the upper wing (denoted by the blue dashed box in Fig. 7.3), the high incidence angle has the opposite effect; the gap between the fuselage and wing is widened because of the high incidence angle, and the airfoil produces a moderately low pressure region on its upper surface. Taking the two opposing Venturi effects into account, the fuselage, despite being pitched at zero incidence relative to the flow, has a low pressure region on its lower surface and a high pressure region on its upper surface and, therefore, can produce a downward-acting lift. The lower wing, as a result of its very low pressure region, can produce a large amount of upward lift, while the upper wing, with its minimal Venturi effect but high incidence angle, can produce a moderate amount of lift.

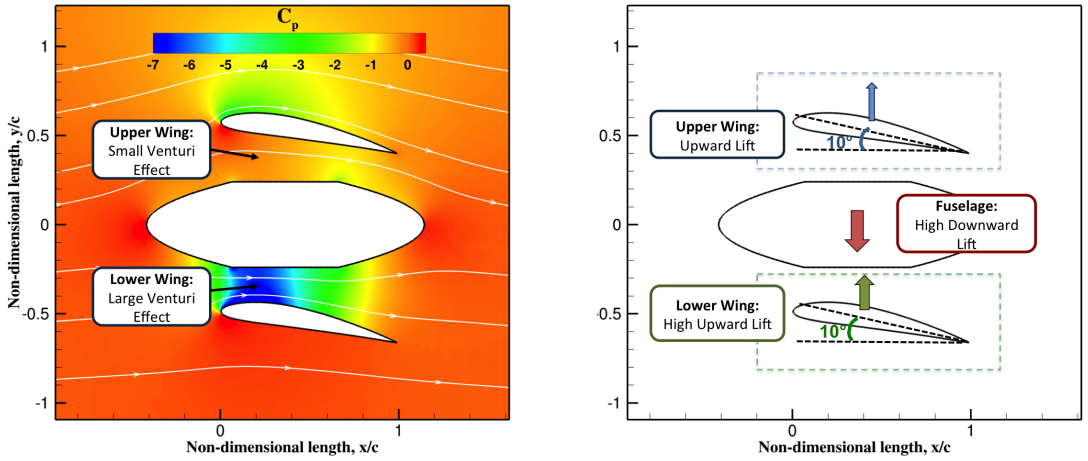

FIGURE 7.3: Total, 2D pressure field for the *Halcyon* generated from CFD.

7.1.4 Calculation of Total Lift

The total vehicle lift was calculated by integrating the pressure field along the surface of the airfoil and applying a correction to account for the small aspect ratio of the wing. The first row of Table 7.1 shows the results of integrating the CFD pressure field assuming *no* effect of aspect ratio, i.e., two-dimensional flow. Consistent with the predictions made in the previous section, the upper wing produces 2,127 lb (964 kg) of positive lift, the lower wing produces 830 lb (376 kg) positive lift, and the fuselage produces 1,055 lb (478 kg) of downward lift.

TABLE 7.1: Lift produced by the vehicle in cruise under a 2D assumption (top row) and after correcting for aspect ratio (bottom row).

	Lower Wing	**Upper Wing**	**Fuselage**	**Total Lift**
2-D Lift	2,127 lb / 964 kg	830 lb / 376 kg	-1,055 lb / -478 kg	1,903 lb / 863 kg
3-D Lift	1,160 lb / 526 kg	453 lb / 205 kg	-575 lb / 260 kg	1,038 lb / 470 kg

When an aspect ratio correction *is* applied to the data in Table 7.1, the lift production drops substantially. Experimental studies on the performance of a Clark Y airfoil for different wing aspect ratios is shown in Fig. 7.2(b), with the relevant design point marked by dark red lines [10]. Geometrically, the Clark Y airfoil is very similar to the NACA 4412: both airfoils have a thickness of 12%, a camber close to 4%, and a maximum lift coefficient C_{lmax} of nearly 1.60. Figure 7.2(b) shows that an aspect ratio of 1.6 wing results in a 45% drop in lift coefficient compared to a high aspect ratio wing at an incidence angle of 10°. The bottom row of Table 7.1 represents the lift produced by the *Halcyon* after applying a low aspect ratio wing correction. This shows that when an aspect ratio correction is applied, a NACA 4412 airfoil at a wing incidence of 10° produce a lift of 1,038 lb (470 kg) which is adequate for wing-borne flight.

The final wing geometry parameters are compiled in Table 7.2. Although only a single combination of wing incidence and airfoil shape is reported here, a total of 7 different configurations, each

representing a different combination of airfoil and incidence angle, were analyzed through the CFD model. Airfoils with camber less than 4% were found to produce insufficient lift for cruise, even at high angles of incidence. The high incidence angle of the *Halcyon* wings, although they increase the vehicle's profile drag, represent the minimum camber and incidence angle required to carry the vehicle during cruise while keeping the fuselage pitched at zero degree relative to the freestream.

In summary, *Halcyon's* wings were designed with several aerodynamic constraints. Packing limitations in the C-130J cargo bay, coupled with the desire for large wing area in deployment and cruise, resulted in two very low aspect ratio wings located in close proximity to the fuselage. The resulting flow field is dominated by interaction effects and losses in lift due to 3D effects on the wing. *Halcyon*'s wings were designed with a high incidence angle and a high camber to overcome its unique, complex flow environment.

TABLE 7.2: Final set of wing parameters.

Wing Geometry	Value (English)	Value (Metric)
Aspect Ratio	1.6	–
Span	7.6 ft	2.3 m
Wing Area	36.1 ft^2	3.35 m^2
Incidence Angle	10°	–
Airfoil Shape	NACA 4412	–

7.2 Wing Structural Design

As discussed in Chapter 8, the wing is built in sections using out-of-autoclave techniques in order to leverage their ability to produce large pieces at relatively low cost. The wing is divided in two for this process, wherein the upper and lower wing skins are cured independently from one another. The lower wing skin is laid on a support and then bonded to the ribs and wing spars. The strut/wing connections are co-cured with their respective spars prior to assembly and require a pass-through to be cut in the wing skin. The desired angle of incidence is controlled via precise manufacturing of these connections, potentially requiring machined sleeves to be inserted Other support elements (e.g., fuel tank straps, connection blocks for junction boxes and controllers, landing gear struts, etc.) are also bonded or fastened into the wing structure at this stage. The wing prior to attachment of the upper wing skin is shown in Fig. 7.4.

The major elements (e.g., fuel tank, junction boxes, controllers, etc.) will be placed into the wing through service doors. These doors are skin panels that are hinged via a UV-stabilized acrylic flexure and secured via stainless steel quarter turn fasteners and nut plates bonded to the wing skin. Galvanic corrosion between the carbon fiber skin and the plates is prevented via application of a fiberglass veil between the fasteners and the skin. The elevon and its actuators can be installed without any such door. Provided that the mounting points have been machined into the ribs, the servo actuator and hinge can be installed via a handheld ratchet and nut driver. The servo arms and spherical bearing of the hinge, shown in Fig. 7.5, can then be individually connected to corresponding spherical bearings on a plate that can be attached to the elevon in-situ. This in-situ installation is enabled by the ±51° deflection allowance afforded the elevon and can be completed using only hand tools, stainless steel bolts, and safety wire. As the elevon

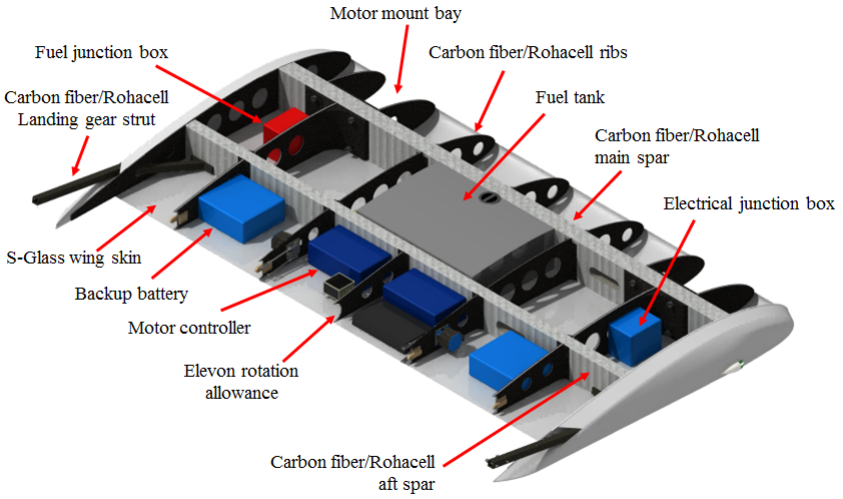

FIGURE 7.4: Wing assembly.

is manufactured from S-glass, galvanic corrosion from contact with anodic fasteners is not a factor here.

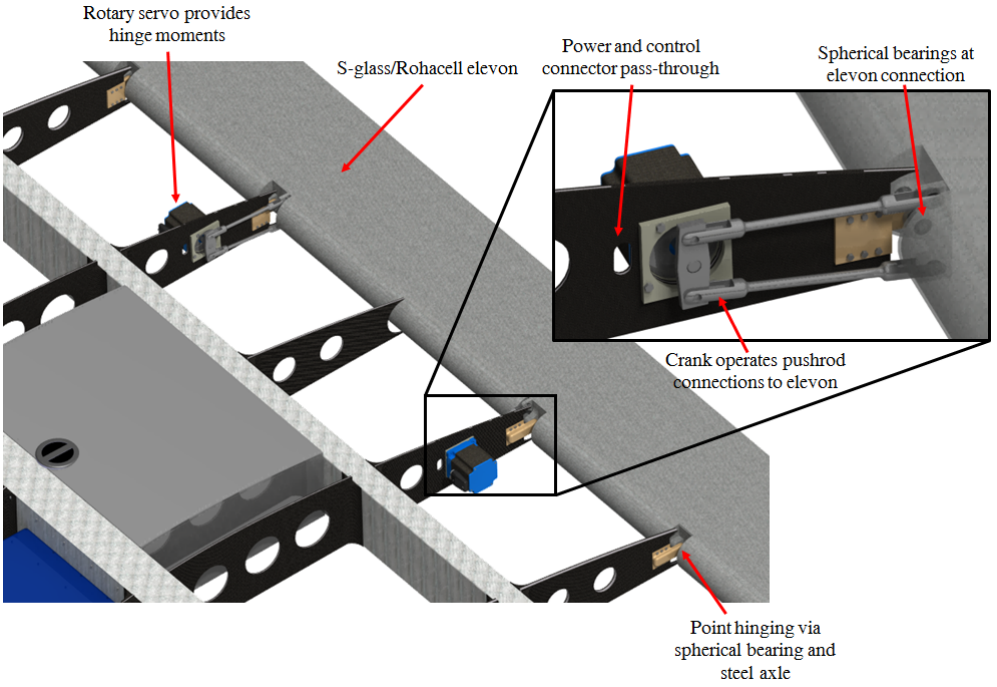

FIGURE 7.5: Elevon actuator detail.

Structural Layout

Landing Gear

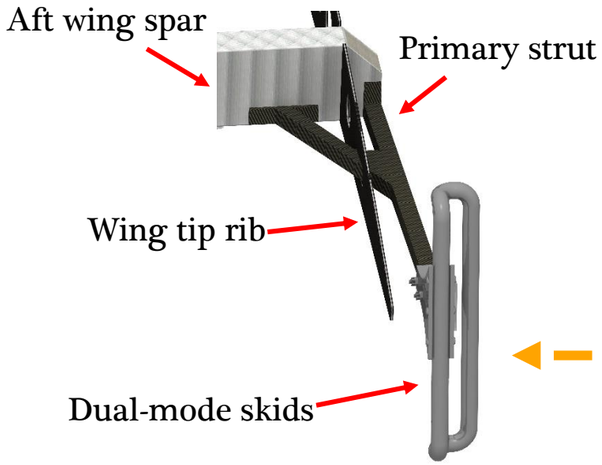

Payload Handling

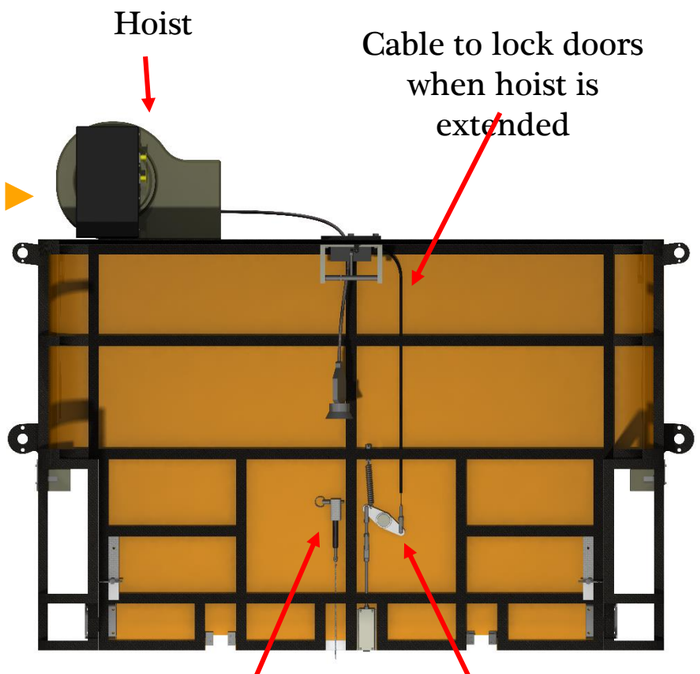

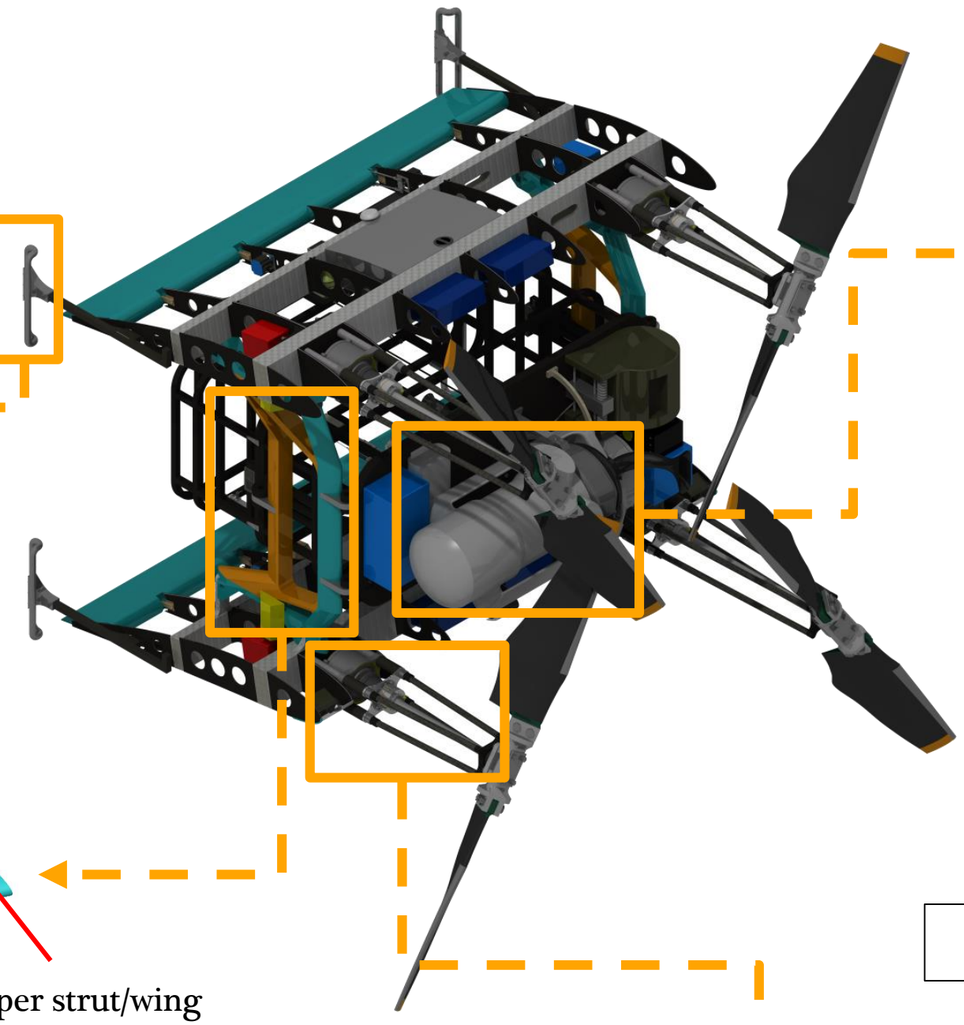

Struts

Push/Puller

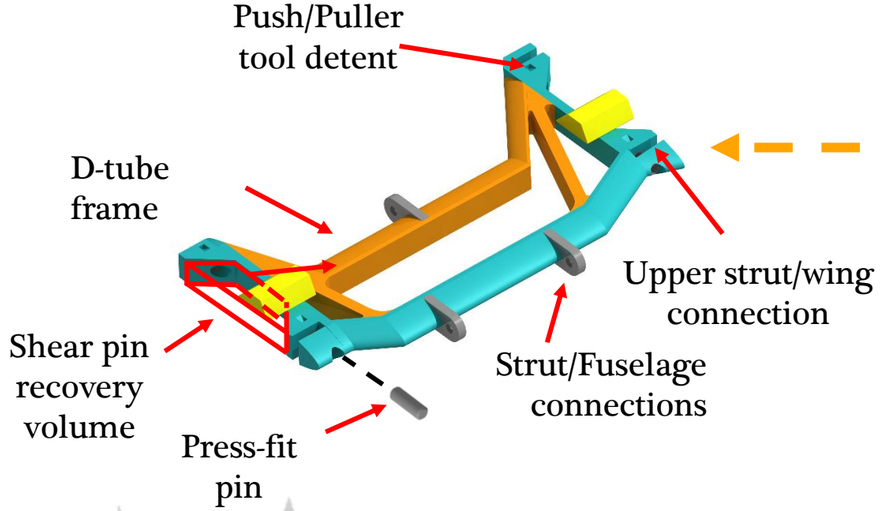

Motor Mount

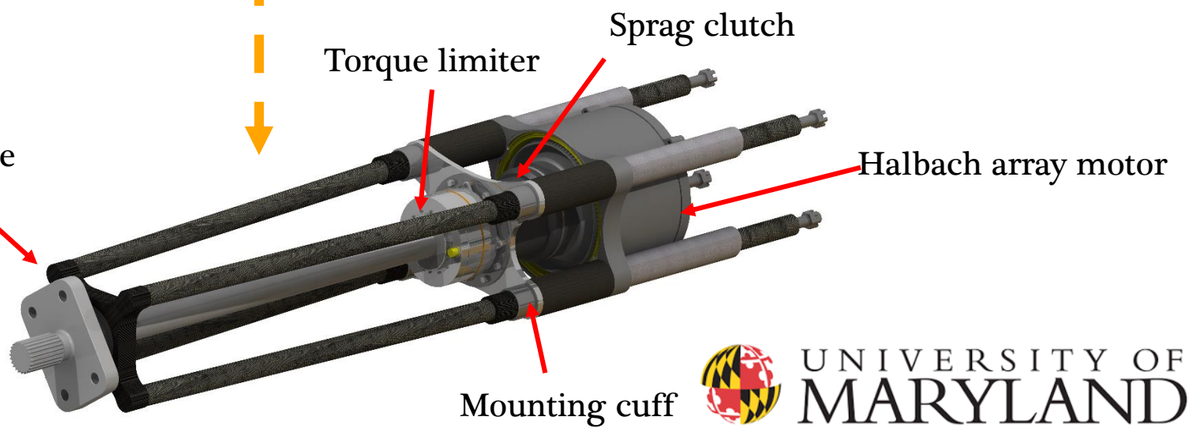

Halcyon

UNIVERSITY OF MARYLAND

8 Structural Design

8.1 Hub Design

Various rotor hub systems were considered before deciding on the current configuration used for *Halcyon*. Due to the unique structural loads resulting from the mission's deployment strategy, stiff hub designs are relevant. Also of interest is that, while both the transition from edgewise to axial flight regimes and typical helicopter controls require blade pitch control, the need for pitch control has been obviated by the use of RPM control. This choice further simplifies the rotor design as RPM control is facilitated through the electric propulsion system and requires no actuators, pitch links, or torsionally compliant mechanisms to operate efficiently in both axial and edgewise flight modes.

Hence, the following qualitative analysis was completed concerning the various categories of rotor hubs currently in use.

Articulated: Articulated hubs contain a high number of parts owing to mechanical hinging of the blades in all axes. Due to high complexity and the inherent compliance of a hinge, these hubs do not fit well with *Halcyon's* mission profile where high impulsive loads will be seen upon deployment, and where a low hub profile is desirable in axial flight.

Semi-Articulated: Several modern helicopters use a semi-articulated hub utilizing flap flexures and the multi-functional nature of elastomeric bearings and dampers. While these hubs are mechanically compact, large impulsive loading upon deployment may not be conducive sensitive materials contained in this style of hub.

Hingeless: The Bo-105, Eurocopter Tiger, and HAL Dhruv all use a hingeless hub with a composite flexure and a bearing pack close to the hub. The Bo-105 has two radial bearings and a tension-torsion bar while the Tiger and Dhruv carry the loads through one conical and one radial elastomeric bearing.

Bearingless: Bearingless rotors are mechanically simple designs which include the torsional degree of freedom in the flexure design and add a torsion tube to transfer pitch link loads to the far end of the flexure. This design adds a significant level of complication to the structural aspects of the flexure. Also, while the central hub is compact, the drag from the torque tube can add to the hub drag.

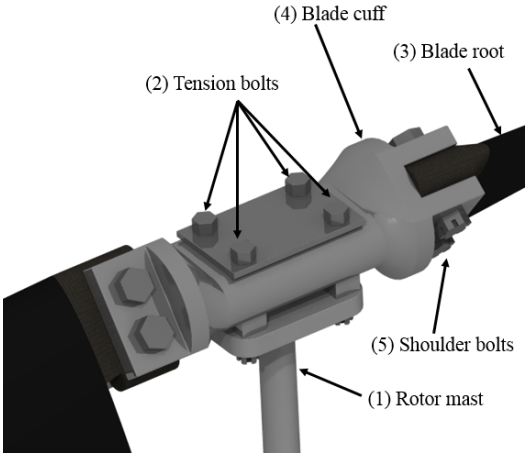

FIGURE 8.1: *Halcyon's* bearingless titanium hub.

The blades are capable of withstanding the stresses of deployment without the aid of compliance in the flap or lag directions, hence, in a move to keep the hub as simple as possible, a bearingless configuration was selected. Since no torque tube is required (as no pitch inputs are necessary) and a high-stiffness blade root is desirable in both flap and lag, this design can be simplified even further and the design of a flexure completely neglected. In lieu of this, the hub is simply a one-piece blade grip that directly attached the blades to the rotor mast. This hub can be seen in Fig. 8.1.

The hub is a titanium forging that connects to (1) the rotor mast via (2) four tension bolts that transmit thrust loads and an interior spline that transmits torque loads. The blades are held at (3) the root in (4) an integral blade cuff by (5) a pair of shoulder bolts made from stainless steel, a choice made both for the material's resilience in hostile environments and to prevent the possibility of corrosion in the steel/carbon joint. This hub has been designed for the extreme load conditions predicted during initial deployment and motor startup, exceeding the strength requirements imposed by both conditions by a minimum factor of 2.

8.2 Airframe Design

Halcyon is designed with quick integration in mind, simultaneously fulfilling mission requirements while integrating seamlessly with the pre-existing cargo handling systems aboard not only the C-130J, but also on legacy models of the aircraft without loss of mission performance. In order to achieve this, a premium was placed on strong and lightweight structures that would be capable of meeting the taxing demands of *Halcyon's* deployment. This includes both the rigors of flight, particularly speaking of stresses produced upon egress from a C-130J at altitude, as well as the extreme climates that the vehicle must operate in to accomplish its mission of providing disaster relief to remote locations in South America.

To this end, a semi-monocoque design was selected, composed of a carbon fiber understructure and load-bearing skin. The composite structures incorporated into *Halcyon* are designed with maintenance in mind and the vehicle can easily be disassembled into its major structural components using only 5 tools and will be detailed in Section 8.2.3.

The rotors are vertically staggered such that, even at their maximum flapping angle no blade will occupy the same plane as any other object within its radius. Hence, each pair of rotors is is spaced 10% of their radius from one another as well as from the fuselage to prevent any possibility of a tip strike. The clearance between the rotors is seen in Fig. 8.2. While this decreases the critical speed of the rotor masts due to the required extension of the rotors away from the aircraft, the maximum operational speed of the rotors falls at less than 70% of this value. These rotors are mounted to the wings to increase the moments generated by each thrust vector, but are also limited in size and location by the restrictions imposed by the available C-130J cabin space.

Since electric motors provide torque for the rotors, the only component of the aircraft that requires aspiration is the engine. Inlet and exhaust ducts are incorporated into the nose of the fuselage to provide adequate flow for aspiration as well as cooling. Similar inlets and exhausts provide flow over the radiators of the aircraft's various liquid cooled components (i.e. motors, motor controllers, generator, and batteries) using NACA ducts.

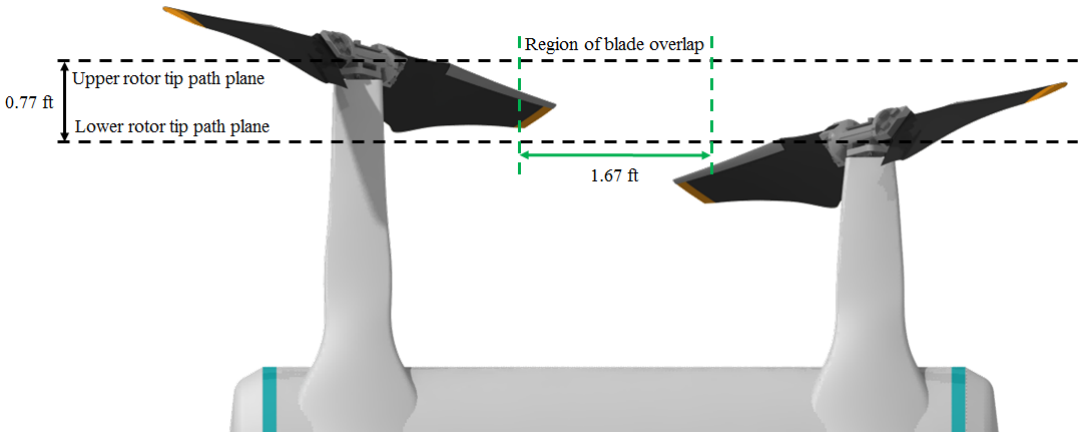

FIGURE 8.2: Clearance between rotor blades.

8.2.1 Load Paths

As seen in Fig. 8.3, *Halcyon's* dual flight modes and configuration yield somewhat atypical load paths. The primary source of aerodynamic loads are, to varying extents, the wings and the rotors. In edgewise flight, rotor thrust is easily the dominant source, although, due to camber, the wings provide some side-force even in hovering flight. In axial flight, where the Venturi effect and body interference effects greatly vary the load distribution between the two wings, the contributions from the wings and fuselage are equal to that of the rotors, albeit the force vector is oriented perpendicularly to that of the rotors. Similarly, the aircraft must also be able to resist vertical loads produced during landing.

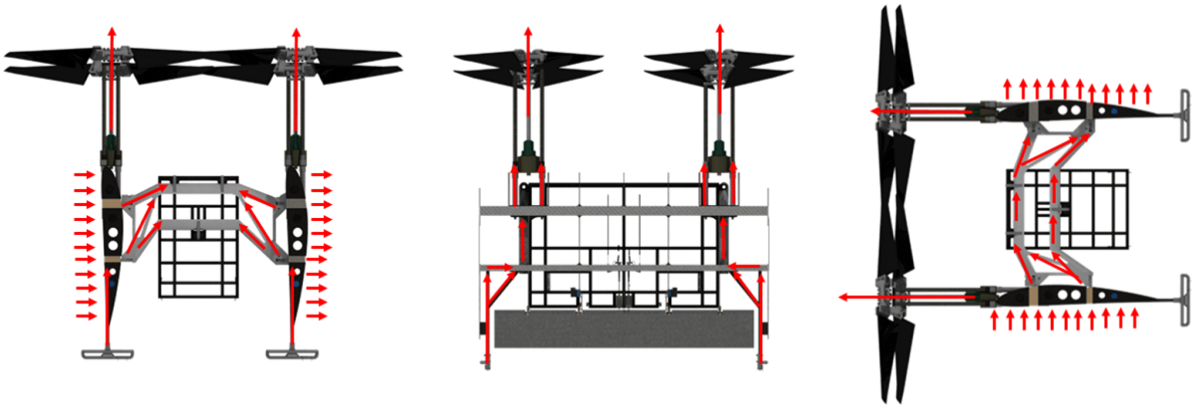

(a) Load paths during hover. (b) Load paths during landing. (c) Load paths during landing.

FIGURE 8.3: Load paths.

These loads are transmitted through the wing spars to the struts. While wing spars are not typically loaded in the chordwise direction, the subsequent bending moments are reduced via the location of the wing/strut connections. These pinned joints, as shown in Fig. 8.4 hold the wing (relative to the strut) in translation and bending in the chord and yaw directions. Placement of the joint relatively close to the axis of the motor thrust vector and the landing gear attachment enables stresses in the wing spars to be relieved in the chordwise direction. These loads are

transmitted through the struts to the fuselage, where the struts are again attached by a series of three press-fit pin joints that completely fix the strut in space.

The stresses are directly transmitted to a series of longerons near the nose bulkhead that transmit the loads to the fuselage body and the payload which is restrained by the fuselage structure itself. The engine, generator, hoist, and battery are all mounted on the nose bulkhead, allowing their loads to be transmitted to the struts directly through this carbon fiber and Nomex honeycomb. The payload weight is held directly by the hoist during edgewise flight and is distributed across several fuselage frames in axial flight. In this latter flight mode, the frames are supported by the aft-most strut/-fuselage connection point. The frames are sized to support this load, particularly under the high accelerations observed during the deployment process.

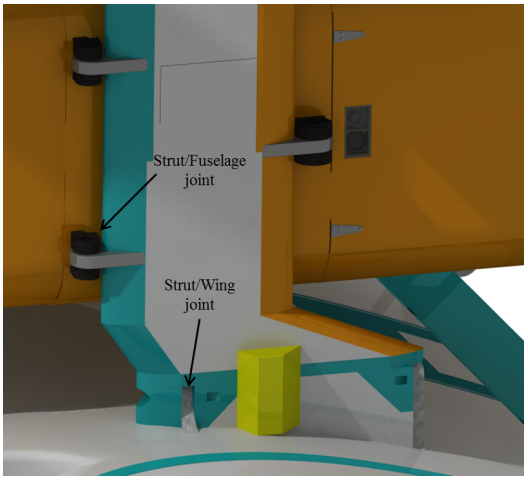

FIGURE 8.4: Structural connections between wing, fuselage, and strut.

The nose bulkhead and the fuselage frame share the load of the payload depending on flight mode. However, in the case of high density loads, the frames have been sized to withstand the full weight of the payload without failure. These frames are built in single pieces prior to co-bonding with the longeron segments and are segmented due to space restrictions. In order to reinforce these segments and provide structural continuity, cap strips of unidirectional carbon fiber are positioned over each longeron and run the length of the fuselage.

8.2.2 Material Selection

Because weight, strength, and stiffness are important design criteria, composite materials are selected to construct *Halcyon's* airframe. A combination of carbon fiber and fiberglass were used as reinforcement materials. Rohacell and Nomex honeycomb were used as core materials.

The wing and fuselage skin panels are constructed using out-of-autoclave (OOA) pre-pregs. Traditional composite manufacturing techniques require expensive tooling that can survive the high temperature and pressure within an autoclave. The use of OOA manufacturing allows the use of less costly tooling, savings that are especially critical for a composite-framed aircraft, and enables the construction of larger panels as a single element than would be possible with autoclave size restrictions. Larger panels also increase overall stiffness and reduce the number of fasteners required. This is of particular interest for *Halcyon* due to its large wing and fuselage area. The use of automated fiber placement (AFP) technology and partially impregnated fabrics facilitate the manufacturing process.

The understructure is produced from a carbon fiber layup over aviation-grade Rohacell cores. Rohacell is a relatively cheap material that is easy to form in a variety of different shapes, decreasing time and expense for structures that do not need the additional rigidity afforded by materials such as honeycomb. These structures are primarily box beams that can be easily manufactured in smaller autoclaves using the aforementioned core material as a mandrel on which to wrap bidirectional fabrics. This methodology produces the wing spars, D-tubes found in the struts, fuselage frames, and longerons. Larger elements within each component (e.g., wings, struts, etc.) are co-cured and then the larger structure is co-bonded in the final assembly.

As carbon fiber is utilized extensively, care is taken in the selection of fastener materials in combination with the use of certain "buffer" components to keep anodic and cathodic materials separated at all times.

8.2.3 Strut Design

The struts are a critical component on this aircraft as they transmit all of the inertial, aerodynamic, and propulsive loads. In steady flight, these loads are expected to be primarily in the axial and vertical directions (corresponding to what are primarily propulsive and aerodynamic forces, respectively). In order to react these loads, the strut is built around a stiff D-tube frame composed of five plies of $\pm 45°$ carbon fiber/epoxy composite laid up on a Rohacell core. These tubes are stiffened by a carbon fiber box beam (of a similar layup) that lends flexural support to the structure and are co-bonded to the D-tubes.

The strut/wing connection platform at either end of the strut are molded carbon fiber-reinforced polymer (CFRP) and are then co-bonded to the structure via a scarf joint at the end of each D-tube. Each connection slot on this platform is precision machined to accept a CFRP connector from the wings with minimal slippage between the two parts. This connector and the strut are connected by a press-fitted, corrosion-resistant stainless steel pin. Installation is carried out using a push/puller tool that locks onto the detents molded into the CFRP and is driven by a cordless impact driver for ease of use. To remove, the push/puller tool is again locked onto the detents and the pin is pressed into the recovery volume for manual removal. The strut/fuselage connections are managed in a similar way. These connections are molded CFRP and are fastened to the D-tubes via an adhesive lap joint.

The strut's response to various flight load cases was evaluated using X3D, a finite element analysis tool capable of analyzing static and dynamic responses [11]. The two load conditions considered for this structure were hover and steady level, wing-borne flight. The applied loads are given in Table 8.1. For all cases, the strut/fuselage connections were considered free only in rotation about their respective pins and the strut/wing connections were free to translate in all directions, simulating motion of the wings relative to the fuselage for a given strut deformation. Following this reference frame, all loads were applied to the strut/wing joints as follows. Each load is given in vector form, corresponding to the longitudinal, lateral, and vertical directions, respectively. No concentrated moments were applied to the joints.

Please note that the applied loads shown here are triple those expected to be expected during flight.

Table 8.1: Load case detail.

Load Case	Joint	Load ([lb, lb, lb])	Load ([kN, kN, kN]))
Hover	Upper	[1320,0,50]	[5.87,0,0.22]
Hover	Lower	[1080,0,300]	[4.80,0,0.99]
Axial Cruise	Upper	[640,0,2860]	[2.85,0,12.72]
Axial Cruise	Lower	[1120,0,9030]	[4.98,0,40.17]

Figure 8.5 shows the stress distributions in the vehicle's flight modes. It should be noted that the applied loads shown here are triple those expected to be expected during flight. At the base of the cross-brace, a stress concentration produces a maximum von Mises stress of 161.4 ksi (1,113 MPa) in hover, resulting in a safety factor of 3 relative to the ultimate strength of the

composite. Similarly, the maximum displacement of each joint was <0.00003 in (0.00063 mm), which is, likewise, acceptable. The modal frequencies were likewise found to be at some variance from the operating frequencies of the rotors.

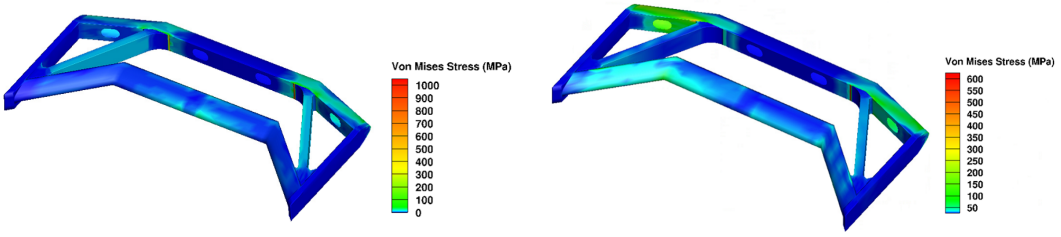

(a) Hover condition. (b) Cruise condition.

FIGURE 8.5: Structural analysis in steady flight.

8.2.4 Fuselage Structure

The fuselage structure is composed from a network of box beams that interface with the nose bulkhead at the interface between the engine compartment and the payload bay. Each frame and longeron is placed so as to distribute the weight of the payload along several load paths to the strut connections. This distribution is facilitated through the proper positioning of the payload. The payload is pulled tight against a series of four delrin wedges that act as bump stops, thus limiting the payload's longitudinal travel along the length of the fuselage. These stops are installed via quick-release pins into a glass-fiber reinforced polymer (GFRP) strip that allows the user to vary the location of the stops based on the payload size so as to best accommodate the load.

The payload is limited from motion in the lateral and vertical directions by the fuselage frame itself. Varied payload sizes can be accommodated on the pallet. The wedge-shaped stops automatically locate the pallet laterally and vertically within the vehicle and ensure that no motion is possible in those axes so long as tension is applied to the payload in the longitudinal direction.

8.2.5 Motor Mounts

The attachment from the motor's mounting flange to the airframe was designed specifically for low weight and ease of maintenance. Four roll-wrapped carbon fiber tubes transmit all loads from the motor to the main spar of the wing, which is connected to the strut as noted in Section 8.2.1.

This mount is directly interfaced to the motor's mounting flange. The motor is connected to a sprag clutch which enables the motor to disengage from the shaft when the shaft has a higher RPM than the rotor. This enables the rotors to have an autorotative startup phase without requiring power to be dissipated from the motors. The sprag clutch connects to a torque limiter which resists torques up to a preset limit and locks the rotors in their storage positions until the motors provide torque to the system. Each of these devices are mechanically simple and require low maintenance. The torque limiter is then attached to the mount on a stainless steel cuff.

In order to produce mounts that were simultaneously lightweight, compact, and strong, the aforementioned FEA solver was again utilized to guide design choices. As seen in Table 8.2

The motor mounts were tested at the maximum loads expected in edgewise and axial flight, respectively, corresponding to maximum thrust and torque in each condition. The torque and thrust were applied as distributed loads across the rotor mast, which were reacted only by the motor itself. These loads are then transmitted to the mount itself via the built-up sections of the mounting tubes and from there to the wing spar via the threaded rod ends. Hence, the initial 3 in. (76.2 mm) of each spar is fixed in all degrees of freedom to simulate where the tubes pass through the wing spar and are bolted in place. The weight of the hub is negligible compared to these other loads (e.g., thrust, torque), but is also considered in the analysis.

TABLE 8.2: Load case detail.

Load Case	Load ([lb, lb, lb]),([ft lb,ft lb,ft lb])	Load ([kN, kN, kN]),([kN m, kN m, kN m])
Hover	[1080,0,0],[900,0,0]	[4.80,0,00] ,[1.22,0,0]
Axial Cruise	[1200,0,-120],[900,0,0]	[5.34,0,0.53],[1.22,0,0]

The results of this study is shown below in Fig. 8.6 for the motor mount's initial design iteration. As in the case of the struts, the motor mounts can easily handle all applied loads as the stresses in the tubes themselves do not exceed 10.2 ksi (70 MPa). While the maximum stress in them model is higher than that, this occurs only around nodal locations where boundary conditions were applied, conditions that generate some localized errors in the solver. Hence, these values can be safely ignored. Similarly, the stress concentrations around the attachment from the simulated motor mounting flange (from which the shaft continues in the positive "x" direction) are softened by the increased material thickness of the actual motor mount. The associated modal frequencies are also not aligned with any operational frequencies of the rotor system.

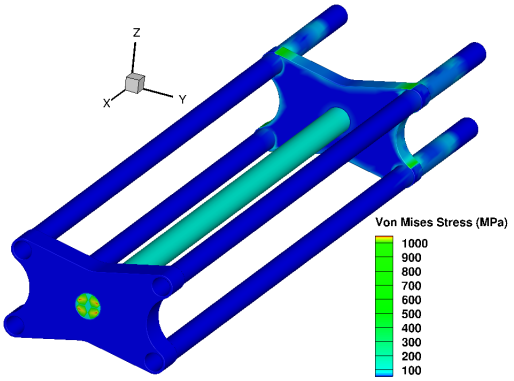

FIGURE 8.6: Stress distribution for hover load case.

Taking advantage of this analysis, the present design features tubes that are 75% the previous diameter. Furthermore, this slight resizing allows for two plies of carbon fiber removed from their construction. The mount tubes now taper to the radial bearing that supports the rotor, decreasing drag and increasing the aircraft's packing factor in the C-130J cabin.

8.2.6 Landing Gear

To quote the USAF publication *C-130 Transportability of Army Vehicles* concerning the 436L cargo rails installed in the C-130J, "Contact between vehicle tracks or wheels could damage the rails. Proper operation of these rails is key to the C-130's alternate missions of airlifting cargo pallets and for airdrop." [12] To prevent damage to the rails when maneuvering *Halcyon* inside

of the C-130J cabin and enable an efficient on-loading and deployment process, the cargo rails will be utilized and protected similar to a C-130J airdrop operation. Hence, *Halcyon's* landing gear was chosen to be a skid that could interface with the rail directly. However, this same skid must also be capable of landing on surfaces, preferably without reconfiguring in order to decrease complexity and weight. Hence, a dual-mode skid was adopted, as shown in Fig. 8.7.

The skid itself is 7075 aluminum tubing that is formed so as to accommodate landing loads and the lighter loads that would be experienced during handling aboard the C-130J. The lower skid is responsible for higher landing loads and is, thus, placed directly in line with the landing gear strut. The main body of the skid in then fixed directly to the carbon fiber strut via a pair of titanium bolts. This strut is a carbon fiber and Rohacell box beam sized to withstand hard ground impacts following a 300 fpm (1.524 m/s) descent [13]. A carbon fiber box bonded to the strut and the wingtip as well as cross-bracing prevent the strut from buckling under these loads and alleviate bending loads on the connections between the strut and the aft wing spar. This connection is managed via two stainless steel bolts to enable removal of the entire strut assembly for major maintenance.

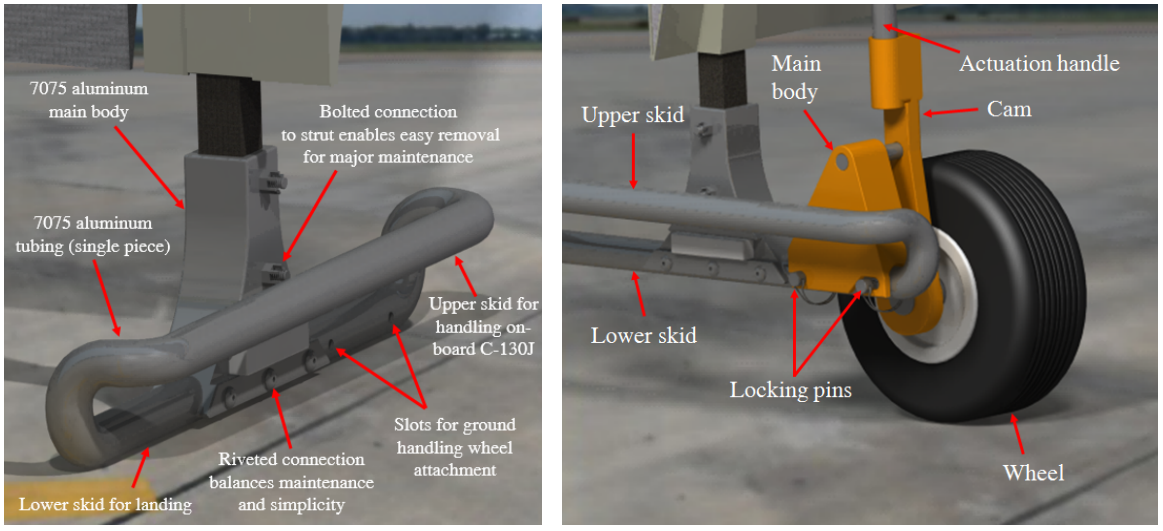

(a) C-130J handling mode.

(b) Ground handling mode.

FIGURE 8.7: Operational modes of the landing gear.

8.2.7 Payload Handling Systems

Halcyon utilizes an FAA-certified helicopter rescue hoist to meet the RFP requirements of a delivery at an impact velocity less than 5 ft/s (1.5 m/s). Hoists, unlike winches, are capable of lifting objects at angles greater than 45^{circ} and were therefore a necessary component for payload delivery from hover.

The hoist chosen for *Halcyon* is the UTC Aerospace Systems Model 76379-040. A cable speed of 215 ft/min (1.1 m/s) which will easily allow us to deliver the package in less than 30 seconds. The hoist is installed above the firewall of the aircraft at the edge of the nose, and the offset cable is routed through the firewall to the cargo bay. A roller box is used to guide the cable to a position directly above the center of the payload. A spring-loaded lever permits the payload doors to lock in place upon retraction or extension of this cable.

9 Vehicle Performance Analysis

As a disaster relief vehicle, *Halcyon* is designed to deploy from a C-130J and efficiently deliver 508 lb (230 kg) of supplies. This mission profile imposes several constraints on the vehicle's design, such as a small storage footprint, passive stability in free-fall, and a robust hover for precision payload delivery. The key to achieving these goals lies in *Halcyon's* unique configuration. As a quad-rotor tail-sitter, the vehicle operates as a helicopter in hover and as an airplane in cruise, improving packing, deployment, and cruise performance. By including two wings, *Halcyon* eliminates the need for a stabilizing tail, making the vehicle small and compact. By transitioning to airplane mode during cruise, *Halcyon* minimizes the cruising power and fuel required. By optimizing its proprotors for hover, *Halcyon* is capable of efficiently hovering at high altitudes and high temperatures.

This section demonstrates the hover and cruise performance of *Halcyon* at a variety of operating conditions. The vehicle will be shown to have a full-load hover ceiling at a pressure altitude of 13,450 ft (4,100 m) and to more than double the RFP's range requirement.

9.1 Hover Performance

As specified in the RFP, *Halcyon's* minimum hover requirement is 10,050 ft (3,060 m), ISA+ 0°C for a duration of one minute. To safely exceed this requirement, *Halcyon* was designed with a goal hover ceiling of 11,000 ft (3,350 m) at its gross takeoff weight of 1,520 lb (690 kg). An initial power estimate was determined based on an underestimation of the vehicle's performance parameters, with the understanding that the actual power required would be different from the estimated power required. Hover power was initially calculated from simple momentum theory equations assuming a download factor of 15%, a turbo-generator efficiency of 80%, and a 10% power surge for gust tolerance. This initial hover power calculation resulted in a required installed power of 480 hp (353 kW), which formed the basis for the propulsion system design detailed in Section 10.

After completing the individual component designs, power required to hover was recalculated with a more accurate blade element momentum theory (BEMT) model and a more accurate value of turbo-generator efficiency. At 10,050 ft and ISA+ 0°C, *Halcyon* operates at only 79% of the total power available. This is a result of over-estimating the hover power during initial sizing. The propulsion system is sized to supply 280 hp (206 kW) at 10,050 ft, whereas BEMT reveals only 225 hp (165 kW) is required. The excess power was included in the propulsion system to maximize the vehicle's operating range and to allow for deployment maneuvers at 13,000 ft (see Section 12.4) .

Figure 9.1(a) shows the power required to hover at a payload weight of 500 lb over a variety of atmospheric conditions. At the design hover conditions (represented by the solid blue and red lines), the hover ceiling is shown to be 13,450 ft pressure altitude, and the maximum operating temperature for hover at 10,050 ft is shown to be ISA+15°C. Therefore, *Halcyon* is capable of hovering up to 13,450 feet pressure altitude at ISA+0°C, far exceeding the RFP requirement of 10,050 ft. If the vehicle is hovering at 10,050 ft, *Halcyon* can operate at temperatures up to ISA+15 °C. For reference, 92% of the populated area of Nepal, a targeted disaster relief area, is located at an altitude less than 12,000 ft (3,660 m), meaning *Halcyon* can perform a controlled hover throughout the country's most extreme elevations.

The excess power in hover also means the vehicle is capable of hovering at gross weights higher

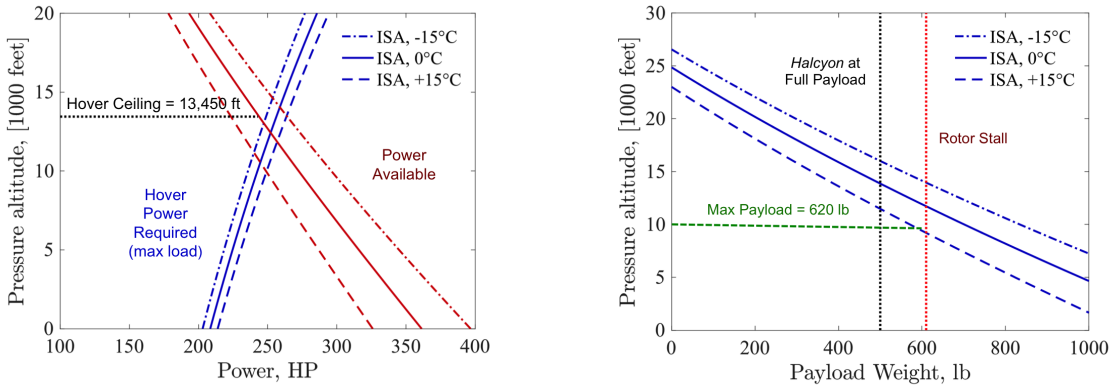

(a) Hover power at payload of 500 pounds.

(b) Hover ceiling under multiple payload conditions.

FIGURE 9.1: Hover Performance.

than the design gross takeoff weight. Figure 9.1(b) shows the variation in hover ceiling with onboard payload weight. The empty weight and fuel weight are assumed to be fixed, and the takeoff weight is changed only by increasing the amount of payload onboard. For an onboard payload weight of 545 lb (247 kg), the vehicle is capable of hovering at a pressure altitude of 11,200 ft (3,414 m), well beyond the design point of 10,050 ft. However, the stall margin at this point exceeds $C_T/\sigma = 0.16$, implying that the outboard portions of the rotor blades will begin to stall in hover. At the design condition of ISA+ 0°C (represented by the solid blue line), *Halcyons* maximum payload weight is shown to be limited by blade stall, not by the hover ceiling.

In summary, Figure 9.1(a) and Figure 9.1(b) demonstrate *Halcyon*'s excellent hover performance. The vehicle is capable of hovering 3,400 ft (1,036 m) above the altitude set by the RFP (an increase of 33%) over a wide range of operating temperatures. At ISA+ 0°C, the maximum onboard payload is not limited by the hover ceiling; instead, the vehicle encounters blade stall when carrying an additional 120 lb (54 kg) of payload.

9.2 Drag Estimation

To calculate the fuel required during *Halcyon's* cruise segment, an accurate estimate is needed for the vehicle's total drag. Drag can be decomposed into three main components: parasitic drag on the fuselage, profile drag on the fuselage, and induced drag on the wings. Assuming a smooth airframe, the parasitic and profile drag components are typically lumped into a single parameter, the equivalent flat plate area, while induced drag is a function of the wing's operating lift coefficient. Based on historical data, a flat plate area of 4.5 ft^2 (0.42 m^2) was assumed during initial sizing [8]. After designing a stream-lined fuselage shape for minimized drag, the vehicle's equivalent flat plate area was recalculated based on a component-by-component drag buildup.

The vehicle's parasitic drag was determined using a drag buildup method outlined by Raymer [14]. Each component of the aircraft was considered separately, and the total vehicle flat plate area was calculated by summing the component flat plate areas. For an individual component of the airframe, the flat plate area was calculated as a product of four factors: the wetted area, the skin friction drag coefficient, the form factor, and the interference factor. The wetted area of each component was estimated by integrating the component's cross-sectional area along its

longitudinal span. The skin fraction drag coefficient, which a function of Reynolds number, was calculated for each component assuming a cruise speed of 70 knots (130 km/hr), an altitude of 10,050 feet, and a fully turbulent boundary layer. The component form factor, which depends on how the component's geometry relates to an elliptical planform, was calculated using Shevell's methodology[15].

TABLE 9.1: Component breakdown of the vehicle's total equivalent flat plate area.

Component	**Flat Plate Area (ft^2)**	**Flat Plate Area (m^2)**	**Percentage (%)**
Fuselage	0.957	0.089	45.57
Wings	0.663	0.062	31.59
Struts	0.184	0.017	8.78
Rotor Hubs	0.281	0.026	13.40
Landing Gear	0.014	0.001	0.67
Total	2.099	0.195	100.00
120%	**2.520**	**0.234**	–

Table 9.1 shows a component-by-component breakdown of the total flat plate area of *Halcyon*. To account for items such as pitot tubes, latch hinges, and sensor antennas, an additional drag of 20% was added to the final equivalent flat plate area based on the recommendation of Prouty [16]. The fuselage, even with its large, nearly elliptical shape, contributes to only 45% of the total vehicle drag, comparable to the induced drag on the wings. Section 8 provides a more detailed explanation of how the fuselage was shaped to minimize drag. The total equivalent flat plate area of *Halcyon* is 2.52 ft^2 (0.234 m^2). This value is used in all futher calculations of the power required to cruise.

9.3 Forward Flight Performance

One of *Halcyon's* distinguishing features is its transition into axial flight during cruise. To analyze the power required to cruise during airplane mode, trim conditions for the vehicle were obtained through linearized vehicle dynamics. Effects of the four thrust vectors from the rotors, lift and drag from the wing as a result of forward airspeed and rotor downwash, and fuselage drag were all considered in the vehicle dynamics. Using these trim conditions, the power required at 10,000 ft ISA while carrying the payload and after dropping the payload was calculated for a range of flight speeds, and is shown in Fig. 9.2. From hover until the transition region, the vehicle flies in helicopter mode with rotors in edgewise flight. After the transition region, the vehicle flies in airplane mode with the rotors in axial flight. Power required in the transition region was calculated for a transitional maneuver from helicopter mode to airplane mode as explained in Section 12.4.

Based on Fig. 9.2, a cruise speed was selected for the vehicle when cruising with its 508 lb payload (i.e., when loitering before payload deliver) and when cruising without its payload (i.e., when returning to base). Without the payload, the speed for best endurance is 70 knots (130 km/hr), and the speed for best range is 91 knots (170 km/hr). With the payload, the speed for best endurance and the speed for best range are 66 knots (122 km/hr) and 113 knots (209 km/hr), respectively. The speed for best endurance maximizes the vehicle's potential loiter time

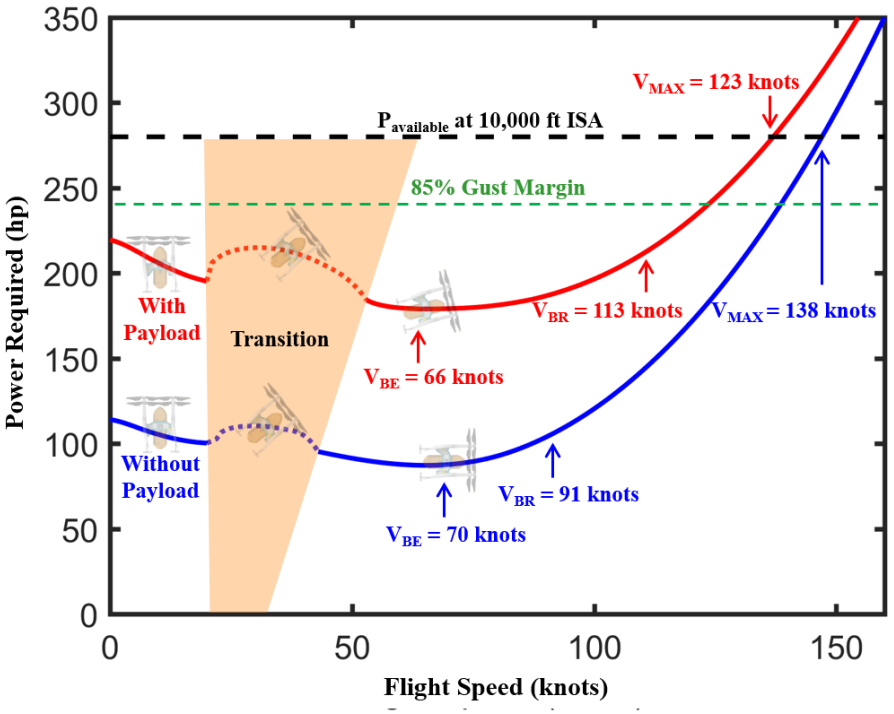

FIGURE 9.2: Vehicle power curve.

before dropping the payload. *Halcyon* is designed for operation at 10,000 ft ISA; therefore, its performance only increases at lower altitudes.

Range and endurance estimates were obtained for the vehicle with and without the payload. Range and endurance plots for the vehicle at 10,000 ft ISA are shown in Fig. 9.3. The range of the vehicle both with and without the payload surpasses the 50 nm minimum range specified by the RFP.

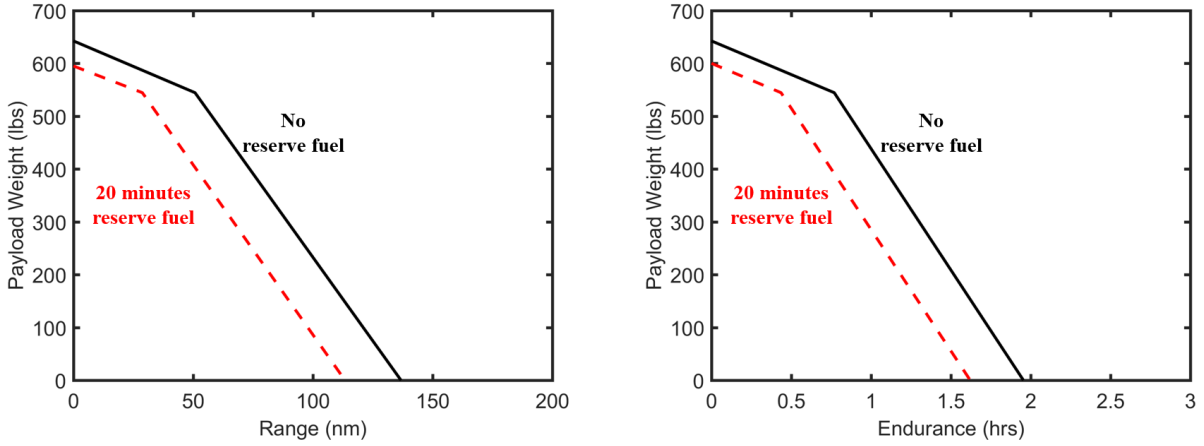

(a) Payload versus range.

(b) Payload versus endurance.

FIGURE 9.3: Range and endurance plots.

Propulsion System

Turbo-Generator Specifications

Turboshaft engine
- 480 shp (360 kW) at 6000 RPM
- Electric starter
- Self-contained lubrication system
- Multiple attitude operation

Generator
- 295 hp (220 kW)
- 400 V, 131 A
- 95% efficiency

Motors
- 4 brushless permanent magnet motors
- 70 hp (52.22 kW) each motor
- 95% efficency
- Liquid cooling

Li-ion Battery
- 6.65 hp-hr (4.96 kWh)

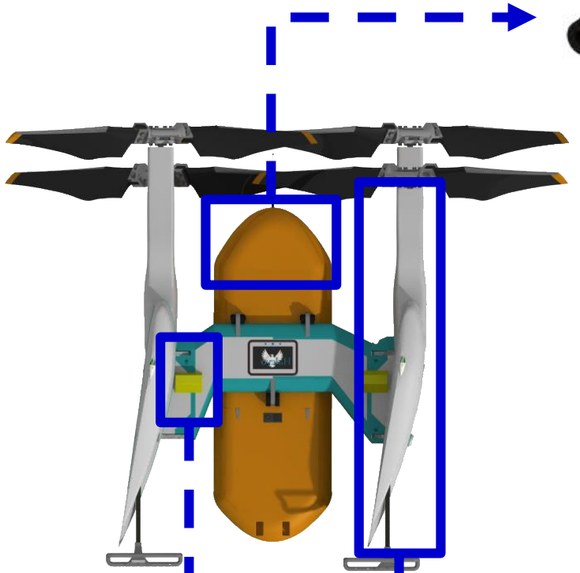

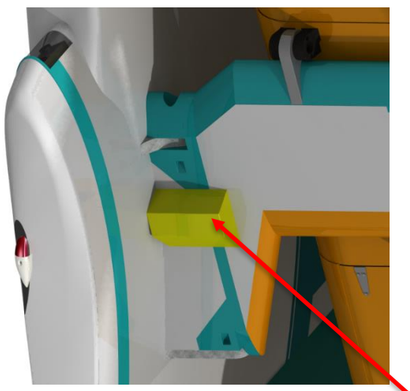

Pass-through for wiring or fuel line

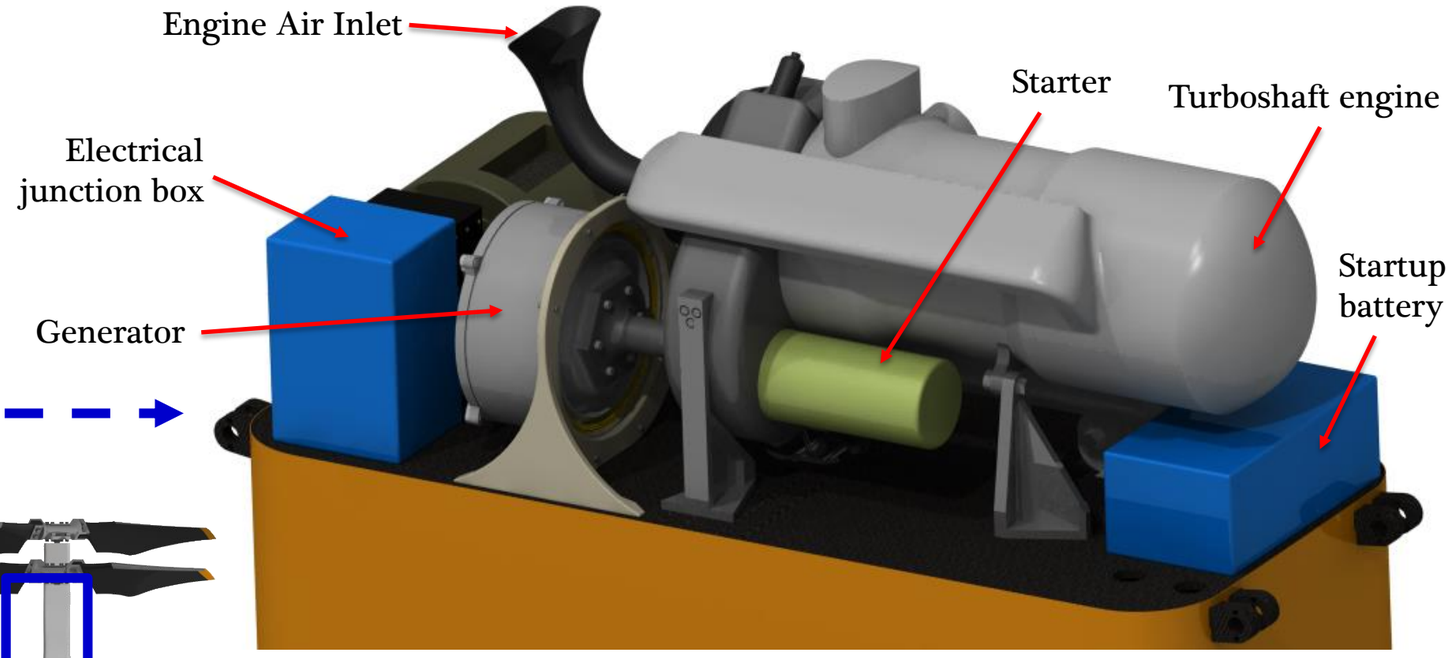

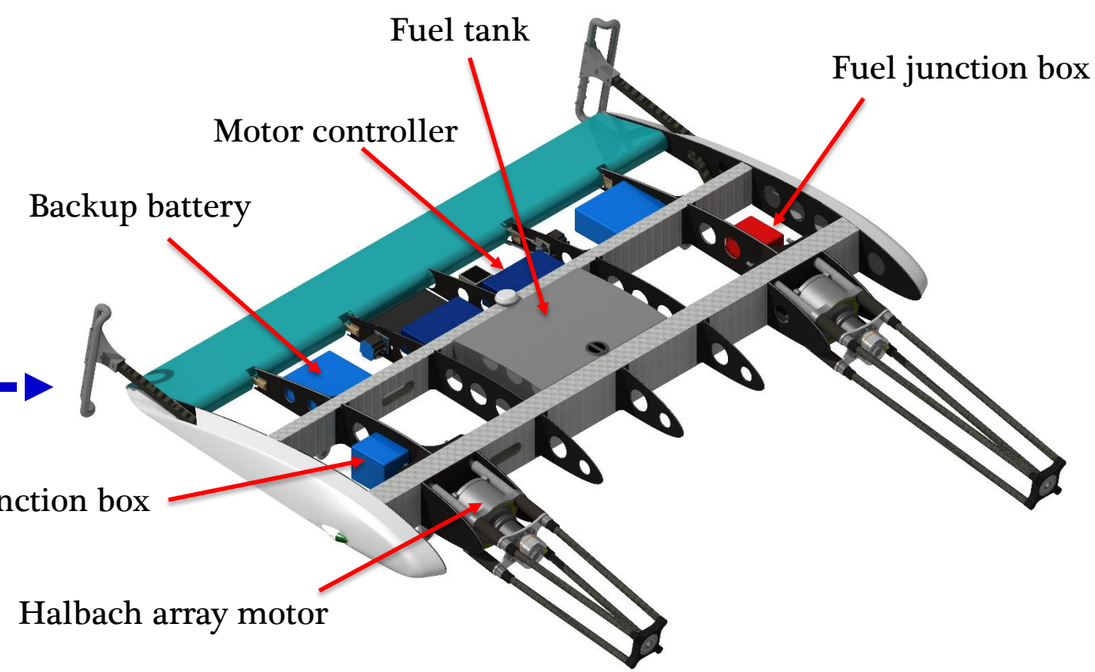

Halcyon

UNIVERSITY OF MARYLAND

10 Propulsion System Overview

Based on the results of initial sizing, *Halcyon's* propulsion system was designed for a power output of 280 hp (206 kW) at an altitude of 10,000 ft. This section will detail the primary components of *Halcyon's* propulsion system, including the primary power source, the transmission, and the system's method for providing differential RPM control.

10.1 Powerplant Selection

In Section 5.5, a turbo-generator configuration, wherein a single turboshaft engine drives an electric generator, was chosen as *Halcyon's* propulsion system. The generator is connected to an electrical transmission, and four variable torque motors control the vehicle through differential thrust. Before performing a detailed design of the system's major components, a brief trade study was conducted on different versions of the turbo-generator configuration, varying the system's power source and number of individual engines. The results of this trade study are summarized in the list below:

- A naturally aspirated internal combustion engine (ICE) was considered as an alternative to the vehicle's efficient but expensive turboshaft engine. Gas ICE's in the 300 hp - 500 hp class were found to suffer from an low power-to-weight ratio compared to turboshaft engines. The reduced cost of a naturally aspirated ICE was outweighed by an excessive increase in overall vehicle weight, eliminating this option from consideration.
- A turbo-charged diesel engine was considered for its low specific fuel consumption (SFC) compared to commercial turboshafts. Again, the diesel option was eliminated due to a very low power-to-weight ratio in the 300 hp - 500 hp range.
- A system of multiple turboshaft engines, each with their own generator, was considered as way of reducing engine size. Section 5.5 found that state-of-the-art turboshafts show little variation in weight when less than 400 hp is required. Therefore, including two or more turboshafts reduces the power output of each engine but dramatically increases the vehicle's takeoff weight. A multi-engine system was eliminated due to its weight penalty.

Halcyon's propulsion system was designed with the same configuration selected in initial sizing: a single turboshaft engine, an electric generator, an electric transmission, and variable torque motors. A detailed weight comparison of all potential propulsion system options is presented in Fig. 10.1. *Halcyon's* propulsion system represents the best combination of mechanical simplicity, controllability, and weight savings.

10.2 Electric Transmission

An electric transmission was chosen to enable differential RPM control of *Halcyon's* four main rotors. In addition to facilitating a simple, low-maintenance design, an electric transmission is highly responsive to autopilot inputs and provides superior vehicle controllability. *Halcyon's* electric transmission consists of three main components: a set of variable torque motors, an electric generator, and a set of motor speed controllers. Each component is described in detail below.

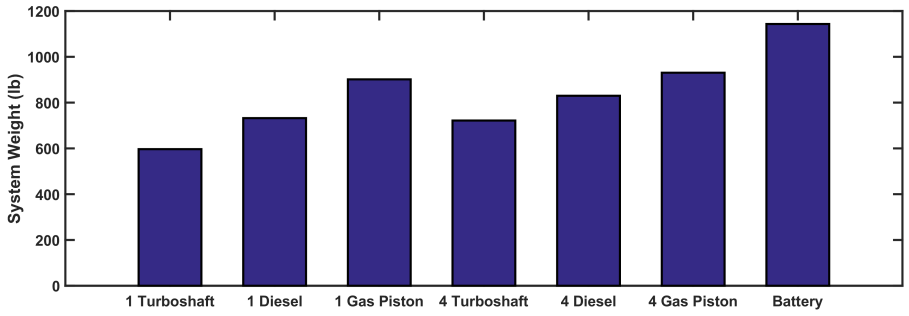

FIGURE 10.1: System Weight for Different Powerplants.

10.2.1 Motors

Halcyon's electric propulsion system was designed for a maximum power output of 280 hp. Therefore, *Halcyon's* four motors were designed to provide 70 hp (52.2 kW) to each rotor. Brushless DC (BLDC) permanent magnet motors with integrated inverters and gearboxes were selected for their favorable power density. *Halcyon's* motor design was based on two commercially available variable torque motors: the Siemens 107 hp (80 kW) motor (used on the DA-36 E-Star 2) and the PowerPhase 75 motor (used on the 2008 Boeing fuel cell demonstrator) [17]. Consistent with the properties of these motors, *Halcyon's* electric motors were designed with a power to weight ratio of 3.18 hp/lb (5.22 kW/kg).

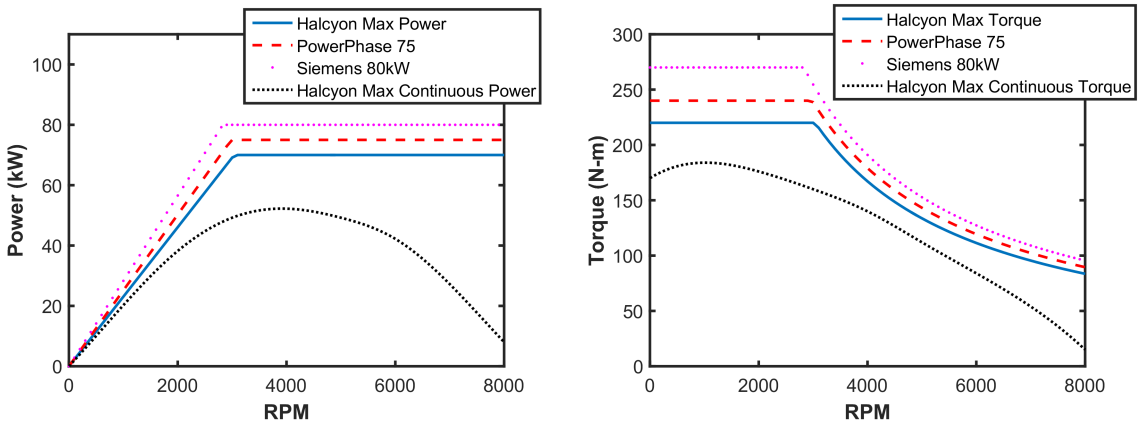

(a) a (b) b

FIGURE 10.2: Variation of power and torque against RPM for various motors without gear reductions.

To ensure that *Halcyon's* motors supply a sufficient torque in the vehicle's two flight modes, several modifications were made to the motor setup. A consequence of its two flight modes, *Halcyon* operates over a range of torque and RPM. In hover, the motors are each required to produce a torque of 168 ft-lb (228 Nm) at 1750 RPM; in cruise, the motors are required to produce a torque of 53 ft-lb (72 Nm) at 2050 RPM. The variation of motor torque with RPM is shown in Figure 10.2(b) for the PowerPhase 75 and the Siemens 107 hp. To achieve the required torque and RPM in hover and cruise, a planetary gearbox with a 3:1 gear reduction was integrated with the motor system. After implementing the gearbox, the motors are able to generate a maximum continuous torque of 405 ft-lb (550 Nm) and can disengage the torque

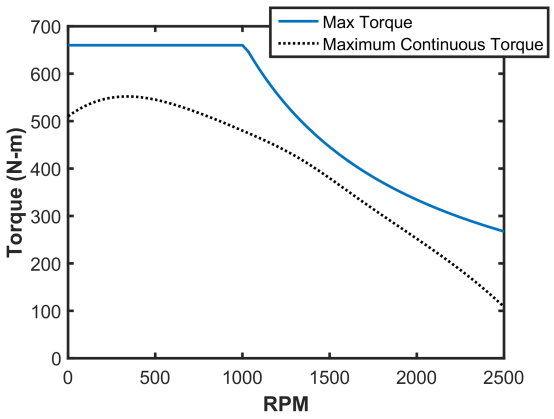

FIGURE 10.3: Torque vs RPM for the *Halcyon* motor assembly.

limiters during rotor start up which require 369 ft-lb (500 Nm) (see Sections 8.2.5 and 6.10.1). A peak efficiency of 95% is estimated for *Halcyon's* operating RPM range. *Halcyon's* motor output can be seen in Fig. 10.3.

10.2.2 Generator

Halcyon's turbine generator was designed with the goal of minimizing weight and maximizing generator efficiency. A survey of commercial turbine generators was conducted to determine the optimal tradeoff of generator weight, maximum power output, and efficiency. A scaled-up version of the Wrightspeed 107 hp (80 kW), a prominent generator from the auto industry, provided the basis for *Halcyon's* electric generator design. Based on the properties of this generator, *Halcyon* was designed with an integrated 1.5:1 planetary gear reduction and integrated power inverters. The generator was scaled to have a maximum continuous power output of 295 hp (220 kW), coupled to the turboshaft engine operating at 6000 RPM. Consistent with the Wrightspeed generator, the turbo generator has a power to weight ratio of 1.15 hp/lb (1.89 kW/kg). Figure 10.4 shows the variation in power with RPM for the *Halcyon's* scaled-up generator with the peak power occurring at 4000 RPM.

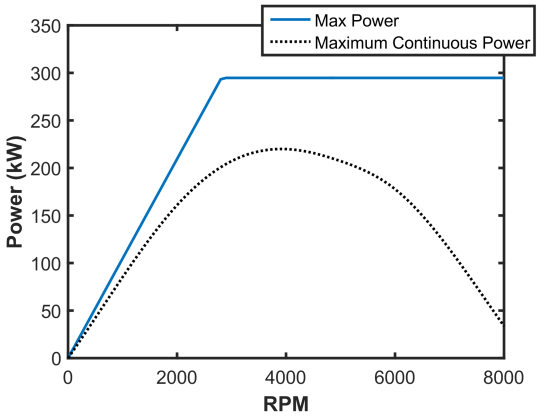

FIGURE 10.4: Electric generator operation.

Based on *Halcyon's* band of operational rotor speeds, a peak efficiency of 95% was estimated for the generator. The generator produces electricity at 400 Volts, resulting in a current of 131 Amps per motor when *Halcyon* operates at maximum power.

10.2.3 Motor Speed Controllers

Controllers are implemented on each of *Halcyon's* motors to control motor torque and RPM. The Sevcon Gen4 Size 8 was selected from a survey of motor controllers based on the maximum power and current requirement of *Halcyon's* motors. This motor has a weight to power ratio of 0.21 lb/hp (0.13 kg/kW).

10.2.4 Cooling

The motors and the generator require liquid cooling. *Halcyon* has provisions of 14 lb (6.4 kg) for the weight of the cooling system and dedicated spaces for the system to be installed. The cooling system consists of a pump connected to a radiator with hoses running a water and ethylene glycol mix.

10.3 Engine

A rubber engine was created for this design to meet *Halcyon's* mission requirements; however, the vehicle's engine weight and size strongly correlate with currently available, off-the-shelf turboshaft engines. *Halcyon* is powered by a 480 hp (353 kW) turboshaft engine that provides a maximum continuous power at 90% of takeoff power. To meet the goal engine output of 280 hp at 10,050 ft, the engine's power rating takes into account the power loss due to high altitudes, using a 3% loss for every 1,000 ft (300 m) ISA, and a component efficiency of 95% for the motors and generator.

Historical data was gathered to compare different types of engines and size the *Halcyon* engine. Findings from the survey are validated with the paper NASA Design and Analysis of Rotorcraft [18]. The *Halcyon* engine has a power to weight ratio of 2.94 hp/lb (4.82 kW/kg). The engine's weight and size is comparable to the Rolls Royce M250 C20R, and to ensure reliable operation during the vehicle's deployment stage, the engine is designed to enable flight in various orientations.

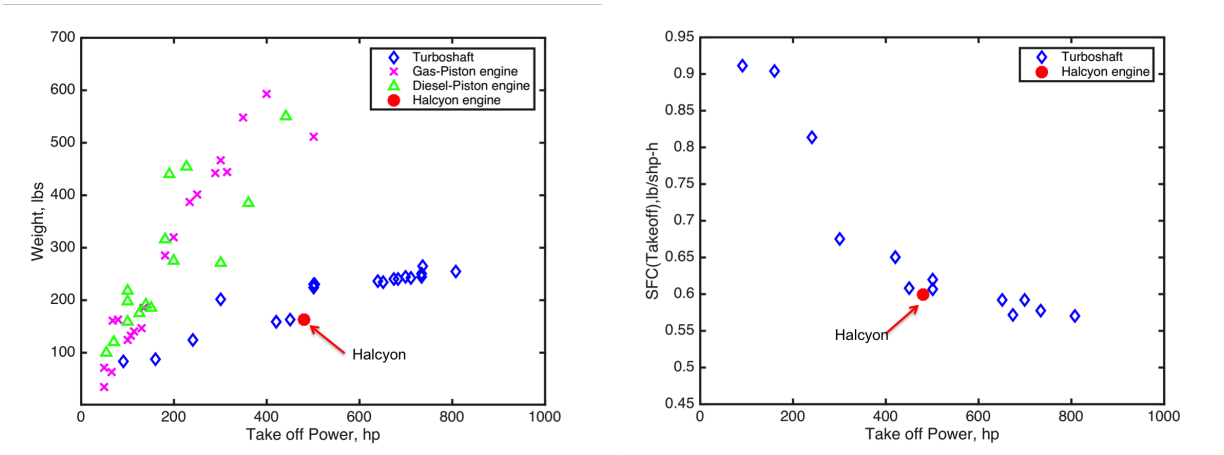

(a) *Halcyon* engine weight

(b) *Halcyon* specific fuel consumption

FIGURE 10.5: *Halcyon* turboshaft engine power-to-weight ratio and specific fuel consumption.

Figure 10.5(b) shows the trend for specific fuel consumption (SFC) corresponding to turboshaft engines. The SFC for *Halcyon's* engine is 0.6 lb/hp-hr (365 g/kW-hr), again comparable to the

Rolls Royce M250-C20R and M250-C28B series. Fuel management and engine performance is controlled by a dual Full Authority Digital Engine Control (FADEC) system, which monitors engine temperatures, engine pressure and atmospheric conditions to optimized engine efficiency at a given flight condition.

10.4 Lubrication System

The lubrication system of a turboshaft engine serves several functions essential for safe and dependable operation of the engine. Its primary function is to provide oil to engine components that are subject to friction loads from the engine's rotation and heat loads in the turbine area. *Halcyon's* engine implements a self-contained lubrication system that allows for operation in each of the vehicle's flight modes. A dry sump lubrication system was chosen for its adaptability to different flight attitudes that prevents oil supply from flooding the engine. In a dry sump system, additional pumps are used to collect and store the oil from the sump in an external reservoir, as shown in Fig. 10.6.

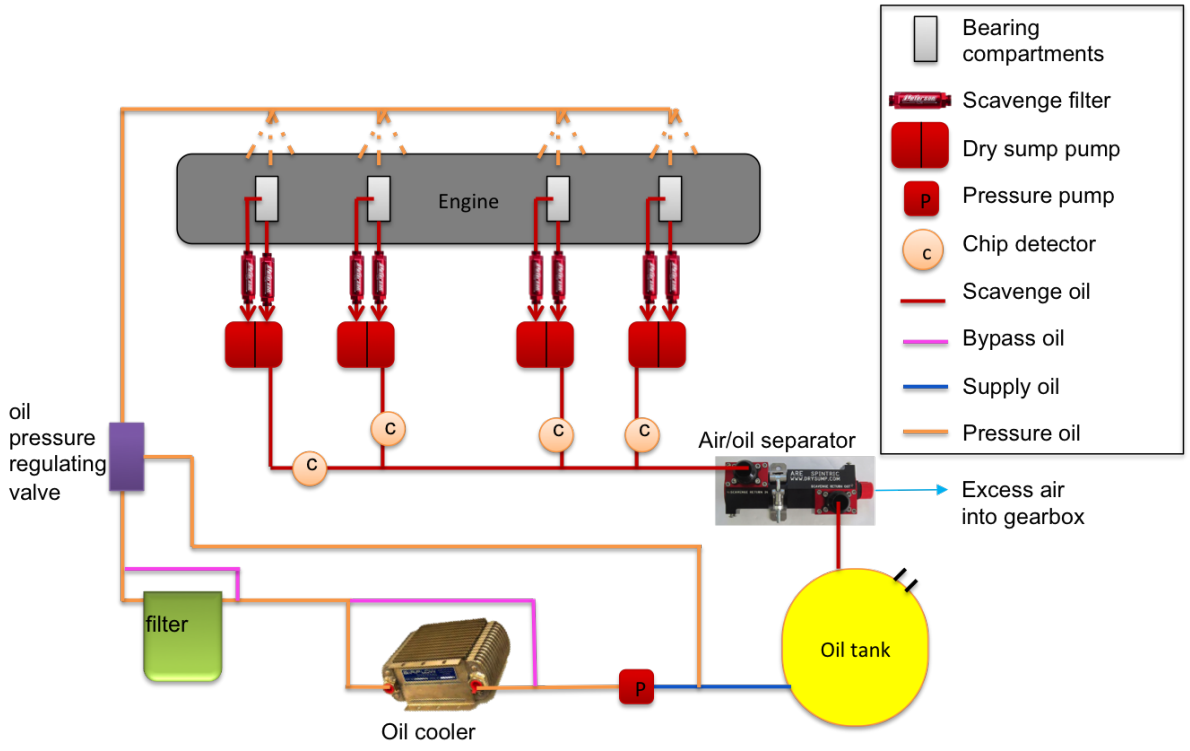

FIGURE 10.6: *Halcyon's* lubrication system enables continued operation in multiple vehicle orientations: vertical dive, edgewise hover, and airplane-like cruise.

Pressure and oil scavenge pumps are utilized to direct oil flow to and from the engine. Interconnecting tubes scavenge the oil at two different locations in each bearing compartment and gearbox, ensuring collection of oil from the engine over a large range of orientations. The scavenge pumps have excess capacity in order to drain each sump without gulping in different flight conditions. Screen filters are placed on each scavenge line to protect the pumps in case of engine failure, and chips detectors are located downstream of the dry sump pumps.

The air and oil mixture passes through a separator to separate the air from the oil. Air is sent to the top of the oil tank where it is vented back to the engine accessory gearbox. The oil tank

is pressurized to approximately 4 psi (27.6 kPa) to provide positive flow of oil and suppress foaming and pump cavitation [19]. A baffle with flap valves is placed in the center of the tank to enable flight in different orientations and operate in negative g loading. The oil tank is designed to provide constant supply of oil with an expansion space of at least 10% for an allowance in increase in oil volume due to thermal expansion and air in compliance with Federal Aviation Regulations section 33.17 [20].

In *Halcyon's* hot-tank lubrication system, the oil cooler is placed in the pressured side of the system, and the returning hot oil goes into the oil tank. In this type of system, smaller oil coolers are used because the maximum heat exchange occurs when the oil has less air. Hot oil from the tank is directed by a pressure valve through the oil cooler that has a bypass valve in case the oil cooler gets clogged. Cooled oil is then filtered through a 10 micron filter with an incorporated bypass valve. Filtered oil flow is delivered through internal passages by a single positive-displacement pump to each bearing compartment. The system is set so the oil pump start pumping oil after the compressor has built up enough inertia. A regulator is used to arrest oil flow until the engine has reached 80% speed.

Lubrication to engine components is provided by nozzles fitted at end of pressured oil lines in the casing of the engine. A last-chance filter is located just before the oil jet nozzles. Oil is sprayed on engine bearings and is then scavenged from each bearing compartments by a dry sump pump.

High performance oil seals are used to maintain the oil inside the sump and the inner cavity of the bearing compartment, which is enclosed by an outer cavity filled with high-pressured air. A slight vacuum is maintained in the outer cavity outside the sump, and labyrinth seals and carbon seals are used for air and oil leakage control.

Accessories such as oil scavenge and pressure pumps, pressure fuel pumps, and the starter/generator are driven by the engine accessory gearbox.

10.5 Fuel and Electric System Integration

The fuel tanks are designed with a low sump that is common to both flight orientations and are located inside the wings, which have an incident angle of 10 degrees that help maintain fuel in the same area. The struts provide fairings for fuel and electrical lines to be run from the wings to the fuselage and vice versa. Each strut provides shelter for either fuel or power lines, and both sets of lines are kept physically separate at all times for safety. These lines connect to junction boxes in the wings and fuselage to enable power transfer.

Once run through the D-tube, the power connections are routed through a small fairing that conceals the wires as they enter the wing itself. The wing junction box is accessible via a removable access panel (secured via quarter-turn fasteners) through which the user can plug in the fuel lines or electrical cables by hand.

10.6 Battery

Halcyon's propulsion system includes a small battery for use during two critical modes of the vehicle's operation: initial deployment and engine failure. As described in Section 6.10.1, *Halcyon* uses battery power during deployment from the C-130J until the engine starts up. Solar Impulse 2, manufactured by in Air Energy, was selected for use in *Halcyon* due to its favorable energy density of 0.16 hp-hr/lb (260 Wh/kg). The battery was sized to provide 6.65 hp-hr (4.96 kWh)

during deployment (i.e., when the vehicle is fully loaded) and to allow for a one minute hover in the event of engine failure. If the engine fails, *Halcyon* quickly ejects its payload and safely lands using the battery power. The battery is connected to the cooling system to prevent overheating.

10.7 Propulsion System Weight Breakdown

Figure 10.7 shows the component-wise weight distribution of the propulsion system. The total weight of the system is 486 lbs (220 kg). Halcyon implements currently available technology for the propulsion system. The engine, generator and controllers account for 70% of the weight of the propulsion system. Future improvements in these items are expected to reduce the weight of the engine-generator combination.

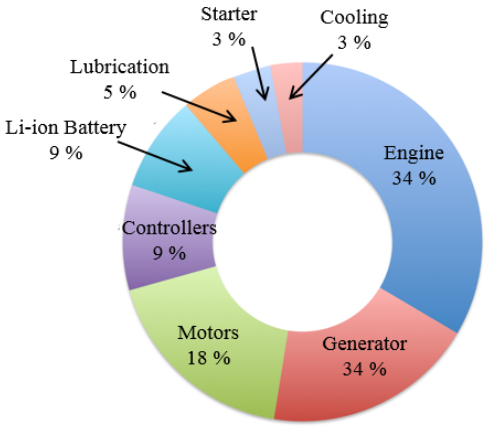

FIGURE 10.7: Weight breakdown of the *Halcyon* propulsion system.

11 Avionics and Sensors

The avionics and sensors suite has been designed to provide full autonomy for the *Halcyon* aircraft system during all phases of its mission. The avionics suite incorporates the latest in proven and commercially available technology to obtain the best performance out of the aircraft while minimizing size, weight and power requirements as much as possible.

11.1 Mission Requirements

Halcyon is designed to be deployable from the cargo bay of a C-130J in flight, precisely deliver a payload to specified GPS location, and then cruise at least 50 nm back to recovery locations. These mission segments introduce a variety of different challenges to the design requirements to successfully complete the mission. The sensor requirements change for each phase of the mission, and the area of coverage provided by the sensors changes as the aircraft transitions from edgewise to forward flight. The requirements identify three key phases for aircraft operation:

1. **Deployment from C-130J:** During the deployment phase, the aircraft system needs to perform the following functions: detect deployment, stabilize itself during initial launch, smoothly trigger rotor-spin up and finally switch to power from engine. This involves a careful selection of measurement techniques. *Halcyon* 's deployment is recorded by a number of sensors, including a strain gauges on each of the four landing gears, gyroscopes and

accelerometers (Inertial Measurement Unit), and the altitude sensing equipment, triggering the lubrication, cooling, and fuel systems to begin priming the engine. Upon launch, the control system must be able to provide orientation feedback to actuate the wing control surface that can be used for rapid stabilization. When the aircraft stabilizes approximately 6 seconds into its descent (see Section 6.10.1), the flight control triggers spin up of the rotors. Approximately 30 seconds after launch,the engine is primed and able to output full power, so the control system switches the power source from the deployment battery to the electric power generated by the engine.

2. **Vertical flight sense-and-avoid for payload delivery and landing:** Vertical flight and payload delivery require precise geographical location, current altitude, and trajectory to be followed. The avionics system must also be capable of obstacle sensing and avoidance to safely reach the designated delivery site. Precision hover is required for payload delivery and the avionics suite needs to provide feedback from the aircraft's sensors that should provide the control system with enough information to achieve steady flight of the aircraft and the underslung payload, even in gusty conditions (see Section 12.4.4). The avionics system must assist payload delivery with the TALON automated cargo hook by controlling the tether and closing the doors after delivery.

3. **Cruise back to recovery location:** During cruise, the aircraft transitions from helicopter to fixed-wing mode with feedback from the inertial measuring units. Cruising requires recognition of other aircraft sharing the airspace along with their trajectory to correct flight path and prevent accidents. The avionics system must provide velocity, orientation, angular rates and trajectory to support the transition maneuver and provide altitude above ground level in forward flight.

11.2 Basic Requirements

In order to select the appropriate sensor suite, it is first necessary to list the basic components required to accomplish the objectives of this mission:

- **Autopilot:** Typically, an autopilot includes a micro-controller as well as the inertial navigation system and some other sensors. This is responsible for providing control inputs to the various actuators based on measurements from all the sensors. Due to the multiple orientations in which *Halcyon* operates, the aircraft requires an autopilot unit capable of rotary-wing flight management as well as fixed-wing operation.

- **Inertial Navigation System (INS):** The deployment phase for the aircraft is critical and for the best movement and orientation accuracy the aircraft will need all 11 pieces of information from the Air Data Aircraft Heading and Reference System (ADAHRS), involving accelerometers (3 degrees of freedom), gyroscopes (3 degrees of freedom), a magnetometer (3 degrees of freedom), a pressure sensor (1 degree of freedom), and a temperature sensor (1 degree of freedom).

- **Satellite Navigation:** *Halcyon* is designed to deliver the payload at a precise location and must maintain a precision hover during drop-off. A Global Positioning System (GPS) receiver typically has 3.3 ft (1.0 m) location accuracy and thus is unable accomplish this requirement [21]. A Differential GPS (DGPS) or other GPS enhancements from ground

based sources are not readily available in all parts of South America, so it would require the installation of expensive transponder reference units if these were to be used. Instead *Halcyon* utilizes multiple satellite constellations like GPS, GLONASS, and Galileo simultaneously by incorporating a Global Navigation Satellite System (GNSS) receiver which can provide the aircraft's position with a precision of 0.8 inches (2.0 cm). Standard GPS receivers are incorporated into the design as a backup system, since GPS fulfills all other mission requirements and can be used to correct sensor drift.

- **Obstacle Sensing and Avoidance:** Obstacle sensing and avoidance is critical to the mission since it affects the safety of the people near the delivery site, other aircraft in the area, and the *Halcyon* . Simultaneous Location and Mapping (SLAM) using Light Detection and Ranging (LIDAR) creates a three-dimensional point cloud used to map potential obstacles. This information will be used by the aircraft for situational awareness and flight pattern adjustment. Infrared sensors will be used to detect people on the delivery site. As a secondary sense and avoidance system, *Halcyon* uses monocular cameras mounted on the wings and fuselage in combination with the Inertial Measurement Unit (IMU) to generate a map using a technique known as Monocular-SLAM. Hence, by combining these two sources of mapping, redundancy is introduced in the system that can be useful if one or more sensors provide errors (such as camera occlusions etc).

- **Traffic Collision and Avoidance System:** *Halcyon* shares the airspace with other disaster relief aircraft, and is therefore required to have constant communication with other nearby aircraft as well as companion *Halcyon* aircraft. A Traffic Collision Avoidance System (TCAS) is integrated into the avionics system for this task.

11.3 Sensors and Selected Equipment

The selection of sensors satisfying the previous capabilities that were defined as essential for the mission is described in the section. These sensors are required for to complete the previous capabilities defined as essential for the mission. The main qualities evaluated for sensor selection are compactness, minimal weight and reduced power consumption to make *Halcyon* as efficient as possible while meeting all the requirements to complete the mission objectives.

- **UAV Navigation VECTOR Autopilot:** This commercially available system was selected as the primary navigational unit for *Halcyon* [22]. It provides automated flight routines for both rotary-wing and fixed-wing aircraft, and its programmable software provides mission flexibility by enabling new maneuvers to be added to the programming. It also includes an integrated GPS and INS with 11 degrees of freedom and 1 kHz sampling rate, errors smaller than 0.5 degrees on pitch and roll, and smaller than 1 degree on heading. The unit has redundant sensors with constant built in monitoring as well as redundant CPUs and redundant power connections as safety features. The unit is compact with a weight of 0.04 lb (180 g) and has a low power draw of 2.5 W. The autopilot connects to the ground control station through a UAV Navigation Datalink transceiver.

- **Trimble BD920 GNSS Receiver:** This receiver module is integrated in the *Halcyon* avionics system to enable access to GPS, GLONASS, Galileo, QZSS and SBAS satellite constellations and provide horizontal location accuracy of 0.8 inches (2.0 cm) and vertical location accuracy of 1.6 inches (4.0 cm)[23]. This sensor acquires its signal in less than

45 seconds following a cold start and features signal re-acquisition in less than 2 seconds. This receiver also provides horizontal velocity with an accuracy of 0.01 kts (0.024 km/hr) and vertical velocity with accuracy of 0.04 kts (.072 km/hr). This receiver will be used with Novatel 42GOXX16A4-XT-1-1-CERT antenna.

- **Velodyne PUCK Lite LIDAR:** Used for obstacle sensing and avoidance, this LIDAR sensor is able to scan 300,000 points per second to generate a three-dimensional point data cloud with a 330 ft (100 m) range and 1.2 inch (3.0 cm) accuracy on a 30 degree horizontal field of view. The aircraft scans the path ahead and below when it is in hover mode. The sensor will be required for vertical navigation, landing, and payload delivery as it will be estimating the height of the aircraft during hover to ensure the aircraft is at the specified altitude of 50 ft.

- **BAE Systems AN/DPX-7 TCAS:** This Traffic Collision and Avoidance System (TCAS), supplied by BAE Systems, was selected for the *Halcyon* aircraft. This system is designed for UAVs, is lightweight and maintains the same capabilities of a full size system. This system is a transponder that operates by sending interrogator signals to nearby aircraft and receiving a return signal with location and trajectory. This information will be used to prevent collisions with the other *Halcyon* aircraft by altering *Halcyon's* course.

11.4 Sensor Operation During Flight

Deployment: During deployment, the crew prepares *Halcyon* by turning on all sensors using an integrated control panel. The electric motors and the engine are connected to the autopilot unit and engage when *Halcyon* is launched from the C-130J cargo bay. *Halcyon* senses it has been deployed using a combination of sensor inputs. States such as free-fall and acceleration in all three axes are determined by the accelerometers. The attitude of the aircraft is determined by the autopilot via onboard Kalman filter estimation using gyroscope and accelerometer measurements. The LIDAR measures distance of Halcyon from the cabin floor and instructs the autopilot when it has been deployed. The LIDAR measures the distance from the *Halcyon* to the cargo bay floor and knows it is not inside the cargo bay once it has been deployed. Airspeed from the pitot-static probe is used to measure the aircraft speed. Strain gauges on the landing gear will read changes in loading. The propulsion system then engages once it has been determined that deployment has occurred. It is important to use a sensor combination instead of a single sensor to avoid any false readings inside the C-130J cargo bay which could happen due to turbulence or other movement during flight.

11.4.1 Vertical Flight and Hover

LIDAR Based SLAM: *Halcyon* operates at low speeds and close to the ground in vertical flight mode especially during payload delivery and landing. In this orientation, *Halcyon* uses LIDAR and INS to provide obstacle sensing and avoidance. Scanning the terrain identifies potential obstacles and slopes which might compromise payload delivery integrity or impede landing, as shown in Fig. 11.1.

Halcyon first scans the location and performs a coarse analysis to determine which sites are most suitable. Sites are assigned a score that incorporates the proximity to the specified GPS coordinates. All the suitable landing sites will then be analyzed with a more robust process to determine the optimal landing zone closest to the specified target, as shown in Fig. 11.2. The

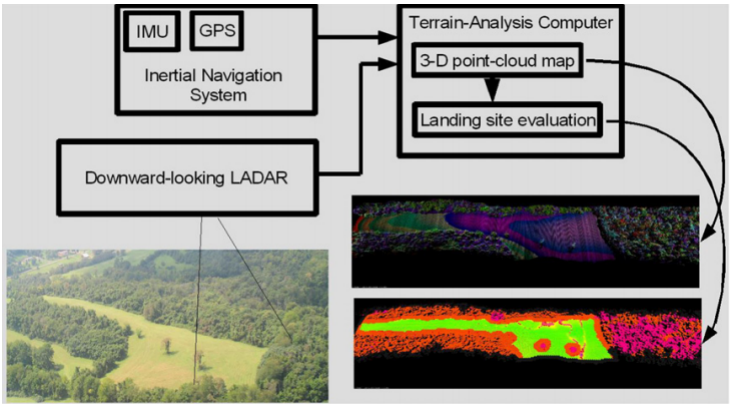

FIGURE 11.1: LIDAR scans local terrain for optimal delivery zones.

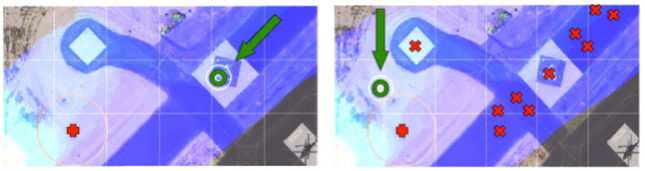

FIGURE 11.2: System selects optimal landing zone, weighted by proximity to specified GPS coordinates. Red crosses indicate debris; green circle indicates best available spot.

originally designated location takes preference, but the aircraft will not use it if it is determined to be unsafe. This method has already been proven to work on the Boeing Unmanned Little Bird [24] and enables use of proven technology on the *Halcyon* for mission effectiveness while ensuring the safety of both the people and other aircraft near the delivery site. The computing power required to make the map and perform the analysis is provided by onboard Intel i7-3610QE processors on a Stealth LPC-480G4 vehicle computer. Use of the LIDAR and computer requires a maximum of 100 W which *Halcyon* is equipped to provide.

Monocular SLAM: For a robust and safe operation, *Halcyon* uses SONY FCB-SE600 cameras mounted on the wings and fuselage in addition to the IMU for Monocular-SLAM as a secondary obstacle sense and avoidance system. This technique has been proven to work on all maneuvers for unmanned aircraft in GPS denied environments [25]. This method of obstacle mapping and avoidance, though less robust than the map created with LIDAR, which provides detailed information of slopes and obstacles on the ground, serves as an adequate backup in case of emergency.

Infrared (IR) Camera: Both obstacle sense and awareness methods will be complemented with Quark 2 IR camera manufactured by FLIR. This camera is able to detect people at up to 935 ft (285m). The IR camera complements the sense and avoidance sensors by identifying people at the delivery site to increase mission safety for the people on the ground. The camera may also be used for reconnaissance (searching for survivors).

11.4.2 Forward Flight and Cruise

Some of the sensors mounted for vertical flight will be unavailable in cruise because of prop-like orientation. Operation in has similar to deployment once the vehicle is stable. In cruise, *Halcyon* travels back to base along a predetermined route selected during mission planning. Navigation is performed mainly using GNSS. Because *Halcyon* will be sharing the airspace with other aircraft,

including other *Halcyon* aircraft also providing supplies or services to the relief effort, constant communication, TCAS, and obstacle detection and avoidance will be required to avoid accidents. *Halcyon* uses the TCAS and FLIR MLR10K-LX rangefinders to identify obstacles and adjust its flight path accordingly. Obstacle detection is constantly active.

11.4.3 Supporting Instrumentation

The following instrumentation is installed on *Halcyon* to safely operate and complete its mission.

- **Alliantech Omniprobe:** This probe, complete with heating provisions to prevent icing, is installed to measure airspeed and outside temperature and pressure. The inputs go to the autopilot unit which has provisions for air data inputs. This probe has capabilities of operating at up to 165 degrees from the probe axis by incorporating 18 different pressure ports on the tip [26]. Heating provisions are installed to ensure there is no icing on the ports. Deicing is critical for this sensor since icing is the most likely cause of malfunction. This data completes all the required degrees of freedom on the INS.

- **Garmin GRA5500 Radar Altimeter (RADALT):** This altimeter will be used to determine aircraft altitude above ground level while in forward flight. This RADALT measures altitude above the ground from 0 to 2,550 ft (777 m) while in forward flight with 5 ft (1.5 m) accuracy. Its function is to assist the pitot-static probe and the GNSS in getting altitude data while if the aircraft flies close to the ground. The RADALT uses a pair of AD43011-F16 antennas installed on the wing.

- **Navigation and Anti-Collision lights:** These are installed on the wings to let *Halcyon* be visually spotted in the air. Landing lights are installed to illuminate the ground beneath the aircraft when it is in hover mode. The lights are also used to give the aircrew signals when *Halcyon* is ready for launch or if a problem has been detected and the aircraft is unable to be launched. When a pre-flight systems check is triggered, a confirmation message appears and indicates progress of the systems check on the touchscreen. When the check is complete it triggers one of the following scenarios:

  1. Solid green LED lights turn on if all systems are in order.
  2. Solid white LED lights turn if there was an error with the system check, requesting the aircrew member to perform the check again.
  3. Flashing strobe LED lights turn on if a problem is detected and the launch needs to be aborted.

- **Astronics 1342 Electronic Circuit Breaker Unit (ECBU):** The ECBU is installed for remote activation of all sensors. This ECBU is programmable and has redundant power supplies and processors for safe operation. In addition to that it also provides voltage and current monitoring and can control relays.

- **Touchscreen Monitor:** The purpose of this monitor is for crew personnel to use while preparing the aircraft for a mission. This touch screen will be used to initiate deployment procedures and will interact with the ECBU to turn on all sensors prior to deployment. The touch screen is a Panasonic Toughpad FZ-M1 which is a MIL-STD-810G and MIL-STD-461F certified ruggedized touch screen computer and has its own battery and processing capabilities. Linked to the aircraft's health monitoring system, the panel is installed under

a side panel on the fuselage and enables C-130J personnel to manually perform a systems check of each component.

- **Strain Gauges:** Strain gauges will be installed on the payload delivery system and on the landing gear. They will provide feedback on payload angle with respect to the aircraft when delivering a package. The gauges on the landing gear will be used to determine the angle of the vehicle while landing and during the deployment phase by reading the change in strain experienced when leaving the C-130J.

De-ice provisions will not be implemented to *Halcyon* outside of the pitot-static probe. De-ice systems are heavy and have high power requirements. There are also large costs associated with developing and certifying an aircraft for flight into known icing conditions [8, 27]. With mission planning this issue will be able to be circumvented by selecting a flight path away from zones with high humidity and low temperature where icing could be a problem.

11.5 Ground Control Station (GCS)

UAV Navigation's GCS system will be used for *Halcyon* [28]. This GCS interfaces with the autopilot through the transceiver installed on the *Halcyon* and communicates at a range of up to 108 nm (200 km), well beyond the 50 nm mission requirement. The GCS transfers data at a rate greater than 37 MB/s, enabling live video feed and real-time operational parameter data-stream . The GCS, shown in Fig. 11.3, will be used to plan and execute missions. *Halcyon* is capable of fully autonomous operation, but the GCS also offers the ability to alter the mission with waypoint navigation and manual intervention during any phase of *Halcyon* 's autonomous operation, an important option in a disaster relief scenario where the situation and priorities may shift rapidly. The GCS is configured with alarms for various failure events such as sensor failures, voltage drops, and low fuel warnings. Up to 16 *Halcyon* vehicles can be controlled with a single GCS at any given time. The operator can see active *Halcyon's* on the screen simultaneously and give individual commands to the unit of choice. Aircraft heading and live video feed can be displayed for any *Halcyon* selected while alarms for any aircraft can show up from any screen.

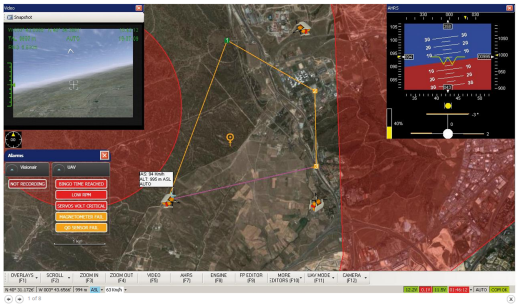

FIGURE 11.3: Sample view of GCS system operation.

11.5.1 Hardware

The GCS consists of a laptop loaded with UAV Navigation GCS software and connected to a bi-directional antenna and a joystick controller. It can be purchased by the customer for $11,175 USD with any laptop of preference and UAV Navigations antenna and controller. The customer also has the option to use the GCASE from UAV Navigation, which includes a Dell Ruggedized Laptop with all the required software and hardware in an integrated waterproof case.

11.6 Safety

All components selected have integrated safety and redundancy measures and are insensitive to rough conditions. *Halcyon* has multiple backup systems and is capable of utilizing the installed systems to complete many of the same tasks, and therefore individual sensor failure will not put people, the aircraft, or the mission outcome at risk.

11.6.1 Navigation

The autopilot unit built-in has a redundant CPUs and can function normally following sensor failure in the integrated INS. This is critical to the *Halcyon* system, since the loss of communications and control would result in loss of the aircraft. For this reason two separate autopilot units will be installed to provide added redundancy to the system. The autopilot is connected in real time to the GCS and is able to send alarms to the operator regarding the loss of any of the sensors or conditions like *Halcyon* loosing altitude or low voltage in the system.

The GNSS receiver, has 220 channels available and operates on multiple satellite constellations. In case of sensor failure, each autopilot unit has a GPS receiver that can be used as an alternate method of navigation. Measures are in place in case of loss of GPS signal, *Halcyon* can use its INS to navigate until the signal is reestablished. In case all satellite positioning receivers malfunctioning and there is no possibility of reestablishing satellite navigation, *Halcyon* will automatically return to the GCS using the INS. The three-tier navigation redundancy is shown in Fig. 11.4. *Halcyon* has an active traffic collision avoidance system and also features navigation and landing lights for visual identification.

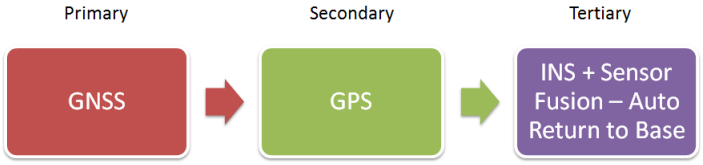

FIGURE 11.4: Navigation system hierarchy.

11.6.2 Obstacle Sensing and Avoidance

Halcyon uses LIDAR based SLAM as primary means of obstacle sensing and avoidance. In case of system failure, the *Halcyon* uses cameras installed on the wings and fuselage to perform Monocular-SLAM. If both systems fail, the aircraft can be piloted remotely by an operator using the GCS live feed from the cameras on the aircraft.

11.6.3 System Power Failure

In case of generator failure, *Halcyon* draws power from two backup batteries. Each battery has sufficient capacity to operate all sensors for 30 minutes. Manufactured and sold by Air Energy, these batteries have a high energy density of 0.16 hp/lb (260 Wh/kg) to minimize weight and volume. Integrated relays controlled by the ECBU ensure that power is routed in the correct direction.

TABLE 11.1: Avionics system bill of materials.

Component	Model	QTY	Power (hp)	Power (W)	Weight (lb)	Weight (kg)	Total cost (2015 USD)
Autopilot	UAV Navigation Vector	2	0.00	2.50	0.80	0.36	$ 15,000
GNSS Receiver	Trimble BD920	2	0.00	1.30	0.10	0.05	$ 5,000
GNSS Antenna	Novatel 42GOXX16A4-XT-1-1-CERT	2	0.00	1.20	1.00	0.45	$ 1,464
LIDAR	Velodyne Puck LITE	2	0.01	8.00	2.60	1.18	$ 16,000
Radar Altimeter	Garmin GRA5500	1	0.01	13.75	3.50	1.59	$ 13,300
Radar Altimeter Antenna	AD43011-F16	2	-	-	0.60	0.27	$ 400
TCAS	BAE Systems AN/DPX-7	1	0.03	40.00	6.00	2.73	$ 28,000
Transceiver	UAV Navigation TELEM06	2	0.01	16.50	4.22	1.92	$ 2,376
Camera	Sony FCB-SE600	6	0.00	1.00	1.12	0.51	$ 1,440
Touch Screen	Panasonic Toughpad FZ-M1	1	-	-	1.20	0.55	$ 3,224
Electronic Circuit Breaker	Astronics 1426-30	1	-	-	10.50	4.77	$ 12,000
IR Camera	FLIR Quark 2	6	0.00	1.00	0.10	0.05	$ 24,000
CPU	Stealth LPC-480G4	1	0.06	84.00	4.80	2.18	$ 1,621
Pitot Static Probe	Omni-probe	1	0.01	10.00	-	-	$ -
Battery	Air Energy	2	0.08	109.38	1.69	0.77	$ 143
Total			**0.16**	**218.75**	**39.03**	**17.74**	**$ 123,968**

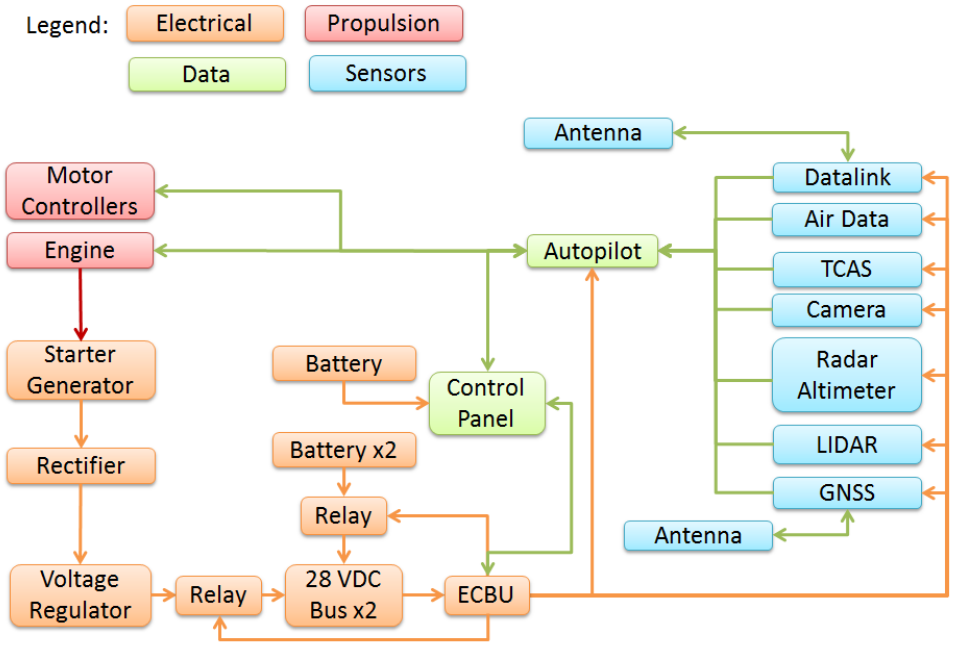

FIGURE 11.5: Layout of *Halcyon's* avionics suite.

11.7 Avionics Package Breakdown

Table 11.1 is a bill of materials for the complete avionics sensor package installed on each *Halcyon* aircraft. Figure 11.5 shows a schematic of how the avionics system is connected.

Control System Performance Simulation

Outbound transition

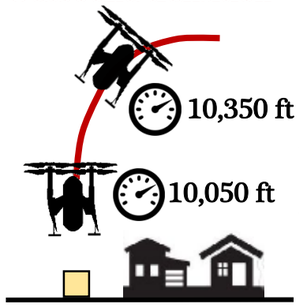

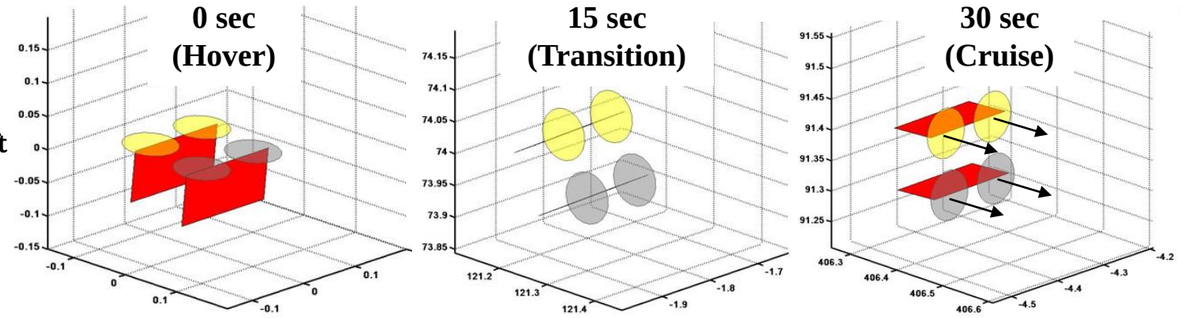

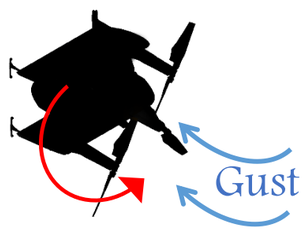

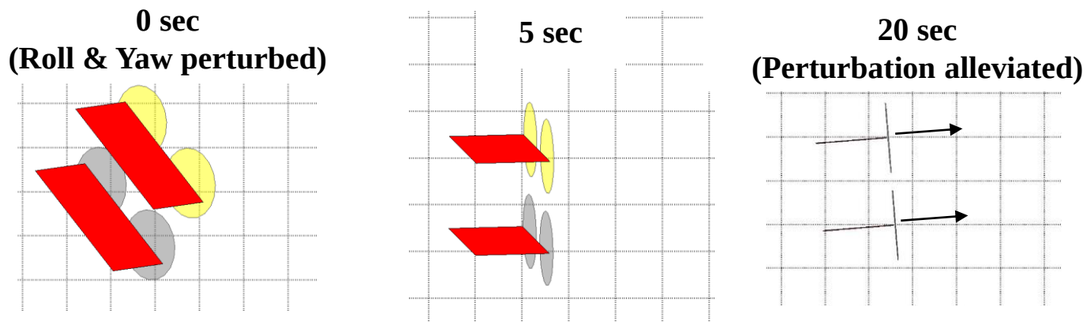

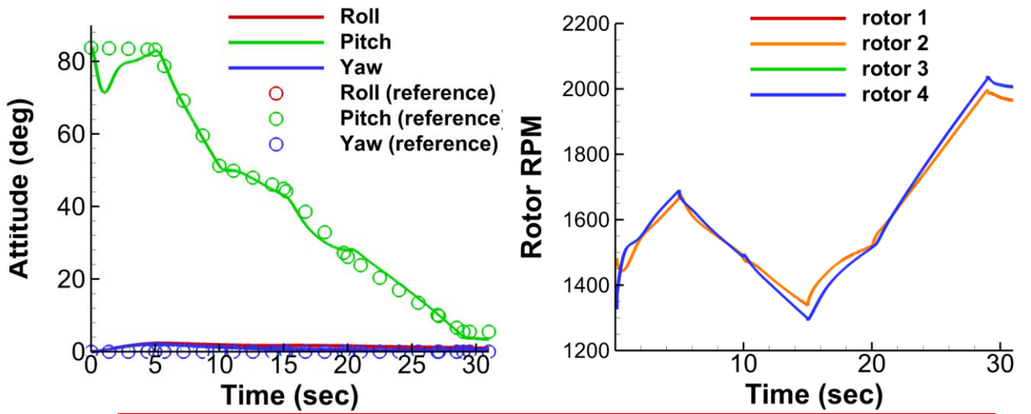

Rotor RPM changes to follow reference attitude

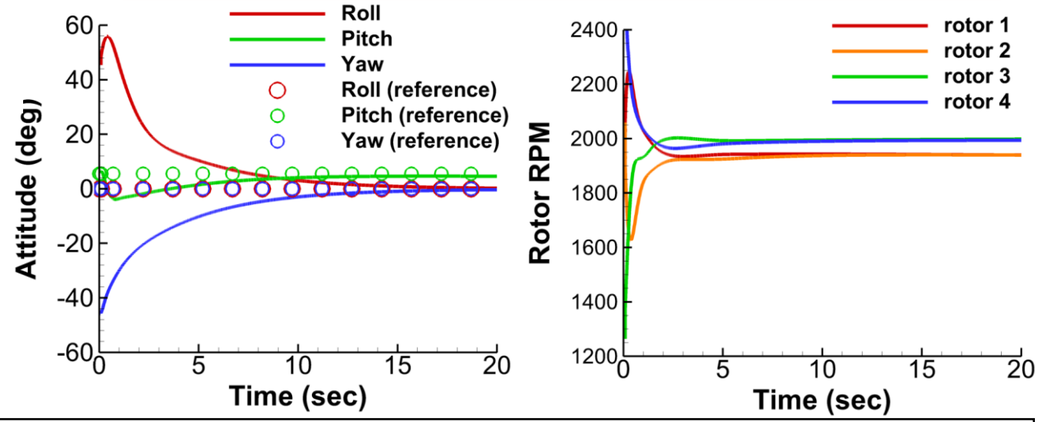

Control System Architecture

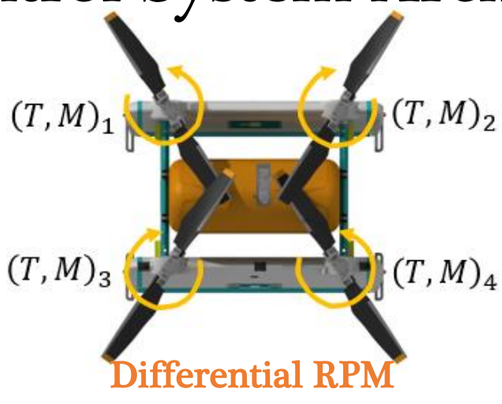

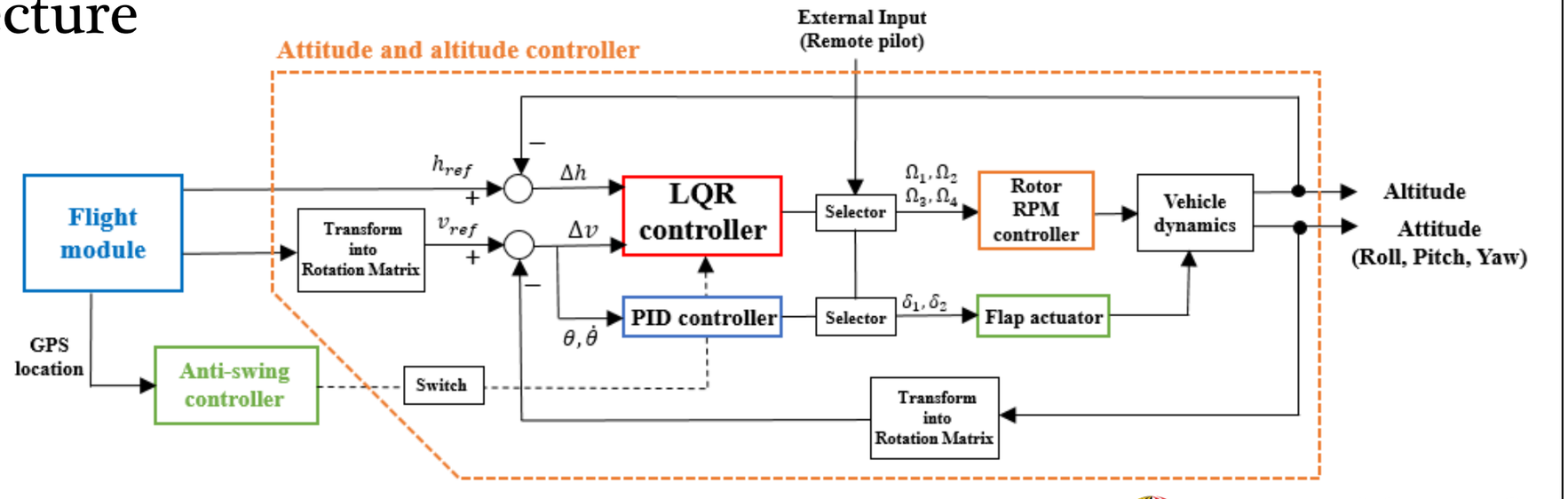

Halcyon

Halcyon features differential RPM control using robust LQR schemes which enable transition maneuvers and gust alleviation during mission.

UNIVERSITY OF MARYLAND

12 Flight Dynamics and Control

To complete the mission successfully, care is taken to design the aircraft to be naturally stable and sufficiently maneuverable. The mission specified in the RFP includes a wide variety of flight conditions, such as the launch from the C-130J into a high speed, turbulent aerodynamic environment [29, 30], descent flight, autonomous precision hover with a descending slung load, steady cruise and inbound/outbound transition from the delivery and landing area. Furthermore, this design also accounts for unexpected perturbations during the launch from the C-130J, wherein the aircraft should attain a stable attitude regardless of potential disturbances experienced during deployment (e.g., gust, non-ideal deployment attitude or pitch/roll/yaw perturbations). The quadrotor configuration selected for this mission allows for four independently regulated rotor thrusts and torques. Therefore, *Halcyon* features a distinct advantage over other configurations, especially for a mission that emphasizes precision hover capability for disaster relief.

12.1 Flight Dynamics Model

A nonlinear rigid body flight dynamic model of the aircraft is used to evaluate *Halcyon's* performance, analyze the stability of the aircraft, and simulate the complicated maneuvers used to describe the filght profile of the aircraft (e.g. deployment and transitions between hover and cruise). The simulations were conducted using an in-house rotorcraft analysis code, which was extended for *Halcyon's* configuration.

Halcyon consists of multiple aerodynamic components, including four rotors and hubs in a tandem arrangement, a lifting-body fuselage, and biplane wings with trailing-edge flaps. Each of these components produce aerodynamic and inertial forces and moments. The vehicle free body diagram operating under representative conditions is shown in Fig. 12.1.

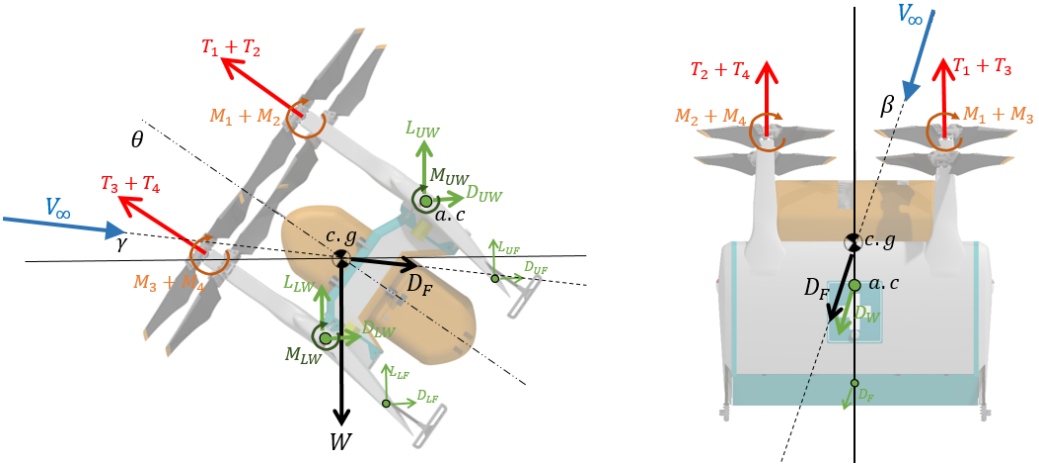

FIGURE 12.1: Free-body diagram of the various forces and moments acting on *Halcyon* .

The rigid-body vehicle flight dynamics which are used for the simulation accounts for the forces and moments acting at the center of gravity, which are generated by the rotors, the wings and flaps, fuselage, and the inertia of the vehicle. Multibody kinematics are used to incorporate rotor-body couplings into the simulation. The individual rotor blades are assumed to be rigid because of the low aspect ratio and high flexural stiffness (see Chapter 6). The rotor aerodynamic forces are calculated from a blade element analysis with the airfoil aerodynamic loads obtained

using look-up tables for angle of attack and operating Reynolds number from experimental data for both normal and reverse flow conditions. The Pitt-Peters dynamic inflow model is used to compute the induced inflow as a function of rotor thrust distribution and flight condition.

Fixed wings are considered to be low aspect ratio three-dimensional lifting surfaces. Oswald's efficiency factor is used to correct the induced drag for wing tip effects and the lift-curve slope is adjusted to account for the aspect ratio. The rotor prop-wash increases the dynamic pressure over the wings and is incorporated into the calculation of aerodynamic loads. The flap control surface included in the wing system is also modeled using two-dimensional airfoil tables with correction for three-dimensional flow effects. The aerodynamic loads for both the wings and flaps were obtained using look-up tables from experiments. To calculate fuselage parasitic drag, the equivalent flat-plate area of the fuselage was obtained using the aircraft's gross weight based on scaling laws, and subsequently updated using a more detailed drag estimation (see Chapter 9).

12.2 Control system

Halcyon is designed with two flight modules: (1) A navigational autopilot, and (2) A stability augmentation system (SAS) for attitude stabilization and gust disturbance rejection. The SAS is always active in flight, while the navigational autopilot can be selectively activated when required. Figure 12.2 shows the control system architecture of *Halcyon*. The altitude and attitude controller was designed based on the flight models of a tail-sitter VTOL which requires transition maneuvers during a mission [31]. Here, v means a state-space representation of flight dynamics, $v = [u, v, w, p, q, r, \pi, \theta, \psi]$. The controller features primarily a linear-quadratic regulator (LQR) based feedback, which regulates the rotor(s) RPM during all other stage of mission, while a proportional-integral-derivative (PID) controller is used to control the deflection of the wing flaps following deployment from C-130J and the hover segment for payload delivery. However, at all times, both control systems are simultaneously active. While the LQR control scheme requires all the state of the system, it is appropriate as the control system because of its performance and robustness. However, a simple PID controller was sufficient as a single degree-of-freedom wing flap contol. The reference altitude and attitude are given by the flight module which operates autonomously using avionics and sensors (see Chapter 11). *Halcyon* features multiple redundancy to increase flight safety in flight module, and a traffic collision and avoidance system (TCAS) is also installed that communicates with other vehicles to maintain safe clearence around each *Halcyon* vehicle.

Another capability of *Halcyon* is delivering a payload using cable even in gusty flight conditions. As shown in Fig. 12.2, an anti-swing flight controller was also designed to minimize the system response to gust perturbation and satisfy mission requirements by using rotor differential RPM (see, subsection 12.4.4). The anti-swing controller tracks two main states: (1) cable angle with regard to vertical and angular rate, and (2) current GPS coordinates offset from target payload point.

12.2.1 Differential RPM

Thrust and torque for each rotor is regulated using RPM control. Control can be achieved in all flight modes using variable RPM and no blade pitch change is required. The rotational speed of each rotor is regulated using a motor controller which operates within the framework of a feedback system that is coupled amongst all four rotors. *Halcyon* operates in hover mode using a conventional quad-rotor control strategy. Transition between helicopter and airplane mode

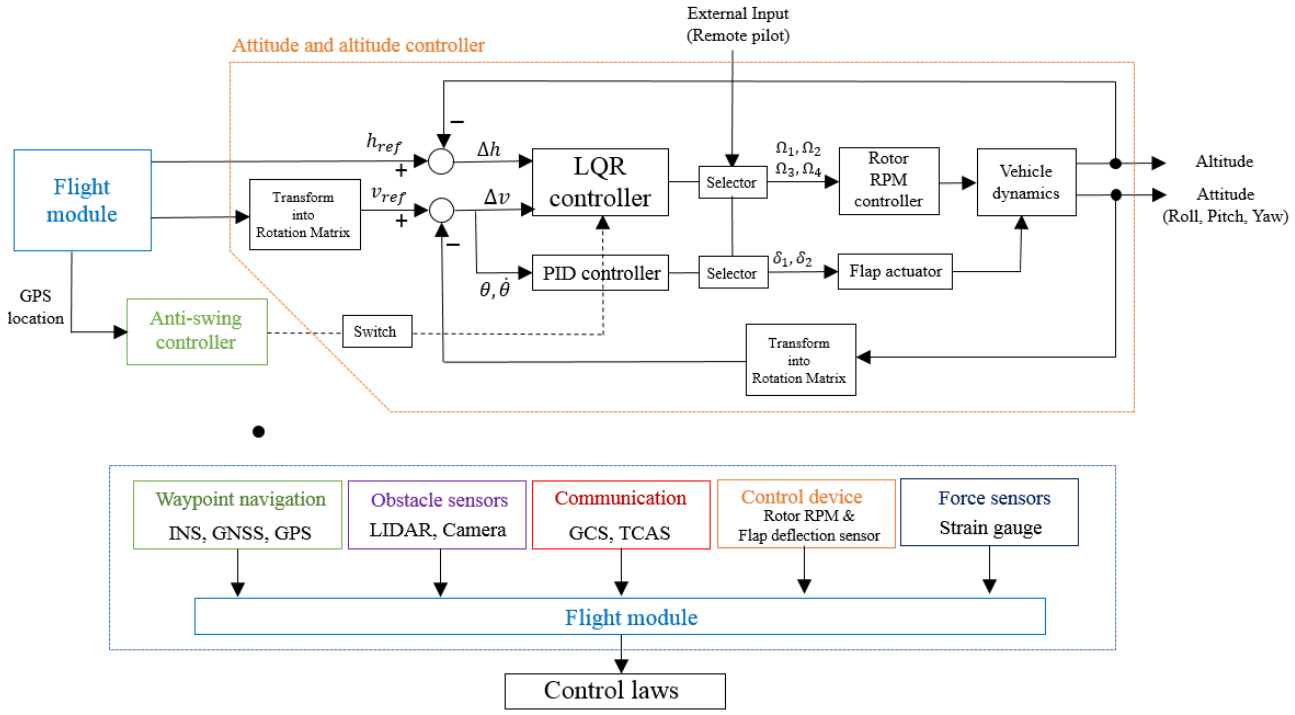

FIGURE 12.2: Control system architecture aboard *Halcyon* .

is attained via the pitching moment provided through RPM variation of the proprotors. The main benefit of this configuration is that the quad-rotor methodology is retained in both hover and forward flight modes with no redundant actuators, reducing the overall complexity of the systems involved [32]. Therefore, a differential thrust or torque of a pair of rotors can induce roll, pitch and yaw motions in both hover and forward flight modes as shown in Fig. 12.3.

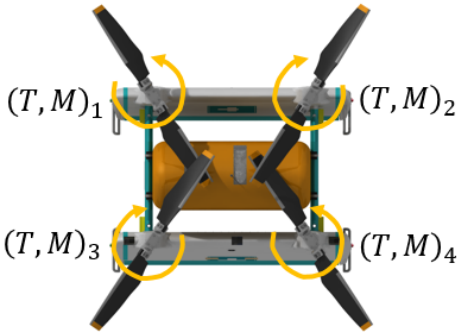

	Roll	Pitch	Yaw
Hover	Differential Thrust $T_{1,3} - T_{2,4}$	Differential Thrust $T_{3,4} - T_{1,2}$	Differential Torque $M_{2,3} - M_{1,4}$
Cruise	Differential Torque $M_{2,3} - M_{1,4}$		Differential Thrust $T_{1,3} - T_{2,4}$

FIGURE 12.3: Attitude control using diffential PRM.

12.2.2 Wing flap

The upper and lower wings are each equipped with a single element trailing edge flap to regulate the pitch attitude control of the aircraft in flight. The flap chord is 20% of the wing chord, and extends for 90% along the span, as shown in Fig. 12.4. The control surface is used as an elevator to orient the aircraft into a gliding cruise (before the rotors are started). This enables safe and predictable conditions during deployment for the rotor blades to spin up as discussed

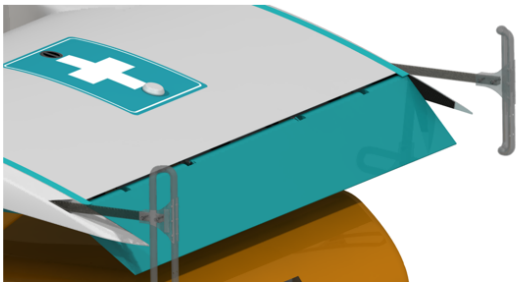

FIGURE 12.4: Wing flap with 25° maximum deflection.

in Chapter 6. The servo-actuators and the structures around the flap are designed to allow up to 25° deflection from the reference position.

Additionally during hover, the prop-wash from the rotors causes a lift on the wings, which results in a hover attitude of 77° in order to offet the lateral forces from the wings (as opposed to the ideal case of 90°). To reorient the vehicle along the vertical in hover, especially during the payload delivery phase of the mission, wing flaps are actuated to alleviate some of the forces generated by the wing. With the flaps deployed to their maximum extent, the hover attitude is reduced to a 84° with regard to horizontal.

12.3 Stability

Dynamic stability refers to the tendency of the aircraft to return to its reference state following a perturbation by exhibiting a damped oscillatory response [33]. To analyze the stability of *Halcyon*, longitudinal and lateral dynamic models were developed based on a linearized six degrees of freedom (DOF) flight dynamics model, which assumes small disturbances about the trim condition. The results are based on fully coupled dynamics models, with longitudinal and lateral modes plotted separately for clarity. Only eigenvalues with a negative real component correspond to stable modes, while the magnitude of the imaginary component is the damped frequency of oscillation.

Figures 12.5(a) and 12.5(b) show the root loci of longitudinal and lateral modes of vehicle, respectively, at various forward flight speeds at GTOW. The longitudinal modes are heave damping, phugoid and short period. Lateral modes are roll damping, dutch roll, and spiral. The modes are well separated in both frequency and damping as a clear distinction can be drawn between the hover modes (0–20 knots) and forward-flight modes (60–100 knots). The results obtained without the payload were similar to those with payload shown in Fig. 12.5, and are omitted for simplicity. The closed loop system is stable over the entire flight envelope. As the flight speed increases from 60 knots (110 km/hr), the controller stabilizing effect on the both lateral and longitudinal modes are increased.

12.4 Mission Maneuvers

The uniqueness and challenge of the current RFP is the deployment of a VTOL capable vehicle from the rear of a cruising C-130J transport. Figure 12.6 shows the current mission profile. The various stages of the mission are divided into: (1) Deployment, (2) Descent flight, (3) Transitions (cruise to hover and hover to cruise), (4) Precision hover for payload drop, (5) Cruise, and (6) Landing at base to complete the mission. Each of these sections present engineering and technical

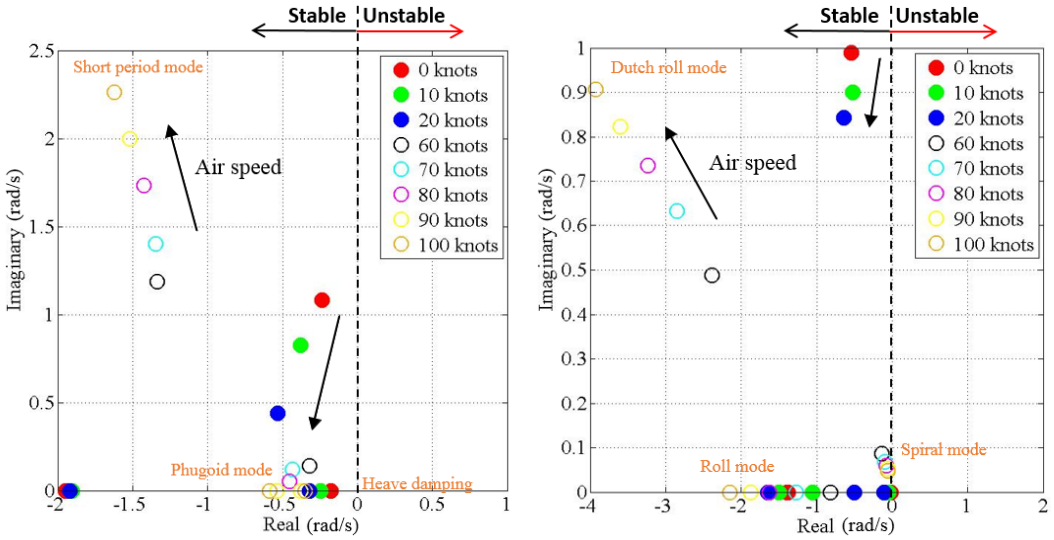

(a) Longitudinal mode

(b) Lateral mode

FIGURE 12.5: Pole diagram depicting the closed-loop stability of *Halcyon* .

challenges in the design and optimization of different sub-systems of *Halcyon* . These challenges and the corresponding solutions are detailed in this section.

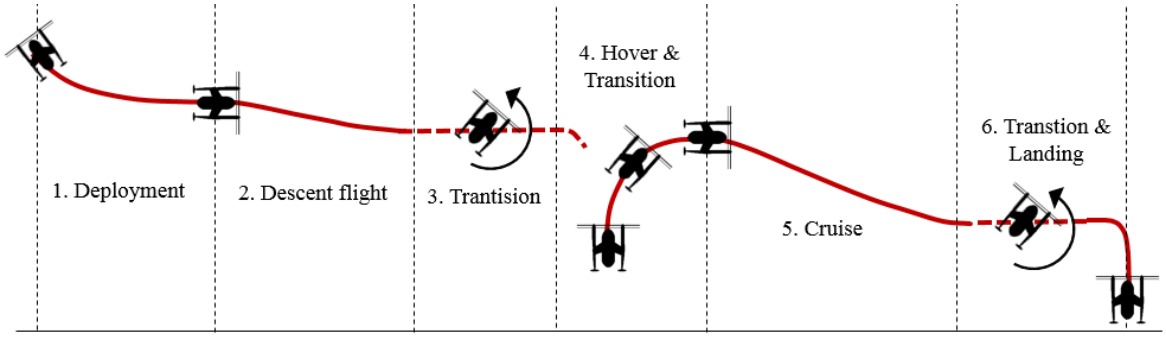

FIGURE 12.6: Mission profile of *Halcyon* .

12.4.1 First Stage: Deployment

The first stage (1^{st} stage in Fig. 12.6) of the mission involves launching the vehicle from the aft ramp of the C-130J while it is flying at 15,000 ft ISA at 175 KTAS. To ensure the safety of the crew and emergency personnel, the rotors or any other engine component cannot be allowed to rotate inside the cargo bay, and instead must be started after the vehicle has achieved sufficient separation from the parent aircraft.

During launch, *Halcyon* rapidly transitions from stationary flow to a high dynamic pressure environment. Upon deployment, most oscillations of the vehicle occur about its pitch degree of freedom. This is because the turbulent flow behind the C-130J ramp is mostly upward with no cross flow components, and the dropped payload pitch attitude changed while yaw and roll attitude are close to 0° [29, 30]. Without stabilizing the aircraft in a pitch attitude, the loads experienced by the rotor blades could (i) cause the blades to strike each other or the airframe;

(ii) lock the blades from rotating; and (iii) tumble the aircraft in an uncontrolled descent from which recovery becomes difficult.

According to the RFP, the vehicle has to achieve stable hover above 11,000 ft. Therefore, *Halcyon* is designed to take full advantage of the aerodynamic forces generated by the wings coupled with the vehicle's CG as it exits the C-130J cargo bay and enters free-fall mode. Designed to orient with pitch down tendency, *Halcyon* uses its wings (cambered NACA 4412 airfoil) and its nose-down pitching moment to achieve a favorable vehicle pitch attitude before spinning up its rotors, much like fixed-wing aircraft that utilize an empennage for shuttlecock stability.

To investigate the feasibility of this strategy, a simulation of the maneuver was conducted in the following manner. The wing flap setting was determined using a proportional-derivative (PD) controller (see Section 12.2) to maneuver the aircraft into cruising forward flight. As specified by AHS in the response to this design team's Request for Information, the maximum deflection of the C-130J ramp angle was assumed to be 12° below the C-130J's longitudinal axis. The ramp deflection as well as the flight speed of C-130J were considered in the initial conditions for the deployment simulation. Furthermore, to account for a non-ideal deployment scenario, pitch moment disturbances of ±65°/s were applied initially based on experimental and numerical studies conducted for a cuboid box deployed out of a generic transport aircraft [30].

The simulation results upon launching from the C-130J are shown in Fig. 12.9, which tracks the vehicle from t = 0 s to t = 37 s, i.e., from deployment to cruising in stable forward flight with the rotor spinning. Time history of the vehicle pitch attitudes were tracked through the deployment phase (t = 0–7 s), for two different vehicle configurations; the vechicle with a wing and without a wing. For the vehicle with the wing case, the time history of flap deflection angle as a means of pitch attitude control is also tracked.

Without a lifting surface, the pitch attitude changes in accordance with the initial pitch moment disturbance, and the aircraft converges to a pitch attitude caused by stationaly rotor drag force, with the free-stream flow going up through the disk as shown in Fig. 12.7(a). The rotor blades are kept from windmilling through the use of a torque limiter in the hub, a lack of which would require the motor to overcome this torque to begin spinning the rotors in the right direction. Therefore, significant aerodynamic loads are experienced by the rotors in this orientation, which may cause structural damage to the blades.

However, with the addition of wings, *Halcyon's* flight dynamics are altered such that the aircraft attains a vertical dive as shown in Fig. 12.7(b). In this orientation, the rotors operate in axial flight similar to a propeller aircraft and the aircraft pulls out of the dive into a gliding cruise using pitching moments generated by the wing flaps as shown in Fig. 12.9, where the flap deflected upward steadly after alleviated all pitch oscillations.

After attaining a favorable vehicle pitch attitude, *Halcyon's* startup of the rotor till stable forward flight cruise is initiated. After t = 7 s from deployment, *Halcyon's* achieves a stable gliding descent. The electric motors engage to rotate the proprotors, enabling the aircraft to transition into powered forward flight through a pull-up maneuver in about t = 30 s. Throughout the startup phase and transition into forward flight of 66 knots, the power required by any of the rotors never exceeds the available power from the electric motors at this altitude. There is a buffer of around 15% of the available power, i.e., excess power, that could be used towards gust tolerance and active stabilization requirements.

Figure 12.8 shows the flight trajectory of the vehicle from launching to powered forward flight (t = 0–37 s). The vehicle flies about 1,000 ft (300 m) in horizontal direction with 400 ft (120 m)

altitude loss at t = 7 s while it achieves a stable gliding descent from launching. After spinning up the rotor, during transition to forward flight, it travels about 3,000 ft (900 m) further in horizontal direction. At that time, the altitude is 14,000 ft (4,300 m) ISA.

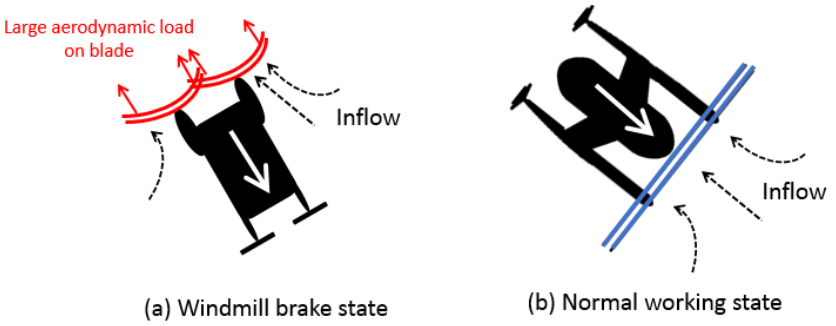

FIGURE 12.7: Orientation of vehicle upon deployment (a) without and (b) with, the presence of wings.

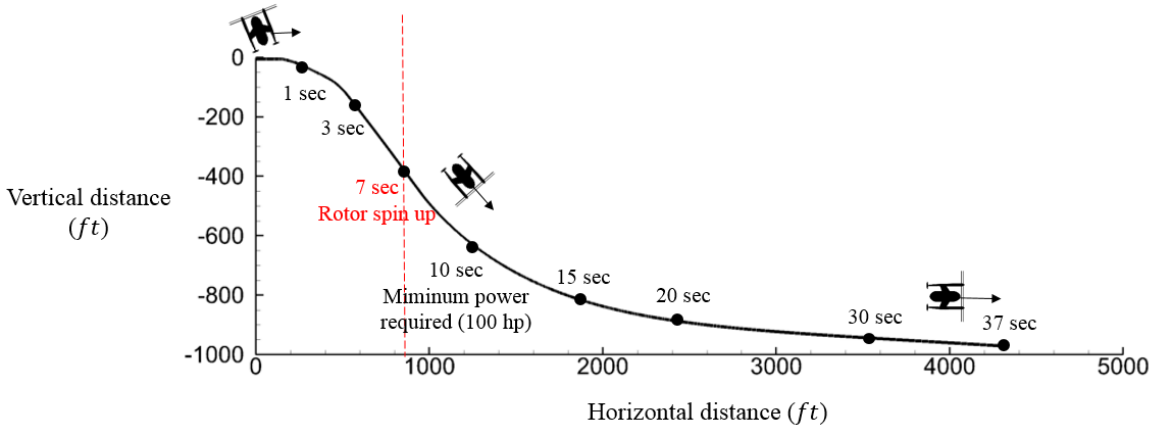

FIGURE 12.8: Vehicle flight trajectory (t= 0–37 s).

12.4.2 Second Stage: Descent flight

As soon as *Halcyon* acheives stable forward flight mode using powered rotors, the autopilot is used to calculate the required descent angle based on GPS coordinates between current location and disaster location for fuel efficient and safe descent flight.

Figure 12.10 shows the required power (upper left) and effective wing angle of attack (upper right) for combination of flight speed (radial direction) and flight path angle (azimuthal direction). The fuel consumption contour are also shown in Fig. 12.10 for the optimum descent condition. The optimum descent angle and speed are obtained by considering wing stall condition (below 20°), autorotation boundary, and moderate speed (below 80 knots),

During descent flight, from altitude of 13,900 to 10,350 ft (4,240 to 3,150 m), the following challenges are encountered: (i) the wing stall occurs due to high pitch attitude for trim condition; (ii) the rotational speed of rotors are accelerated by inflow at high descent angle and velocity, and the vehicle have difficultly recovering from gusts because the differential RPM is used as a flight attitude control module; and (iii) fast descent velocity requires more power and range for transient maneuver during or at the end of descent flight. By considering those conditions, optimum descent conditions are shown in the black box (descent speed from 60 to 80 knots (110

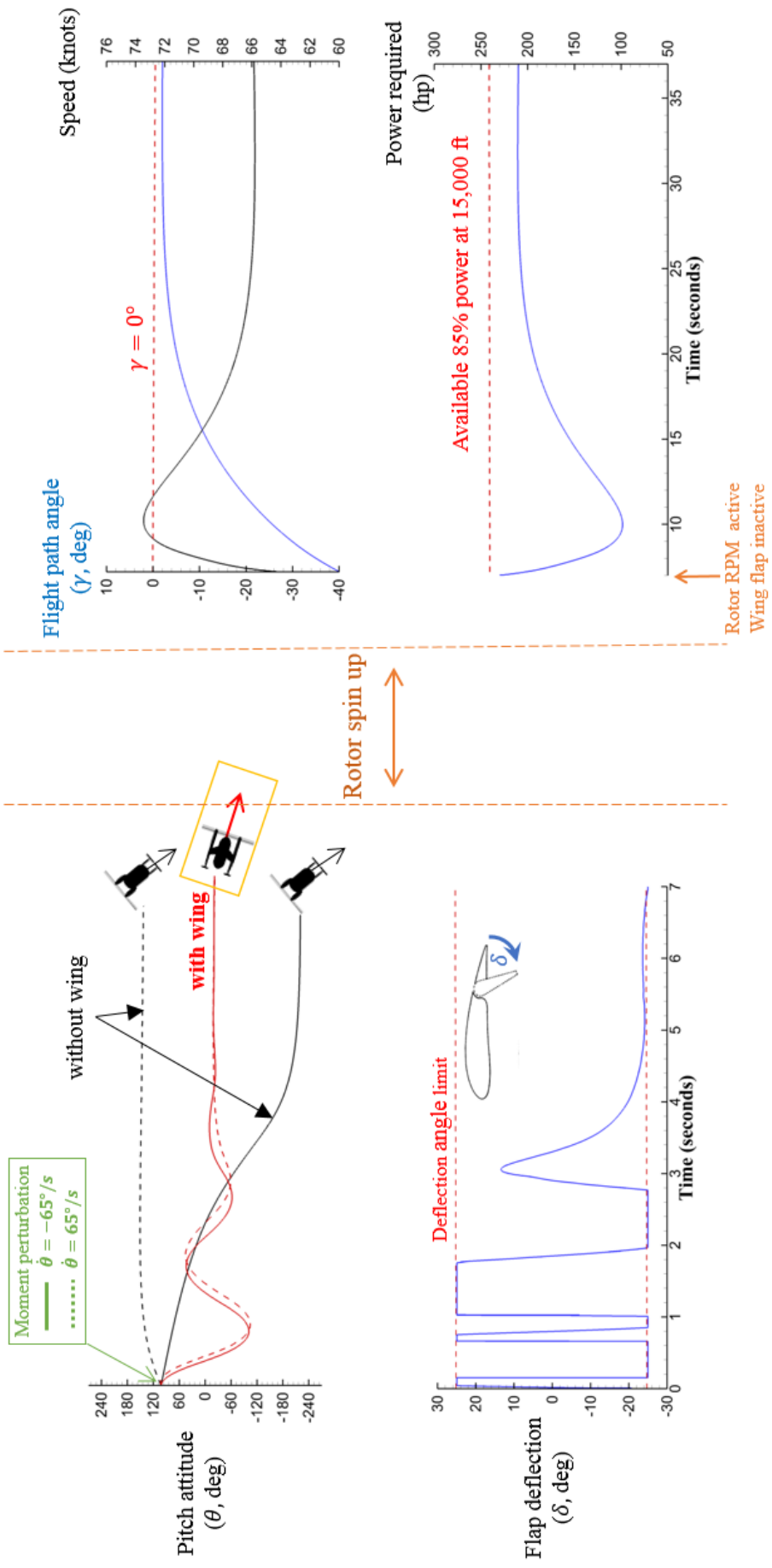

FIGURE 12.9: Vehicle history before(t= 0–7 s) and after(t= 7–37 s) spinning of the rotor.

to 150 km/hr) and descent angle from -20° to 0°). The fuel consumption during the descent flight are estimated for the optimum descent conditions, ranging 0.16% to 10.34% total fuel.

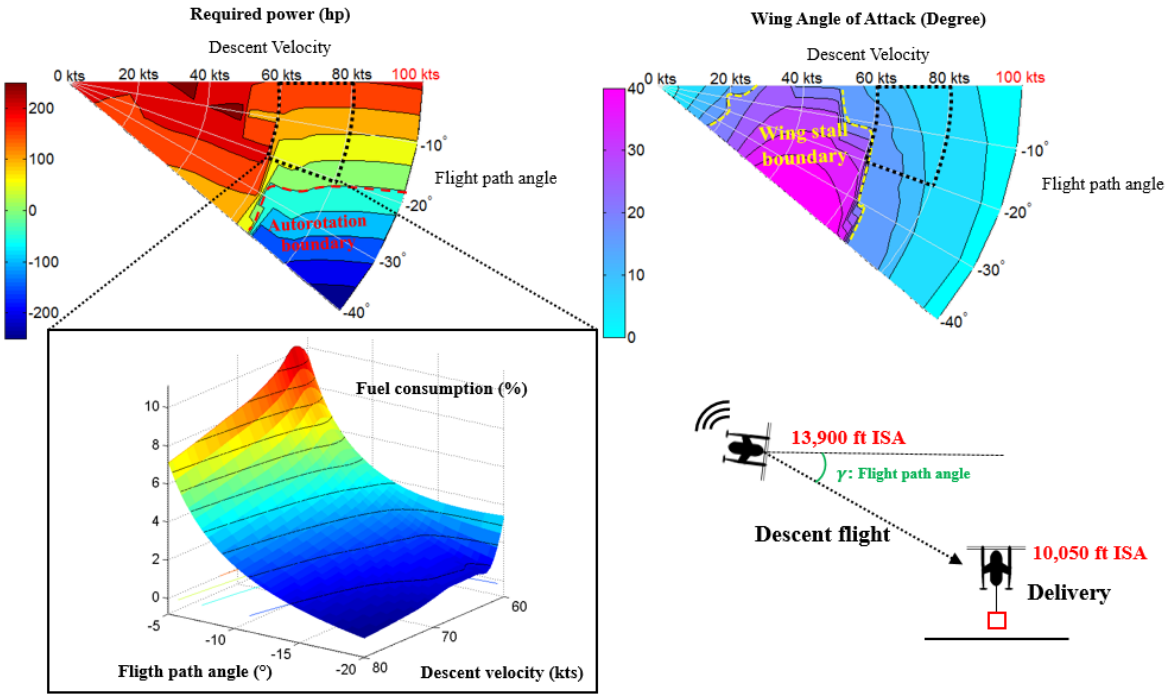

FIGURE 12.10: Fuel consumption for recommended descent flight conditions.

Although the vehicle requires another descent flight after delivery (5^{th} stage in Fig. 12.6), the flight conditions are gentle and approximated to forward flight cruise (1°–2° descent angle). This is because the minimum required flight range of 50 nm is much longer than the altitude difference of 6,000 ft between the disaster area and the base.

12.4.3 Third, Fourth, and Sixth Stages: Transition

Halcyon takes off, hovers, and lands vertically like a typical helicopter, but cruises like a fixed-wing turbo-prop aircraft. Therefore, a transition maneuver is required to change from helicopter to airplane mode. To complete the mission, the aircraft should fly through the following three transition maneuvers:

1. Inbound transition **with payload**, in which the aircraft decelerates and pitches nose-up to move into precision hover in preparation for delivery.

2. Outbound transition **without payload**, in which the aircraft accelerates and pitches nose down to move into airplane-like cruise after delivery.

3. Inbound transition **without payload**, in which the aircraft decelerates and pitches nose-up to move into hover in preparation for landing.

During each transition maneuver, four variable-RPM rotors are used as the primary means of control. Especially, a differential thrust between pairs of the rotors is used as a pitch controller. Depending on the atmospheric conditions, the autopilot selects a specific trajectory from a family of maneuver profiles. The feasibility of these maneuvers were investigated by the in-house flight

simulation tool that includes full nonlinear rotor-body coupled dynamics. To construct a transition maneuver, trim conditions (obtained in Section 12.1) were utilized as reference points [34]. It is essential to choose flight profile that are safe, efficient, and robust from disturbances. Therefore, two primary metrics were considered in deciding an optimal transition maneuver; the power margin and stall of the fixed wing.

Figure 12.11 shows the optimal inbound and outbound transition paths for the mission. The contour plot on the right is required total power, and the plot on the left is effective wing angle of attack for a combination of flight speed and flight path angle. The ranges of flight speed are from 0 to 100 knots, and the the range of flight path angle are from $-30°$ to $90°$. Also indicated on these plots are the wing stall boundary of $20°$ and the available 85% power at 10,000 ft. The fastest inbound transition requires climbing flight wherein kinetic energy of the vehicle is converted to its potential energy. This maneuver admits rapid deceleration, but subsequently requires slow descent in helicopter mode prior to package delivery or landing. While such a maneuver could be executed, for the current mission a "level transition" is preferred, wherein the altitude of the vehicle remains relatively constant throughout the transition.(A→B) This stall brake maneuver requires lesser power than pull-up maneuver as the drag from wings, fuselage and rotors are used to decelerate the vehicle. For the outbound transition after delivering the payload, the aircraft executes an axial climb using the excess power in the system, and then transitions into airplane mode using rotor RPM control. During transition, climbing flight is preferred than level flight because it increases stall margin, and the altitude gain helps avoid obstacles near the ground area. For the mission, therefore, optimum maneuver consists of the following sequence; first vertical climb with $V = 20$ kts and then transient with a $45°$ climb angle. This maneuver increases the altitude to 300 ft (90 m) and increases the cruise speed to 70 knots (130 km/hr). (B→C→D→A)

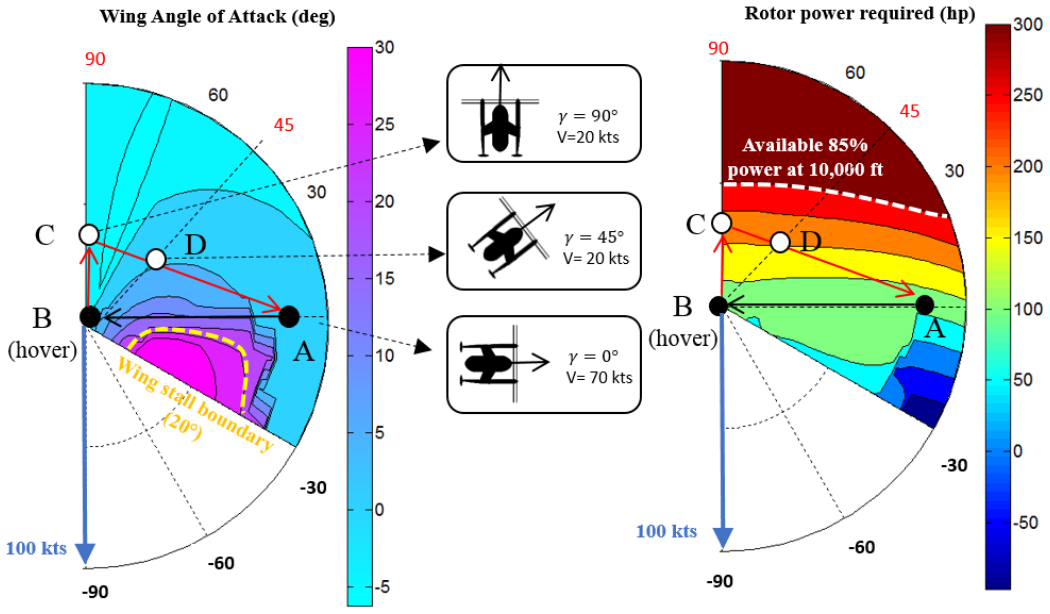

FIGURE 12.11: Inbound transition along A→B, outbound transition along B→C→D→A.

12.4.3.1 Inbound transition

For the inbound transition, there are two different conditions: with payload and without payload. The weight of payload is about half of empty vehicle weight; therefore, the power required and the

vehicle trim settings during each inbound transition are significantly different. Figure 12.12 shows the inbound transitions from steady level forward-flight to hover, with and without payload. The dashed line shows the flight trajectory and the arrows show the pitch attitude and the position of the vehicle. With payload, the inbound transition takes 21 seconds, and requires 1,000 ft (300 m) of forward travel. Without the payload, the inbound transition requires about 10 seconds, traveling 600 ft (180 m) horizontally due to its lower weight. Figure 12.13 shows the time history of power required during each transition maneuvers. The maximum power required are less than available 85% power, and during transition, 0.7% and 0.2% of total fuel was consumed for each case.

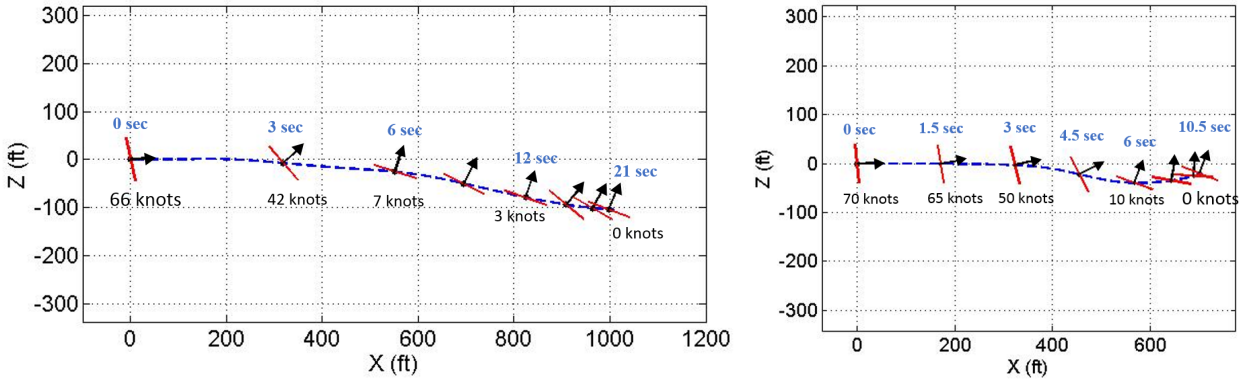

(a) Before payload drop-off

(b) Before landing

FIGURE 12.12: Inbound transition trajectories: flight profiles (a) with and (b) without payload.

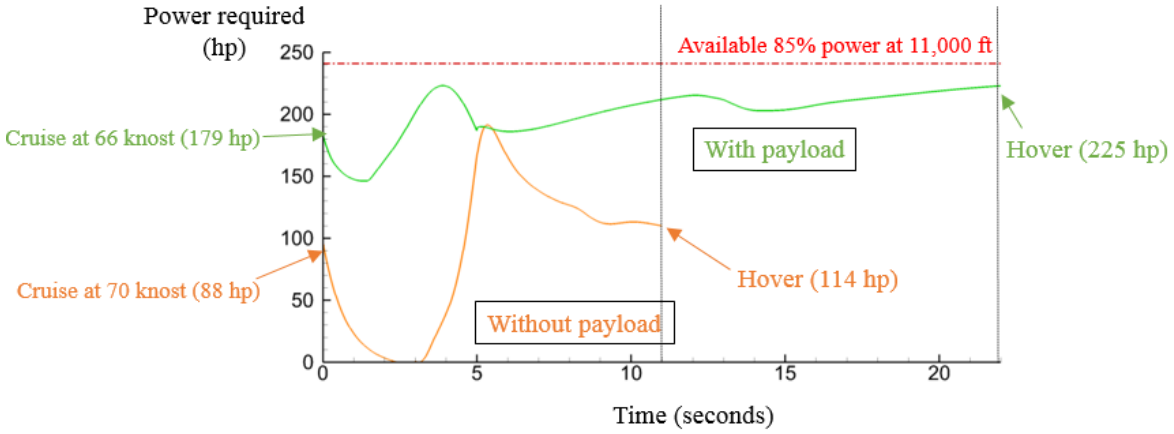

FIGURE 12.13: Time history of power required duing inbound transition.

12.4.3.2 Outbound transition

After successful delivery, the vehicle executes a climb maneuver to reach cruise altitude (300–400 ft AGL). Initially, the vehicle climbs 100 ft (30 m) to make altitude above ground level of 150 ft (45 m). During climb, the vehicle velocity is limited to 20 knots (40 km/hr) to avoid drawing excessive power and damaging the motors. After, *Halcyon* initiates the transition maneuver with $\gamma = 45°$, the optimal trajectory in terms of power efficiency. Figure 12.14 shows the flight profile of the outbound transition simulation. Outbound transition requires 30 seconds to reach a cruise velocity of 70 knots (130 km/hr) at about 400 ft (120 m) above the ground. For this maneuver, 0.7% of total fuel was required.

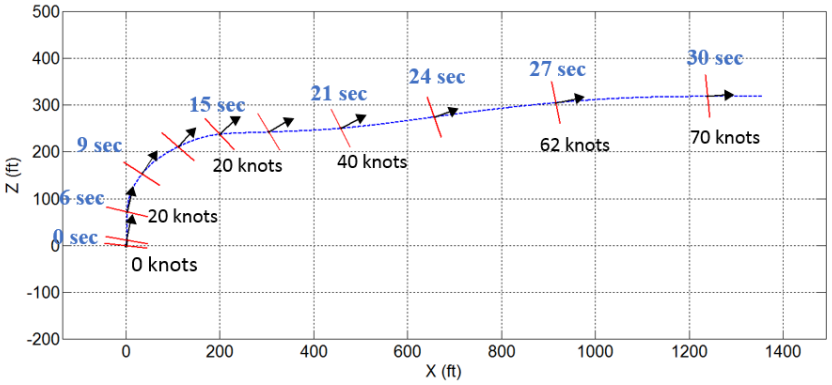

FIGURE 12.14: Outbound transition simulation result.

12.4.4 Fourth Stage: Precision Hover

The payload must be delivered to the designated area using a tether released 50 ft above the ground. As listed in the RPF, total delivery time may not exceed 60 seconds and the maximum allowable impact velocity of the payload is 5 ft/s (1.5 m/s). Using a tether 50 ft in length and an FAA-certified helicopter rescue hoist, the requirements are easily met without any gusts.

Gusts can perturb the payload and initiate weakly-damped pendulous swing motions, and such motions require significant time intervals to decay to acceptable levels. Gust disturbances may result in potentially exceeding the 60 second delivery period and/or maximum impact velocity. To minimize the vulnerability to gust perturbations, *Halcyon* features an anti-swing flight controller which works by sensing the sling cable angle and angular rate at every moment during delivery as shown in Fig. 12.15. To obtain information, each directional force components by cable tension are measured using strain gauges on the rollers that redirect the cable as it leaves the hoist (see Chapter 11). This controller is designed not only for suppressing payload swing motion but also for delivering the payload at an exact location using GPS.

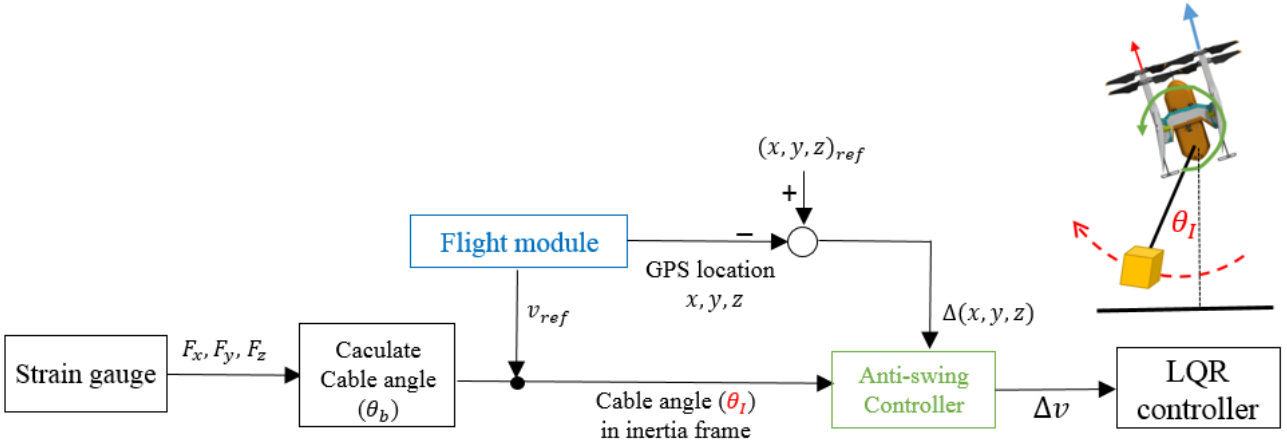

FIGURE 12.15: Anti-swing control architecture.

The vehicle can move in a horizontal plane tilting the body axis using differential RPM control; the horizontal movement of the vehicle can counteract the pendulum movement of the payload and return to a steady state. For verification, a simulation was conducted by applying pendulum motion for payload motion at end of tether with moving hinge point to simulate vehicle. The

gust is modeled as an initial perturbation of 20 ft/s (6 m/s), which was imposed on both vehicle and payload, when they are connected by 50 ft tether above the delivery point. To move vehicle horizontally within available range, a maximum side thrust of 200 lb was set, which can be achieved by 7° tilted body-pitch angle.

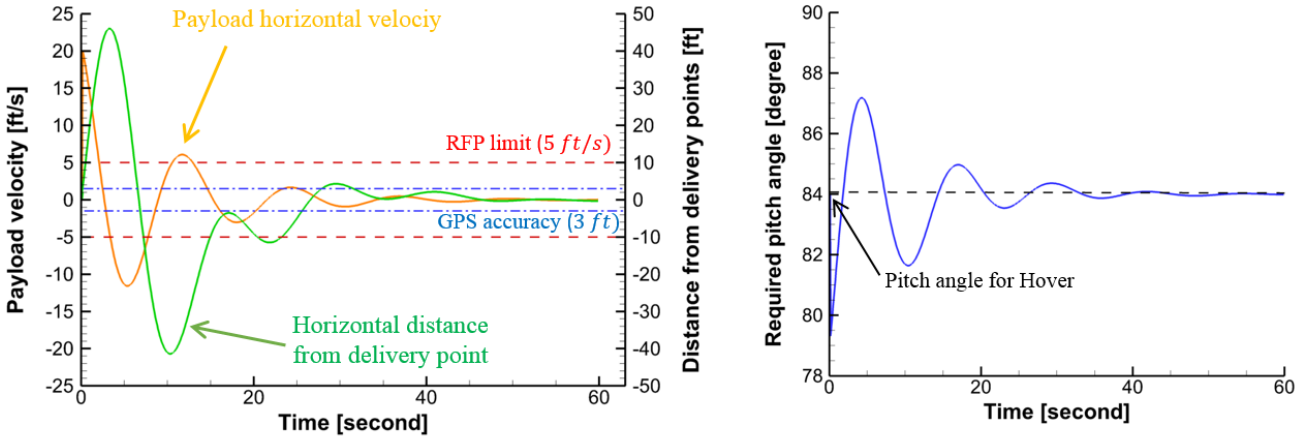

(a) Time history of payload swing motion and offset distance from delivery point

(b) Time history of vehicle pitch attitude

FIGURE 12.16: Simulation of gust alleviation during delivery.

Figure 12.16 (a) shows the time history of payload swing velocity and offset distance from delivery point. Figure 12.16 (b) shows history of body pitch attitude needed to suppress swing motion. By regulating vehicle accelerations, the payload could be positioned at the delivery point within GPS level precision of 3 ft. *Halcyon* with anti-swing system could deliver the payload, satisfying both delivery time and maximum allowable impact velocity of the payload.

13 Acoustics

Considering *Halcyon* is a disaster relief vehicle designed for operation in remote locations and over rough terrain, the vehicle may be exempted from strictly complying with acoustic requirements. In a report to Congress [35], the Federal Aviation Administration (FAA) outlines that emergency helicopter service should be exempt from restrictions as these services are time-critical and provide a noise-excusable public service. However, any aircraft intended for military or civilian use should reduce its acoustic signature to combat noise pollution, detection, and certify its use in areas other than the intended arena.

13.1 FAA Noise Requirements

There are no official regulations for the noise level of an *Halcyon*-sized (1,520 lb [690 kg]) unmanned aerial vehicle by the FAA. Instead, because *Halcyon's* two flight orientations are similar to a tiltrotor, the Federal Aviation Regulation (FAR) guidelines regarding a tiltrotor were applied. The sound pressure levels (SPL) in decibels (dB) were obtained for *Halcyon's* two flight conditions; helicopter-like hover and airplane-like cruise.

In hover, the sound pressure levels were calculated on a plane located 50 ft (15.2 m) below the vehicle to simulate the noise level experienced by ground personnel during a payload delivery mission. In forward flight mode, the SPL levels were calculated for a 400 ft (120 m) radius hemisphere surrounding the vehicle and a plane located 400 ft below the vehicle, which is the

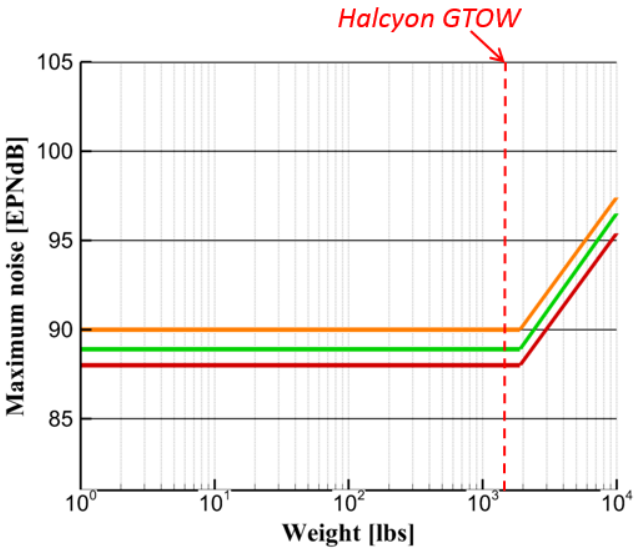

FIGURE 13.1: FAA noise limit requirements (Extrapolated from FAR 36.1103).

effective transition altitude from hover to cruise after dropping the payload. The noise level limit for a 1,500 lb vehicle for different flight conditions lies in a band between 88 and 90 ENPNdb (Effective Perceived Noise Level in decibels), as shown in Fig 13.1.

13.2 Noise Assessment

TABLE 13.1: Acoustic study shows maximum noise levels.

	Thickness Noise (dB)	Loading Noise (dB)	Total Noise (dB)
Hover	91.5	77.8	91.5
Cruise	68.4	85.8	86.2

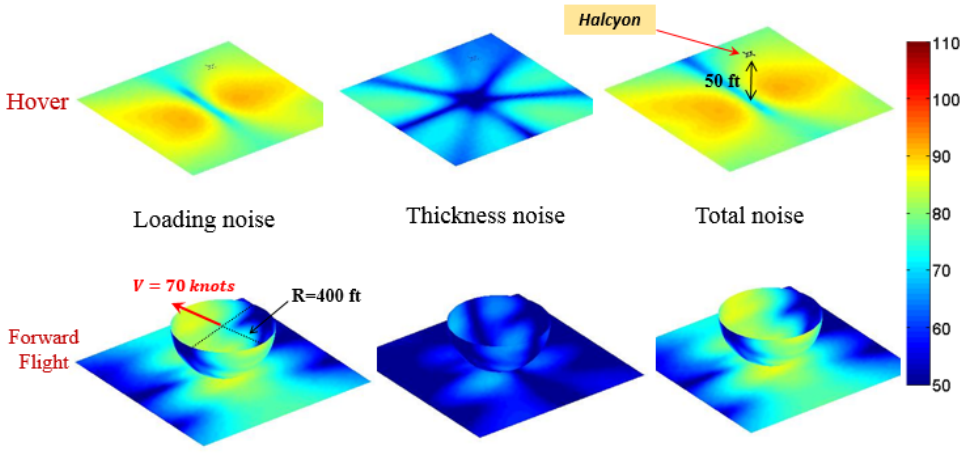

FIGURE 13.2: The thickness, loading, and total noise of the vehicle in hover and cruise conditions.

Halcyon's four overlapping rotors are the main noise source of the vehicle. The overall SPL is comprised of: 1) Thickness noise, which caused by the air displaced by a blade, 2) Loading noise,

which is caused by the accelerating force on the air induced by the blade surface, and 3) High-speed impulsive (HSI) noise and blade vortex interaction (BVI) noise. Noise calculations were obtained using a code developed in-house based on the Ffowcs–Williams–Hawkings (FWHA) equation, which considers thickness noise and loading noise. Contour plots of the loading, thickness and total noise (in dB) around *Halcyon* are shown in Fig. 13.2. The loading noise is the the major source of rotor noise in both hovering and cruising conditions because of the disk loading (12 lb/ft^2 [59 kg/m^2]) being relatively high compared to conventional helicopters. In hover, the noise signature is symmetric about the lateral plane, which is reflective of the arrangement of the rotors. A higher noise signature was observed ahead of the vehicle as airspeed increases. However, in forward flight, the total noise is lower relative to hover. This reduced noise is primarily because of the lower disk loading (2 lb/ft^2 [10 kg/m^2]), which results in a lower loading noise.

The SPL in decibel is summarized in Table 13.1. The maximum noise level in cruising flight is 86.2 dB, which is lower than the FAA noise requirements, while the noise level in hover is only slightly higher (91.5 dB) than the requirement as described by FAR 36. However, if *Halcyon* was required to operate in an urban arena for reasons other than disaster relief, noise reduction techniques could be applied [36] making the vehicle safe to operate in any environment.

14 Failure Modes Analysis

As with any emergency vehicle operating in the chaotic post-disaster environment, safety and survivability are essential aspects of a successful relief effort. The safety of each person involved in the relief effort — including the C-130J crew, emergency personnel, and the disaster victims in need of aid — was a major concern for the designers of *Halcyon* . The ultimate goal of the given mission is to save lives, and therefore great emphasis was placed on aircraft redundancy and safe operation through all levels of operation, from loading the payload into *Halcyon's* cargo bay at the base location to cruising low over potentially mountainous terrain. Possible failure modes at each stage of operation were reviewed, and the cause, impact, and likelihood for each failure mode was identified and mitigated to ensure no excessive risks were taken in the design or operation of the *Halcyon* aircraft.

14.1 Failure Modes, Effects, and Criticality Analysis

Though redundancies and mitigation strategies are necessary in case of an unexpected or unlikely failure, regular inspections, maintenance, and repairs are the best way to identify an issue before it becomes a failure during the mission. Preventative action before the aircraft is deployed will protect personnel and the aircraft itself from damage or injury.

To identify the potential risks involved in this design, a Failure Modes, Effects, and Criticality Analysis (FMECA) was performed and Table 14.1 shows the classification levels of the likelihood of occurrence and the degree of impact for each failure mode.

Each failure level is assigned a letter, A-E, to indicate the likelihood of its occurrence and a Roman numeral, I-V, to indicate the potential degree of impact each failure may have on the mission. Failures with the highest likelihood and impact, receiving a rating of I-A, pose the greatest risk to the success of the mission and must be thoroughly identified and mitigated to ensure the safety of both the aircraft and personnel. Failures with lower rating combinations are considered less of a priority. Mitigation strategies are employed to reduce the risk to an

TABLE 14.1: FMECA classification levels.

Level of Impact	Description
I	Catastrophic - injury or loss of life possible
II	Major concern - vehicle unrecoverable
III	Moderate concern - failure to deliver supplies
IV	Low concern - delay in supply delivery
V	No concern - delivery completed as planned

Level of Likelihood	Description
A	Very high likelihood (>75%)
B	High likelihood (50-75%)
C	Moderate likelihood (25-50%)
D	Low likelihood (5-25%)
E	Negligible likelihood (<5%)

allowable level.

The likelihood of occurrence, degree of impact, consequences, and mitigation strategies of each failure mode is shown in Table 14.2. There are no A-I events, and the three level-I events have a low likelihood of occurring. Therefore, the system has adequate safety.

14.2 Electrical Systems

Because *Halcyon* employs an electrically-powered transmission, flight control system, and avionics and sensors system, the reliability of the electrical routing and components is absolutely critical.

The fly-by-wire flight control system draws its power from the turbo generator in flight, and utilizes an electric transmission system to power the rotors and actuate the wing control surfaces using a rotary servo. The flight control system consists of four motors, each with an individual speed controller, to ensure continuous power to the other three rotors in the event of a rotor or hub failure and enable the aircraft to return to base. If the electrical generator fails and no longer provides power to the rotors, the backup battery will engage and force the aircraft to transition into hover and identify a location for immediate landing.

The avionics and sensors on the aircraft are powered by a separate battery to protect against failures in the transmission and flight control systems, and flight critical components are connected to the backup battery in the event of power loss. *Halcyon* is completely autonomous, and therefore the reliability of the avionics system is essential to maintain control of the aircraft. To this end, *Halcyon's* autonomous system has triple redundancies to ensure continuous control. *Halcyon* uses GNSS as its primary navigational system for enhanced accuracy and precision, but can also use a standard GPS as a secondary system and the INS accelerometers, gyroscopes, and sensor data to navigate with a lesser degree of precision. The obstacle avoidance system also utilizes a triple-redundant network, using LIDAR-SLAM and Monocular-SLAM for primary and secondary sensing, respectively; however, *Halcyon* operators have the ability to take control from the autopilot as a last resort. This is described in further detail in Chapter 11.

14.3 Engine Failure

Halcyon relies on multiple sources of power generation, including the main turbo generator as well as a backup battery capable of safely landing the aircraft from any flight orientation. The backup battery is capable of two minutes of maximum power to enable the aircraft to locate an open area to safely land, which is maximized by dropping any internal payload and transitioning into low-power cruise.

Failure Mode	Impact	Likelihood	Consequences	Mitigation
Engine failure	II	D	Crash landing of vehicle	Backup battery installed to allow 1 minute of max power for transition to hover and safe landing
Electrical propulsion system failure	II	D	Crash landing of vehicle	Backup battery installed to allow 1 minute of max power for transition to hover and safe landing
Delivery mechanism failure	III	C	Unable to delivery emergency aid, supplies impact the ground at high velocity, cargo doors lock in open position	Door lock falls open in event of power loss; automatic return to base for recovery and repair
Unexpected weather or gusty winds	III	B	Flight path altered, delivery delay, unexpected wing/rotor stall	Gust tolerance capability, multiple control surfaces, and additional fuel for 10% extended range
Lightning strike	III	B	Electrical system failure	Expanded copper mesh embedded within blades and airframe skin
Failure of actuated wing flap	III	D	Aircraft cannot pull into level cruise without rotor thrust	Transition to edgewise flight and land immediately with backup power
Vehicle airframe structural failure	II	E	Loss of balance, lift, and control; crash landing of vehicle	Routine maintenance schedule and automated system checks in place
Loss of GNSS navigational awareness	III	C	Loss of centimeter-level precision	GPS and INS/Sensor Fusion awareness engages
Loss of LIDAR-SLAM obstacle awareness	III	D	Loss of close range, refined obstacle avoidance	Less robust Monocular-SLAM uses onboard cameras for obstacle avoidance
Loss of monocular camera	III	D	Safe delivery and landing zones cannot be confirmed	Multiple cameras are installed on the aircraft
Loss of autopilot	I	E	Aircraft loses autonomous flight capability	Operators can take manual control from GCS using live video feed and sensor data
Pre-flight check senses a problem with aircraft	II	D	Aircraft deemed unsafe or in need of repair; mission aborted	C-130J personnel return to base for repair. Standard procedures include initial system check before loading up the C-130J
LED panel fails to complete pre-flight check	III	E	C-130J personnel cannot proceed with deployment procedures	Indicator light system on LED panel clearly indicates Abort (strobe), Go (solid color), or Error (solid white)
Avionics battery is dislodged	I	D	Aircraft loses autonomous flight capability	Backup battery engages to power the sensors and avionics
Control system malfunction	I	D	Loss of control; crash landing of vehicle	Land immediately with backup battery power

TABLE 14.2: Identified failure modes and mitigation strategies.

14.4 Adverse Weather Conditions

To protect against damage to the electrical components within *Halcyon's* structure from lightning strikes or electrostatic buildup, an S-glass isolation layer topped by an expanded 0.04 lb/ft^2 (1.68 g/m^2) copper mesh, capable of withstanding Zone 1A lightning strikes per FAA regulations, is embedded within the skin of the blades, wing, and nose of the aircraft. The main fuselage body, which is much less exposed to a direct lightning strike than the extremities of the aircraft, uses an ultralight 0.01 lb/ft^2 (0.42 g/m^2) copper mesh embedded within the skin to maintain conductivity [37]. This is particularly important for *Halcyon*, which consists primarily of a non-conducting carbon fiber structure.

Halcyon's sensors and avionics systems are fully capable of operation in rain as well as light snow and fog, with dual LIDAR and radar altimeter sensing ability to penetrate a degraded visual

environment. Because *Halcyon* is stored in the C-130J cargo bay before flight, it will not be susceptible to significant ice buildup on the blades and fuselage. *Halcyon's* flight control systems are also capable of maintaining precision hover in gusts up to 20 ft/s (6 m/s), as discussed in Section 12.4.4. For short periods of time, *Halcyon* is capable of operation in polluted air environments, such as wildfires, by utilizing backup battery power. Because the turbo generator fully recharges the battery over the duration of the given mission, *Halcyon* could return to the polluted site after that time and perform another maneuver through the polluted area.

14.5 Downwash and Disk Loading

Ensuring low rotor downwash was a major design goal during the design process. In hover, the aircraft operates only 50 ft above the ground; the downwash from the rotors must be kept low to protect ground personnel at the payload delivery site and to prevent blowing debris around in the rotorwash.

As discussed in Section 5.4.1, *Halcyon* small rotors produce a disk loading of 12lb/ft^2 (59kg/m^2) and a fully-contracted wake velocity of only 116 ft/s (35 m/s). During delivery, *Halcyon* hovers at a vertical distance of 15 radii from the ground, further dissipating a mass flow rate of 5.17 lb/s (2.34 kg/s). For comparison, the CH-53K cargo transport helicopter has a higher disk loading of 17lb/ft^2 ((289kg/m^2)), and its nearly 80 ft (24 m) diameter rotor produces an enormous mass flow rate of 604 lb/s (274 kg/s). Therefore *Halcyon* is shown to have a low rotor downwash, one of the primary objectives of the design of this aircraft.

14.6 Slope Limitations

Fully loaded, *Halcyon* is capable of landing on slopes up to 36°. At the completion of the mission, when the payload has been delivered, *Halcyon* can land on slopes up to 31°.

15 Cost Breakdown

The total cost of the *Halcyon* vehicle can be broken down into four major categories: (i) the development cost, (ii) the production cost, (iii) the operational cost, and (iv) the end of life cost. Operational cost can be further broken down into direct operating costs, which include aircraft maintenance and repair, replacement parts, inspections, and day-to-day operation, and indirect operating costs, which account for training, management and administration, and overhead expenses. The life cycle cost is the sum of each of these four cost elements.

The Bell Helicopter model for cost estimation was used to calculate the expected production costs of each aircraft in 2015 USD. This model is based on the total quantity of the aircraft to be manufactured as well as the rate of production each year. The life cycle cost estimates of this design assume that 600 *Halcyon* aircraft will be produced within the next 20 years.

15.1 Development Cost

The *Halcyon* design makes use of entirely existing and commercially available technologies. By using commercial off-the-shelf (COTS) avionics, power and propulsion components, flight controls, and structures, *Halcyon* minimizes research and development costs and maximizes available resources for testing and certification. Assuming the development cost is approximately three times the aircraft cost of production, this results in a total development cost estimate of

TABLE 15.1: Aircraft production and mission cost

(a) Breakdown of aircraft production cost

Component Description	Cost (2015 USD)
Wings	$ 104,500
Rotor Group	$ 161,600
Fuselage Group	$ 127,900
Landing Gear Group	$ 6,000
Flight Controls Group	$ 60,000
Propulsion Group	$ 314,000
Turbo Generator	$ 300,000
Battery	$ 1,300
Structure	$ 12,800
Basic Avionics Package	$ 86,800
Empty Aircraft Total	**$ 861,000**
Cargo Delivery System	$ 234,200
Door Release	$ 50,000
Rescue Hoist	$ 234,000
Mission Fuel	$ 50
Mission Avionics	$ 37,200
Payload Package	$ 8,800
Mission Aircraft Total	**$ 1,054,400**

(b) Breakdown of mission production cost

Component Description	Quantity	Unit Cost (2015 USD)
Software	Set	$ 23,800
Specialty Carrying Crate	6	$ 250
Optional Ground Wheels	6	$ 250
Kit Tooling	6	$ 1,000
WH Annual Storage	600 sq ft	$ 6,000
Ground Control Station	1	$ 11,200
Total Cost for Mission Set		**$ 84,500**

approximately **$3.16 million**.

15.2 Production Cost

The production costs for the airframe and structural components, including the wings, fuselage, rotors, landing gear, and powerplant structure, were calculated from the 2002 Bell Helicopter model and converted to 2015 USD. The costs for the turbo generator engine, batteries, flight controls, and cargo system were estimated based on the cost of COTS components, such as the UTC Aerospace variable-speed Rescue Hoist. The lithium-ion batteries used in *Halcyon's* design were priced using General Motor's 2016 estimate of $145/kW-hr [38]. The complete cost breakdown is given in Table 15.1(a), and shows that a fully-fueled *Halcyon* aircraft outfitted for the given mission will cost approximately **$1.05 million**, while the basic model with a baseline avionics system costs only **$861,000**.

In addition to the cost of producing each aircraft, the system costs must also be considered. Each mission flown by *Halcyon* utilizes up to six aircraft at a time; thus, the cost of production for a mission includes costs for six *Halcyon* aircraft. The *Halcyon* system includes the tooling required for the aircraft kit option, and *Halcyon* aircraft require adequate floor space for storage. The summary of this cost is shown in Table 15.1(b) and amounts to a total of **$84,500**.

TABLE 15.2: Direct and indirect operating costs.

Operating Cost		
Repair Parts	$	158,200
Battery Replacements[a]	$	730,800
Monitoring Labor	$	420,000
R&M Labor	$	360,000
Indirect Operating Costs[b]	$	667,600
TOTAL	**$**	**2,336,500**

[a] Six aircraft require 24 0.26kWh/kg batteries at $145/kWh over 6 month relief period
[b] Assumed to be 40% of direct operating cost

15.3 Operating Cost

The operating costs are calculated for a standard disaster relief mission lasting over a period of six months. In the first two weeks after a disaster when large amounts of supplies are most needed, each *Halcyon* aircraft is assumed to accrue 20 flight hours per day, equivalent to 20 one-hour resupply missions. During this time, the operators are assumed to work 80 man-hours per day. Assuming a payload weight of 500 lb per aircraft and the utilization of all six *Halcyon* aircraft in each mission, 60,000 lb of emergency supplies would be delivered every day for fourteen days.

After the initial two weeks the daily operation reduces to 10 flight hours per day per aircraft, and operators work 20 man-hours a day. The cost of labor for operators and aircraft monitors is $100/hr for engineers and technicians, and the cost of labor for repairs and maintenance is $100/hr for mechanics and technicians. 4,200 total man-hours and 1,820 total flight hours are accrued over a six month relief effort. The lithium-ion batteries that provide power in deployment last for 500 cycles [39], which is equivalent to 500 one-hour missions. Thus four battery packs would be used by each of the six *Halcyon* aircraft over the six month relief effort, totaling 24 battery packs. Repair parts are assumed to total 15% of the mission-ready *Halcyon* aircraft. Indirect operating costs were assumed to be 40% of the total direct costs. Table 15.2 summarizes the total operating cost.

15.4 End of Life Cost

At the end of an aircraft's usable life, the aircraft is broken down and reusable materials are sent to a recycling facility. This cost is based on the amount of recyclable material used in the aircraft's design; composite components cannot be reused, while the batteries, electronic equipment, and parts of the propulsion system and mechanical components are able to be recycled. Approximately 60% of *Halcyon's* design is recyclable, corresponding to a net end of life cost of **$2.1 million**, or **$350,000** per aircraft.

15.5 Total Life Cycle Cost

Assuming a lifetime operation of 20 years, the total life cycle cost is the sum of the above costs, amounting to **$9.68 million**.

16 Weight Analysis

TABLE 16.1: Weight breakdown according to MIL-STD-1374A specifications.

Component Description	Weight (lb/kg)	% Empty Weight	x_{CG} (in/cm)
1 Wings	80.0 / 36.4	9.0%	-20.1 / -53.3
Wing Structure	70.0 / 31.8	7.9%	-17.4 / 44.2
Trailing Edge Flaps	10.0 / 4.54	1.1%	-41.0 / 104
2 Rotor Group	93.0 / 42.2	10.5%	22.7 / 57.7
Blades	8.54 / 3.88	1.0%	27.8 / 70.6
Hubs	84.5 / 38.3	9.5%	27.8 / 70.6
3 Fuselage Group	52.9 / 24.0	6.0%	14.8 / 37.6
4 Landing Gear Group	20.0 / 9.09	2.3%	-58.0 / -147
5 Flight Controls Group	156.4 / 70.9	17.6%	-15.0 / -38.1
BLDC Motors	88.0 / 39.9	9.9%	-5.80 / -14.7
Electronic Speed Controllers	48.4 / 21.9	5.5%	-38.0 / -96.5
Rotary Servo	20.0 / 9.07	2.3%	-38.1 / -96.8
6 Propulsion Group	377 / 171	42.6%	0.63 / 1.60
Turbo Generator	247 / 112	27.9%	8.78 / 22.3
Cooling System	14.0 / 6.35	1.6%	-1.30 / -3.30
Starter System	16.6 / 7.53	1.9%	-0.60 / -1.52
Lubrication System	30.0 / 13.6	3.4%	0.00 / 0.00
Fuel System	6.80 / 3.08	0.8%	-12.0 / -30.5
Plumbing and Supports	14.6 / 6.62	1.6%	0.00 / 0.00
Backup Battery	48.0 / 21.8	5.4%	-38.0 / -96.5
7 Avionics Group	34.5 / 15.6	3.9%	5.46 / 13.9
Autopilot	0.80 / 0.36	0.0%	-32.0 / -81.3
Obstacle Avoidance	11.6 / 5.27	1.9%	17.4 / 44.2
Navigational System	5.10 / 2.32	0.6%	-36.7 / -93.2
Communication System	0.40 / 0.18	0.1%	-32.4 / -82.3
Health Monitoring System	14.50 / 6.59	0.1%	-13.0 / -33.0
Battery	2.00 / 0.91	1.1%	12.2 / 31.0
8 Cargo Delivery System	73.0 / 32.7	8.2%	0.90 / 2.29
Cargo Door Mechanism	15.0 / 6.82	1.7%	-51.0 / 130
Rescue Hoist	58.0 / 26.3	6.5%	3.14 / 7.98
Empty Weight	**887 / 403**	**100.0%**	**-2.38 / -6.05**
Fuel	88.0 / 37.0		-12.0 / -30.5
Payload Package	545 / 247		-22.2 / -56.4
Gross Weight	**1520 / 691**		**-9.73 / -24.7**

Halcyon's center of gravity (CG) is designed to enable natural stability in deployment and to properly orient the aircraft's four rotors. Table 16.1 shows the CG placement from the leading edge of the wing according to MIL-STD-1374A grouping specifications. The x direction indicates the vector oriented along the body of the aircraft and out through the nose. The y and z directions are not included because the aircraft is designed to be symmetric about those axes, resulting in a CG of zero.

17 Summary

The *Halcyon* system represents a revolution in modern disaster relief practices. Enabling rapid response through simplicity in design, operation, and control, *Halcyon* is a compact, efficient, and agile configuration integrated into a system of systems approach to disaster relief. This proposed design features the following:

- **Delivery of over 3,000 lb of emergency supplies:** Designed to deliver supplies, *Halcyon's* quadrotor biplane tailsitter configuration is optimized for the specified mission's unique constraints. Its small footprint enables six *Halcyon* vehicles, each carrying more than 500 lb of payload, to deliver a total of 3,045 lb of emergency supplies with a single C-130J flyover. The *Halcyon* system, capable of delivering more than 6 times the RFP requirement, maximizes the impact of the relief effort and saves time, minimizes cost, and reduces the required manpower.

- **Precise navigation and control:** Strategic placement of the vehicle's center of gravity enables passive stabilization and parachute-free deployment. *Halcyon's* four thrust vectors, variable-speed rotors, and highly responsive electric motors enable superior vehicle controllability. The rotors and wings provide multiple control surfaces for both helicopter and fixed wing orientations, and *Halcyon's* advanced navigational system guides the aircraft to its prescribed delivery location with 800 mil (2 cm) precision.

- **Simple, low maintenance design:**
Halcyon's composite structure and integrated subsystems are designed in a modular fashion to support low maintenance and repair among the *Halcyon* fleet of aircraft. Designed for on-site assembly, *Halcyon's* modular design can be delivered as a self-contained kit and constructed in minutes with just five tools. Components are easily exchanged or replaced between each *Halcyon* aircraft, enabling fleet readiness when a disaster strikes.

- **Superior performance:** With a Figure of Merit of 0.79, *Halcyon* demonstrates outstanding hover efficiency while maintaining a fuel-efficient cruise of 70 knots. *Halcyon's* serial hybrid propulsion system combines an advanced turboshaft engine with high power density electric motors to support simplicity, increased controllability, and extended range capability.

- **Ready to deploy:** *Halcyon* was developed using proven, commercially available technology to minimize the time and cost of development, resulting in a production cost of $1.05 million for a mission-equipped *Halcyon* vehicle.

- **Safe operation at every level:** *Halcyon's* rotors are unpowered and the vehicle's skids are locked onto the cargo rail system while inside the C-130J, protecting crew personnel from injury. Additionally, low rotor downwash combined with a hover distance 15 radii above the ground guards ground personnel against flying debris. *Halcyon's* triple-redundant avionics system maintains control of the vehicle at all times and an auxiliary battery system provides backup power in case of engine failure.

Bibliography

[1] Johnson, J., "South America - Earthquakes and Tectonics," March 2016, [Online].

[2] Richard Benney, Andrew Meloni, Mike Henry, Kristen Lafond, "Joint Medical Distance Support and Evaluation (JMDSE) Joint Capability Technology Demonstration (JCTD) and Joint Precision Air Delivery Systems (JPADS)," Paper 8304, Special Operations Forces Industry Conference, 2009.

[3] "Defense Transport Regulations," Regulatory document, U.S. Transportation Command, June 2014.

[4] "C-130 Operations Procedures," Instruction, U.S.A.F., February 2013.

[5] Jamie Bartz, D. S. M., "An Experimental Analysis of Camber Effects of a 6-Bladed Flapped Autorotational Aerodynamic Decelerator," *17th AIAA Aerodynamic Decelerator Systems Technology Conference and Seminar*, 2003.

[6] Aviation, L., "Product Details," May 2016, [Online].

[7] Marat Tishchenko, V. T. N., "ENAE634 Helicopter Design Lecture Notes," University of Maryland, College Park, 2008.

[8] Leishman, J. G., *Principles of Helicopter Aerodynamics*, Cambridge University Press, New York, NY, 2006.

[9] Stahlhut, C. and Leishman, J. G., "Aerodynamic Design Optimization of Proprotors for Convertible Rotor Concepts," *68th Annual Forum of the American Helicopter Society*, 2012.

[10] C.H. Zimmerman, "Characteristics of Clark Y Airfoils of Small Aspect Ratio," Technical Report 431, National Advisory Committee for Aeronautics, 2011.

[11] Datta, A. and Johnson, W., "X3D – A Solid Finite Element Multibody Dynamic Analysis for Rotorcraft," *American Helicopter Society Technical Meeting on Aeromechanics Design for Vertical Lift*, 2016.

[12] Cassidy, J. F., "C-130 Transportability of Army Vehicles," Technical report, U.S. Army, June 2001.

[13] Roskam, J., *Airplane Design Part IV: Layout of Landing Gear and Systems*, Design, Analysis and Research Corporation, Lawrence, Kansas, 2004.

[14] Raymer, D. P., *Aircraft Design: A Conceptual Approach*, American Institute of Aeronautics and Astronautics, Inc., 2nd ed., 1992.

[15] Shevell, R., *Fundamentals of Flight*, Prentice-Hall, New Jersey, 1989.

[16] Prouty, R., *Helicopter Performance, Stability, and Control*, PWS Engineering, Boston, 1986.

[17] "Electric propulsion components with high power densities for aviation," Siemens, August 2015, Transformative Vertical Flight Workshop.

[18] Johnson, W. R., "NDARC NASA Design and Analysis of Rotorcraft," Paper, NASA Ames Research Center, Moffett Field, California 94035-1000, Dec 2009.

[19] "Aviation Maintenance Technician Handbook Powerplant, Volume 2," U.S Department of Transportation Federal Aviation Administration.

[20] "Federal Aviation Regulations, Section 33.71-Lubrication System," [Online].

[21] William J. Hughes, "FAA GPS Performance Analysis Report," July 2014, [Online].

[22] Navigation, U., "Vector Technical Specification," [Online].

[23] Trimble, "BD 920 Data Sheet," [Online].

[24] Sebastian Scherer, Lyle Chamberlain, Sanjiv Singh, "Autonomous landing at unprepared sites by a full-scale helicopter," Paper, Robotics Institute, Carnegie Mellon University, Pittsburgh, PA, USA, 2012.

[25] Stephan Weiss, Davide Scaramuzza, Roland Siegwart, "Monocular-SLAM?Based Navigation for Autonomous Micro Helicopters in GPS-Denied Environments," Paper, Journal of Field Robotics 28(6), 854?874, 2011.

[26] Alliantech, "Omni-Probe Data Sheet," [Online].

[27] Jose Luis Palacios, "Design, Fabrication, and Testing of Ultrasonic De-icing System for Helicopter Rotor Blades," Thesis, Pennsylvania State University, May 2008.

[28] Navigation, U., "GCS Software," [Online].

[29] Yannick Bury, T. J. and Klockner, A., "Experimental investigation of the vortical activity in the close wake of a simplified military transport aircraft," *Experiments in Fluids*, Vol. 54, 2013.

[30] Schade, N., "Simulation of Trajectories of Cuboid Cargos Released from a Generic Transport Aircraft," *17th AIAA Applied Aerodynacmis Conference*, 2011.

[31] Atsushi Oosedo, Atsushi Konno, Takaaki Matsumoto, Kenta Go, Koji Masuko and Masaru Uchiyama, "Design and Attitude Control of a Quad-Rotor Tail-Sitter Vertical Takeoff and Landing Unmanned Aerial Vehicle," *Journal of Advanced Robotics*, Vol. 26, 2012, pp. 307–325.

[32] Christopher Bogdanowicz, V. H. and Chopra, I., "Development of a Quad-Rotor Biplane MAV with Enhanced Roll Control Authority in Fixed Wing Mode," *AHS 71st Annual Forum*, 2015.

[33] Nelson, R. C., *Flight Stability and Automatic Control*, McGraw-Hill, 1998.

[34] Kubo, D. and Suzuki, S., "Tail-Sitter Vertical Takeoff and Landing Unmanned Aerial Vehicle: Transitional Flight Analysis," *Journal of Aircraft*, Vol. 45, No. 1, 2008, pp. 292–297.

[35] Federal Aviation Administration, "Nonmilitary Helicopter Urban Noise Study," Tech. rep., Federal Aviation Administration, 2004.